

**Created on 4/16/2002 9:07 PM**

**FINAL DRAFT**

**Comparison of the EO-1 Advanced Land Imager  
Performance with the Landsat Data Continuity Mission  
Specification**

J. A. Mendenhall, D. R. Hearn, D. E. Lencioni  
Lincoln Laboratory  
Massachusetts Institute of Technology  
April 16, 2002

---

This work was sponsored by NASA/Goddard Space Flight Center under U.S. Air Force Contract number F19628-00-C-0002. Opinions, interpretations, conclusions, and recommendations are those of the authors and are not necessarily endorsed by the United States Air Force.

## **Table of Contents**

List of Figures.....	iii
List of Tables.....	v
Introduction .....	1
Noncompliance of ALI to LDCM Specification .....	2
Data Collection .....	2
Spectral Bands.....	3
Spatial Resolution.....	5
Radiometry .....	8
Summary.....	11
Appendix A: LDCM Specification Compliance Matrix.....	A-1
Appendix B: Stray Light Analysis and Impact on Flight Data.....	A-1
Appendix C: Focal Plane Contamination .....	B-1
Appendix D: Leaky Detector Analysis and Correction .....	C-1
Appendix E: Edge Response Calculation .....	D-1
Appendix F: Coherent Noise .....	E-1
Appendix G: Publications.....	F-1

## **List of Figures**

Figure 1: Spectral response curves of the Advanced Land Imager.....	3
Figure 2: ALI point source transmittance Y = pitch direction, X = roll direction..	7
Figure B-1: Earth limb scan history for detector 100, Band 3.....	B-3
Figure B-2: Stray light model and flight data for Band 3.....	B-4
Figure B-3: Effects of stray light for bands 1 (solid), 2 (dotted), 3 (dashed).....	B-5
Figure B-4: Stray light impact example for West Coast, Africa scene.....	B-6
Figure B-5: Raster scan for a typical ALI Lunar calibration.....	B-8
Figure B-6: Direction of a typical Lunar calibration scan on the SCA module.....	B-9
Figure B-7: Images of the moon from a typical Lunar calibration.....	B-10
Figure B-8: Stretched images from a typical Lunar calibration.....	B-11
Figure B-9: Ghosting effects observed in Mount Etna lava flows (Band 7).....	B-12
Figure B-10: Cross section of ALI SCA.....	B-13
Figure B-11: Generation of Lunar ghosts by scattering off the VNIR/SWIR filter boundary.....	B-15
Figure B-12: Generation of lava flow ghosts by scattering off the VNIR/SWIR filter boundary.....	B-16
Figure C-1: Illumination of the ALI focal plane using the internal reference lamp assembly.....	C-1
Figure C-2: Image of a portion of the top surface of the focal plane filters.....	C-2
Figure C-3: History of focal plane contamination for two periods during instrument characterization.....	C-3
Figure C-4: Pan Band on-orbit contamination history.....	C-4
Figure C-5: Pan Band on-orbit contamination history.....	C-4
Figure C-6: Pan Band on-orbit contamination history.....	C-5
Figure C-7: Pan Band on-orbit contamination history.....	C-5
Figure D-1: Band 2 image of Lincoln Laboratory before the effects of the leaky detector (1149) are corrected....	D-1

**FINAL DRAFT**  
Created on 4/16/2002 9:07 PM

Figure D-2: Band 3 image of Lincoln Laboratory before the effects of the leaky detector (864) are corrected.....	D-2
Figure D-3: Photograph of ALI filter assembly.....	D-4
Figure D-4: Photograph of detector rows for Bands 1-4 .....	D-4
Figure D-5: Example of geometric correction performed on images before the leaky detector correction .....	D-5
Figure D-6: Effects of leaky detector corruption of frame 1050 of the Band 2 image of Lincoln Laboratory .....	D-6
Figure D-7: Frame 1050 difference array as a function of weighted standard detector radiance. ....	D-7
Figure D-8: Frame 1050 difference array as a function of weighted standard detector radiance. ....	D-7
Figure D-9: Frame 1050 with leaky detector correction applied. ....	D-8
Figure D-10: Band 2 image of Lincoln Laboratory before (left) and after (right) leaky detector correction .....	D-9
Figure D-11: Band 3 image of Lincoln Laboratory before (left) and after (right) leaky detector correction. ....	D-9
Figure E-1: ALI spatial transfer function for Band 4p (static).....	E-2
Figure E-2: ALI edge spread function, Band 1p.....	E-3
Figure E-3: ALI edge spread function, Band 4p.....	E-3
Figure E-4: ALI edge spread function, Band 7.....	E-4
Figure E-5: ALI edge spread function, Pan band. ....	E-4
Figure E-6: Nominal ALI edge responses. ....	E-5
Figure E-7: Sharpened ALI edge responses.....	E-5
Figure F-1: Maximum autocorrelations in ALI dark data, plotted by band and Sensor Chip Assembly.....	F-2
Figure F-2: Simulated noise and autocorrelation, with common-mode variance .....	F-3

**List of Tables**

Table 1: ALI/LDCM Noncompliance.....1

Table 2: Spectral response summary for the Advanced Land Imager.....3

Table 3: LDCM PST Specification.....6

Table 4: ALI total integrated scatter.....8

Table B-1: Stray Light Parameters .....B-2

Table B-2: Radiance errors derived from the stray light model and flight data.....B-5

Table B-3: Ghost generation model predictions.....B-17

Table E-1: ALI edge slopes, duty cycle = 91.53% case.....E-1

Table E-2: ALI edge slopes, duty cycle = 50% case.....E-2

## Introduction

The performance requirements for the Advanced Land Imager were developed under NASA's New Millennium Program and were intended to facilitate the validation of new sensor technologies and architectures for potential application in future remote sensing missions. The Advanced Land Imager (ALI) was designed and flown well before the Landsat Data Continuity Mission (LDCM) specifications were developed. Nevertheless, the science focus of the ALI technology validation was Landsat data continuity. Therefore, although exact compliance by ALI is not expected, the performance should demonstrate a path to a compliant sensor system.

The performance of the ALI, as determined from preflight and flight data, is compared to the LDCM specification. Twenty-one noncompliances have been identified: four data collection, four spectral, six spatial, and seven radiometric (Table 1). All but six of these are considered minor. The six major noncompliances are the result of stray light, leaky detectors, and contamination. Appendix A replicates the LDCM specification and contains ALI compliance notes where appropriate. Details of the ALI stray light, contamination, and leaky detectors are provided in Appendix B, C, and D respectively. Additional information pertaining to the calculation of the ALI edge response and coherent noise is presented in Appendix E and F. A list of ALI related publications is provided in Appendix G.

Table 1: ALI/LDCM Noncompliance

Parameter	LDCM Specification Number	Noncompliance Classification
Data Collection	3.1.1.1	Minor
	3.1.2	Minor
	3.1.3	Minor
	3.2.1	Minor
Spectral	4.1.a	Minor
	4.2.1.1.1	Minor
	4.3	Unknown
	4.4	Unknown
Spatial	5.3.1	Minor
	5.3.4	Minor
	5.4.1	Minor
	5.4.2	Unknown
	5.5.1	<b>Major</b>
	5.5.2	<b>Major</b>
Radiometric	6.1	<b>Major</b>
	6.2.3	Minor
	6.2.4	Minor
	6.3	Minor
	6.5	<b>Major</b>
	6.6.1	<b>Major</b>
	6.6.2	<b>Major</b>

## **Noncompliance of ALI to LDCM Specification**

ALI noncompliances to the LDCM specification are listed. Instances labeled 'minor' are considered to be technically 'out-of-spec' but should be easily achievable in an LDCM instrument. Instances labeled 'major' are considered important noncompliances and would significantly impact the LDCM if not properly addressed.

### *Data Collection*

Four noncompliances were found in reference to the ALI data collection capability.

#### **3.1.1.1 Daily LDCM Global Archive Coverage**

**Specification:** The unprocessed LDCM digital image data captured into the LDCM active and long term archive(s) shall provide an average daily coverage of at least 250 full WRS-2 (see 2.4.1) land scenes per any 90 day period. WRS-2 land scenes are defined in the WRS Land Database, Revision 2.1, to include continental regions, coastal areas, islands, ice caps, and reefs.

**Implications:** Minor

**Comment:** The ALI thermal control system is 'frozen' during periods when the focal plane is powered. This mode of operation was adopted after it was discovered that when the focal plane is powered, noise is fed back into the thermal control circuitry and the logical thermal control is lost. Although burdensome, adequate thermal stability of the instrument is achieved during normal ALI data collection sequences (1-120 seconds). If continuous data collection were required over long periods (>120 seconds), the original thermal control system, if properly configured, would provide the stability needed.

#### **3.1.2 Minimum Cross-Track Extent**

**Specification:** The unprocessed LDCM digital image data stored in the LDCM archive shall have a minimum cross-track extent of 185 km.

**Implications:** Minor

**Comment:** Technology demonstration with three degree field of view. However, design would meet specification if focal plane fully populated.

#### **3.1.3 WRS-2 Orientation**

**Specification:** The unprocessed LDCM digital image data shall be acquired in accordance with the Worldwide Reference System 2 (WRS-2) grid, such that the swath center of the unprocessed LDCM digital image data shall be within 5 km of the center of the corresponding WRS-2 path.

**Implications:** Minor

# FINAL DRAFT

Created on 4/16/2002 9:07 PM

**Comment:** Three degree field of view positioned on outer edge of WRS-2 path. However, design would meet specification if focal plane fully populated.

### 3.2.1 United States Coverage

**Specification:** Archived LDCM data shall provide coverage of the fifty United States and the District of Columbia and their coastal areas at least once every 16 days or less, regardless of cloud cover, subject to the solar zenith requirement 3.3.1.1.

**Implications:** Minor

**Comment:** Technology demonstration with three degree field of view. However, design would meet specification if focal plane fully populated.

### *Spectral Bands*

Five non-compliances were found in reference to the ALI spectral bands. Figure 1 and Table 2 are provided for reference.

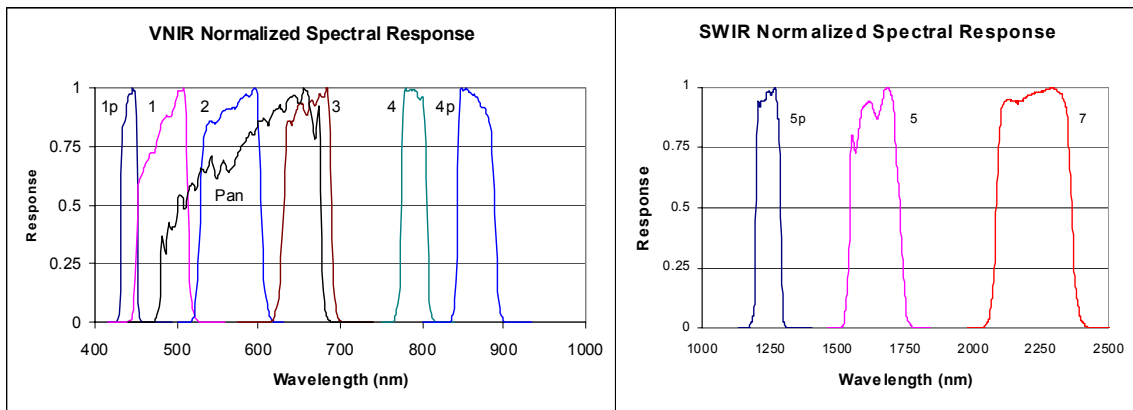


*Figure 1: Spectral response curves of the Advanced Land Imager.*

Table 2: Spectral response summary for the Advanced Land Imager.

ALI Bands	1p	1	2	PAN	3	4	4p	5p	5	7
Wavelength ( nm )	442	485	567	592	660	790	866	1244	1640	2226
Bandwidth ( nm )	19	53	70	144	56	31	44	88	171	272

## 4.1 Spectral Band Widths

### 4.1.a

**Specification:** The full-width-half-maximum (FWHM) points of the relative spectral radiance response curve for each spectral band shall fall within the range of the minimum 50% lower band edge and the maximum 50% upper band edge as listed in Table 4.1-1.

**Implications:** Minor

**Comment:**

Green Band Maximum Upper Band Edge	(spec = 600 nm, ALI = 605 nm)
Red Band Maximum Upper Band Edge	(spec = 680 nm, ALI = 690 nm)
NIR Band Minimum Lower Band Edge	(spec = 845nm, ALI = 842 nm)
NIR Band Maximum Upper Band Edge	(spec = 885 nm, ALI = 890 nm)
SWIR 1 Band Minimum Lower Band Edge	(spec = 1560 nm, ALI = 1545 nm)
SWIR 1 Band Maximum Upper Band Edge	(spec = 1660 nm, ALI = 1730 nm)
SWIR 2 Band Minimum Lower Band Edge	(spec = 2100 nm, ALI = 2080 nm)
SWIR 2 Band Maximum Upper Band Edge	(spec = 2300 nm, ALI = 2360 nm)

### 4.2.1.1.1 Average Response

**Specification:** The average response shall be greater than 0.8.

**Implications:** Minor

**Comment:** Average ALI pan band response is 0.7-0.75.

## 4.3 Spectral Uniformity

**Specification:** The bandwidth shall vary by no more than  $\pm 3\%$  across pixels within a band. Additionally see Section 6.2.3.

**Implications:**

**Comment:** Unknown, only checked SCA 3 and witness sample checks by Barr. The results for SCA 3 complied with the specification.

## 4.4 Spectral Stability

**Specification:** Band center wavelengths and band edges shall not change by more  $\pm 2$  nm over the expected life of the mission.

**Implications:**

**Comment:** Not checked.

### *Spatial Resolution*

The ALI spatial response does not comply with the LDCM specification in six areas.

#### **5.3.1 Standard Band Edge Response Slope**

**Specification:** The mean relative edge response slope for LDCM spectral bands 2, 3, 4, 5, 6, and 7 (<30 m GSD) shall exceed 0.027/meter for Level 1R digital image data across the entire Field-of-View.

**Implications:** Minor

**Comment:** All VNIR MS bands (1', 1, 2, 3, 4, and 4') satisfy this specification at the nominal integration time of 4.05 ms (duty cycle = 91.5%). SWIR bands (5', 5, and 7) meet the specification if duty cycle is reduced to 50%. The most stressing case is band 7 (2200 nm), for nominal duty cycle, and edges perpendicular to the ground track. The above statements hold true for all angles of the edge with respect to the ground track. These results are described in Appendix E.

#### **5.3.4 Edge Response Uniformity**

**Specification:** The mean relative edge response slope shall not vary by more than 10% in any band across the Field-of-View and by not more than 20% between LDCM spectral bands 2,3,4,5,6,and 7 for Level 1R digital image data.

**Implications:** Minor

**Comment:** ALI: Band-to-band variations = -8% to +3% from overall mean for MS bands, OK. Edge slopes across FOV not computed. Laboratory measurements do show variations of in-track MTF from SCA to SCA, possibly leading to ±10% variations of edge slope. Partially populated FPA makes full comparison difficult.

#### **5.4.1 Level 1R Product Aliasing**

**Specification:** The product of the mean relative edge response slope and the GSD shall be less than 1.0 for Level 1R digital image data for both the in-track and cross track directions.

**Implications:** Minor

**Comment:** OK for all bands, for nominal duty cycle. At 50% duty, for edges at 45°, the product is slightly greater than 1, for bands 1, 2, 3, 4, and 4'. This is described in more detail in Appendix E.

#### **5.4.2 Level 1G Product Aliasing**

**Specification:** The product of the mean relative edge response slope in a Level 1G digital image data, resampled using the cubic convolution method, and the maximum GSD specified in Table 5.3-1 shall be less than 1.0 for both the in-track and cross track directions.

**Implications:** Minor

**Comment:** Not computed. Given the smoothness of the ALI edge response functions, no suspected reason why the re-sampled data would not also meet this specification.

### 5.5 Stray Light Rejection and Internal Light Scattering

**Implications:** Major

**Comment:** ALI has significant stray light. A summary description of the ALI stray light analysis performed to date and the impact stray light has on flight data is provided in Appendix B.

#### 5.5.1 Point Source Transmittance (PST)

**Specification:** For any detector in the sensor and for all bands, the normalized point source transmittance (PST) (peak point source response normalized to unity) shall be less than the values given in Table 5.5-1 for the corresponding off-field angles over the entire field-of-view of the system.

**Implications:** Major

**Comment:** ALI PST is an order of magnitude too large. Table 3 and Figure 2 are provided for reference.

Table 3: LDCM PST Specification

Off-axis Field Angles	PST for all Bands
$.30 < Q < 1^\circ$	$<10^{-2}$
$1^\circ < Q < 3^\circ$	$<10^{-3}$
$3^\circ < Q < 10^\circ$	$<10^{-4}$
$10^\circ < Q < 20^\circ$	$<10^{-5}$
$20^\circ < Q < 25^\circ$	$<10^{-6}$

EO1 Point Source Transmittance  
TracePro ray-trace simulation

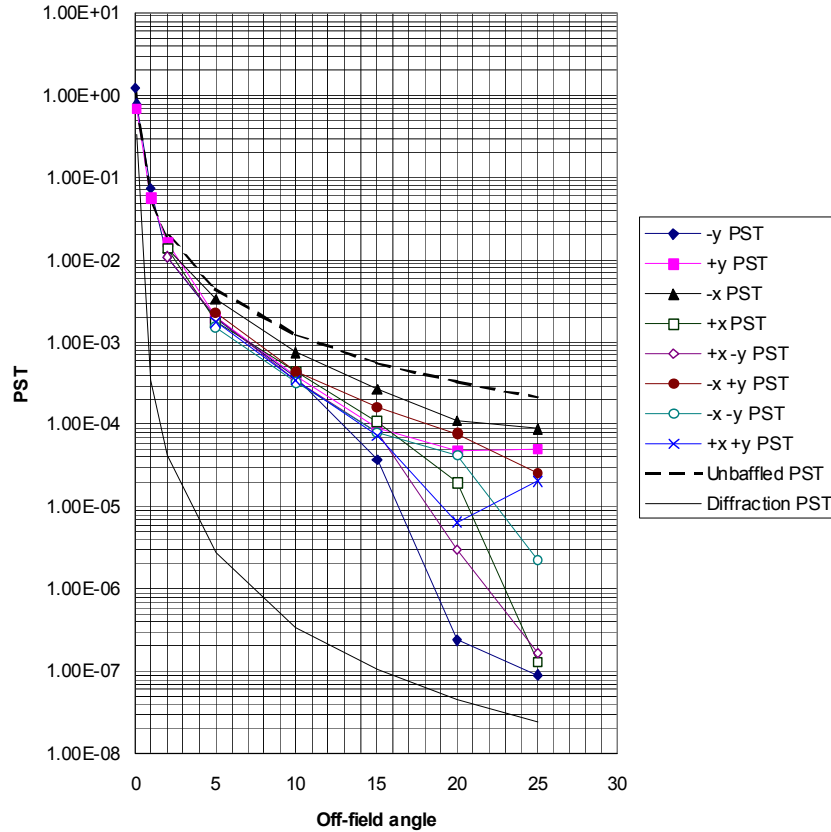


Figure 2: ALI point source transmittance  $Y = \text{pitch direction}$ ,  $X = \text{roll direction}$ ..

### 5.5.2. Total Integrated Optical Scatter (TIS)

**Specification:** The total integrated scatter for 1 degree or greater for a point target imaged onto a detector in any band shall be less than 1%.

**Implications:** *Major*

**Comment:** ALI TIS exceeds 1% for 5 out of 7 bands. Worst case is by a factor of 16 for the Blue Band. Table 4 is provided for reference.

# FINAL DRAFT

Created on 4/16/2002 9:07 PM

Table 4: ALI total integrated scatter.

Band	Total Integrated Scatter (%)
1	15.5
2	10.9
3	7.6
4	4.4
5	0.9
7	0.5
Pan	3.5

## Radiometry

The ALI does not meet the LDCM specification in seven areas.

### 6.1 Absolute Radiometric Accuracy

**Specification:** The digital values in a Level 1 data product shall be linearly scaled to at-aperture spectral radiance with an uncertainty less than or equal to 5% (1 sigma) **with a goal of 3%** (1 sigma) across the range of 0.3  $L_{\text{typical}}$  to 0.9  $L_{\text{max}}$  (Table 6.1-1) with all accuracies established relative to National Institute for Standards and Technology (NIST) standards.

**Implications:** *Major*

**Comment:** This spec is not met for ALI for some targets due to stray light (e.g. dark targets in bright background). See Appendix B.

### 6.2.3 Pixel-to-Pixel Uniformity

**Specification:** For a uniform source above  $2 * L_{\text{typical}}$  the standard deviation of the calibrated values across pixels within a line of Level 1R digital image data within a band shall not exceed 0.25% of the average radiance for bands 2-7 and 0.5% of the average radiance for band 8. Temporal noise may be averaged to verify compliance with this specification.

**Note:** This requirement applies for target radiances with spectral characteristics as follows: the spectral radiance of the source used in pre-launch calibration, spectral radiance from bare soil as observed through a dry atmosphere, spectral radiance proportional to the exoatmospheric solar irradiance, and spectral radiance from a dense vegetation target as observed through a moist atmosphere (See Figure 6.2.3-1 and Top of Atmosphere Radiance Values , MODTRAN 4 Model table values, Reference d).

**Implications:** Minor

**Comment:** OK for prelaunch calibration and solar but not verified for all other spectra.

#### 6.2.4 Coherent Noise

**Specification:** The magnitude of the autocorrelation of a dark (zero-radiance) scene, computed after subtraction of detector-by-detector direct current offset, and normalized to 1.0 at zero lag, shall not exceed 0.25 at any non-zero spatial lag.

**Implications:** Minor

**Comment:** The maximum values of the autocorrelations computed are spread over a range from 0.08 to 0.60, when all bands and all SCAs are considered. There are clear differences between the SCAs, with SCA 3 having the highest autocorrelations (~0.35 to ~0.60), and SCA 4 having the lowest range (~0.08 to ~0.30). No secular trends are apparent in the autocorrelations, though there are considerable variations from DCE to DCE. These results are described in more detail in Appendix F.

#### 6.3 Dynamic Range

**Specification:** The LDCM Level 0 and Level 1 digital image data shall cover, without saturating, signals up to the L max as shown in Table 6.2.1-1. Note: For bands 2- 8, this corresponds to the radiance reflected off of a Lambertian target of 100% reflectance illuminated by the sun at a solar zenith angle of 20°.

**Implications:** Minor

**Comment:** Red Band spec = 470 W/m<sup>2</sup>/sr/u, ALI = 450 W/m<sup>2</sup>/sr/u  
NIR Band spec = 285 W/m<sup>2</sup>/sr/u, ALI = 240 W/m<sup>2</sup>/sr/u  
SWIR 2 Band spec = 24.7 W/m<sup>2</sup>/sr/u, ALI = 22 W/m<sup>2</sup>/sr/u

#### 6.5 Radiometric Stability

**Specification:** The LDCM Level 1 digital image data for radiometrically constant targets with radiances greater than or equal to L<sub>typical</sub> shall not differ by more than ± 1 % over any time up to 16 days nor by more than ± 2 % in any period between 16 days and five years.

**Implications:** Major

**Comment:** ALI contamination and stray light violate this. In principal, the contamination could be accounted for, but not stray light to the 1% level. See Appendix C for a description of the ALI contamination.

#### 6.6.1 Bright Target Recovery

**Specification:** The unprocessed data in the archive shall be such that the recovery region around an image pixel which has been exposed to a radiance level of less than or equal to 1.5 times that of the source sensor's saturation level shall be contained within a 7 x 7 pixel region centered on the exposed pixel.

**Implications:** Major

## FINAL DRAFT

Created on 4/16/2002 9:07 PM

**Comment:** Apparent reflections at the 1% level have been observed in the SWIR bands for lava flows. Also, a 1% in-track 'halo' has been observed during lunar observations. See Appendix B.

### 6.6.2 Pixel-to-Pixel Crosstalk

**Specification:** The crosstalk-induced artifacts in neighboring pixels caused by a region of pixels having a radiance level of less than the saturation level and which is more than ten pixels away, shall not exceed 1% after radiometric correction.

**Implications:** *Major*

**Comment:** The ALI has two detectors with significant cross-talk. An algorithm has been developed to account for 'leaky detector' effects to the 1-2% level for most instances. However, in some scenes with 80% clouds you will see substantial LD effects in regions where there are holes in the clouds. See Appendix D for a description of the leaky detector effects.

Optional Reflective Band Note: No additional noncompliances, outside of those listed above, were found when considering the LDCM optional reflective band.

## **FINAL DRAFT**

Created on 4/16/2002 9:07 PM

### **Summary**

The performance of the Advanced Land Imager has been compared the Landsat Data Continuity Mission specification. Twenty-one noncompliances have been identified. All but six of these are considered minor. The major noncompliances are the result of stray light, contamination, and leaky detectors. These issues are discussed in detail in Appendix B, C, and D respectively. However, none of the identified noncompliances are the result of an inherent flaw in the design of the instrument. Stray light may be avoided on future missions by improving the mirror finishes. Improved baffling of the interior of the telescope, particularly behind the secondary mirror, will greatly reduce the stray light effects of the black paint. Careful assembly of the filters should reduce filter boundary scattering. Thorough screening of SCAs prior to focal plane population will eliminate leaky detectors. Finally, careful selection and bakeout of materials and paints used within the telescope will help prevent contamination of the filter surfaces.

**FINAL DRAFT**  
Created on 4/16/2002 9:07 PM

## Appendix A: LDCM Specification Compliance Matrix

Verification Method Legend: D = Demonstration, I = Inspection, A = Analysis, T = Test, YES = ALI satisfied specification, NA = not applicable to ALI, NO = ALI did not satisfy specification, ?? = unknown if ALI satisfied specification.

Requirement Number	Requirement	Pre-Launch Verification Method	Post-Launch Verification Method	ALI Compliance Notes
2.0	<b>LDCM Data and Data Products</b> (overview)			
2.1	<b>Archived LDCM Data</b> The LDCM shall archive unprocessed LDCM digital image data, metadata, browse images, and associated ancillary data.	D	D	NA
2.1.a	The unprocessed LDCM digital image data and ancillary data shall include all information necessary to generate the LDCM data products specified in Section 2.2.	A	D	NA
2.1.b	The unprocessed LDCM digital image data and ancillary data shall be of a quality and quantity necessary to ensure that the LDCM data products meet the data specifications found in Sections 3, 4, 5, 6, and 7.	—	—	NA
2.1.c	The archived LDCM digital image data shall afford at a minimum the geographic coverage and temporal resolution specified in Section 3.	—	—	NA
2.1.1	<b>Unprocessed LDCM Digital Image Data</b> [definition - Unprocessed LDCM digital image data are those digital image data directly generated by the LDCM sensor(s) and transmitted from the LDCM satellite(s). The numerical value of the digital image data from sensor to archive shall be preserved.]			
2.1.1.1	<b>Unprocessed LDCM Digital Image Data Lossless Compression</b> Unprocessed LDCM digital image data, after any compression and decompression, shall be identical to the data prior to compression.	I	—	NA
2.1.1.2	<b>Unprocessed LDCM Digital Image Data Quality</b> (header only)			

**FINAL DRAFT**  
Created on 4/16/2002 9:07 PM

<b>2.1.1.2.1</b>	<b>Dead or Inoperable Detectors</b> Less than 0.1% of the unprocessed LDCM digital image data archived daily shall be produced by dead or inoperable detectors.	T	T	<b>YES</b>
<b>2.1.1.2.2</b>	<b>Transmission Errors</b> The bit error rate resulting from the transmission (from observatory to archive) of unprocessed LDCM digital image data shall be no greater than 1 bit in $10^8$ bits.	A	—	<b>NA</b>
<b>2.1.1.2.3</b>	<b>Archive Errors</b> The LDCM ground data processing and archival shall introduce no more than one bit error in $10^{12}$ bits processed and archived.	A	—	<b>NA</b>
<b>2.1.2</b>	<b>Ancillary Data</b> The LDCM shall archive ancillary data associated with the archived unprocessed LDCM digital image data. The ancillary data shall consist of:	—	—	<b>NA</b>
<b>2.1.2.a</b>	satellite and sensor housekeeping data required to generate the specified data products	A	D	<b>NA</b>
<b>2.1.2.b</b>	calibration data required to generate the specified data products.	A	D	<b>NA</b>
<b>2.1.2.c</b>	any other supplementary data required to generate the specified data products.	A	D	<b>NA</b>
<b>2.1.2.1</b>	<b>Sensor and Satellite Housekeeping Data</b> The archived housekeeping data shall:	—	—	<b>NA</b>
<b>2.1.2.1.a</b>	quantify the state of the LDCM sensor and satellite systems during acquisition of the unprocessed LDCM digital image data	A	T	<b>NA</b>
<b>2.1.2.1.b</b>	at a minimum provide the sensor/satellite state information required to generate the specified LDCM data products	A	D	<b>NA</b>
<b>2.1.2.1.c</b>	at a minimum provide the sensor/satellite state information required to verify the performance of the LDCM sensor(s) and satellite(s)	A	D	<b>NA</b>
<b>2.1.2.1.d</b>	either be in metric engineering units or the archive shall provide the conversion factors required to convert the housekeeping data to metric engineering units.	A	D	<b>NA</b>

**FINAL DRAFT**  
Created on 4/16/2002 9:07 PM

2.1.2.2	<b>Pre-Launch Characterization and Calibration Data</b> The LDCM shall archive all pre-launch test data acquired for the purpose of characterizing and calibrating the performance of the LDCM sensor(s), including the radiometric response and the image geometry.		D	NA
2.1.2.3	<b>On-Orbit Characterization and Calibration Data</b> (header only)			
2.1.2.3.a	The LDCM shall archive all data acquired in orbit for the purpose of characterizing and calibrating the performance of the LDCM sensor(s), including those data acquired to characterize and calibrate radiometric response and image geometry.		D	NA
2.1.2.3.b	The calibration data shall include, but not be limited to, data acquired while viewing radiometric reference sources or geometric targets.		D	NA
2.1.2.3.c	The archived calibration data shall also include all of the derived calibration coefficients required to generate the specified LDCM data products including radiometric gains and biases and detector, sensor, and satellite alignment parameters.		D	NA
2.1.2.4	<b>Supplementary Data</b> The LDCM shall archive all of the supplementary data required to generate the data products described in Section 2.2.	A	D	NA
2.1.3	<b>Metadata</b> (header only)			
2.1.3.a	The LDCM shall archive metadata for each granule of archived, unprocessed LDCM digital image data.	D	D	NA
2.1.3.b	The metadata shall adhere to the Federal Geographic Data Committee (FGDC) standards for metadata.	D		NA
2.1.3.c	The metadata shall include but not be limited to:	—	—	NA
2.1.3.c.1	The WRS-2 path and row for each WRS-2 scene within an archived digital image granule	D		NA
2.1.3.c.2	The acquisition date for the archived digital image data granule	D		NA

**FINAL DRAFT**  
Created on 4/16/2002 9:07 PM

<b>2.1.3.c.3</b>	The acquisition start time and end time for the archived digital image granule and the acquisition start time and end time for each of the WRS-2 scenes within the granule	<b>D</b>		<b>NA</b>
<b>2.1.3.c.4</b>	Solar azimuth and zenith angles (in degrees, accurate to 3 decimal places) at the center of each WRS-2 scene within an archived digital image granule at the date and time of data acquisition		<b>D</b>	<b>NA</b>
<b>2.1.3.c.5</b>	Identification of the satellite and sensor that acquired the digital image data	<b>D</b>		<b>NA</b>
<b>2.1.3.c.6</b>	Identification of the ground station that initially received the digital image data granule	<b>D</b>		<b>NA</b>
<b>2.1.3.c.7</b>	Identification of the data's path to the LDCM archive		<b>D</b>	<b>NA</b>
<b>2.1.3.c.8</b>	The spectral bands provided by the digital image data	<b>D</b>		<b>NA</b>
<b>2.1.3.c.9</b>	The geographic location of the corner points of the archived digital image data granule with an uncertainty of less than or equal to 250 meters (90% circular error), excluding terrain effects		<b>A</b>	<b>NA</b>
<b>2.1.3.c.10</b>	The geographic location of the corner points of each WRS-2 scene within an archived digital image data granule with an uncertainty of less than or equal to 250 meters (90% circular error), excluding terrain effects		<b>A</b>	<b>NA</b>
<b>2.1.3.c.11</b>	The geographic location of the center of each WRS-2 scene within an archived digital image data granule with an uncertainty of less than or equal to 250 meters (90% circular error), excluding terrain effects		<b>A</b>	<b>NA</b>
<b>2.1.3.c.12</b>	The percentage cloud cover for each WRS-2 scene within an archived digital image data granule with an uncertainty of plus or minus 10%, 95% of the time		<b>A</b>	<b>NA</b>
<b>2.1.3.c.13</b>	The percentage cloud cover for each of the four quadrants of each WRS-2 scene within a digital image data granule with an uncertainty of plus or minus 10%, 95% of the time		<b>A</b>	<b>NA</b>
<b>2.1.3.c.14</b>	Data quality metrics for each WRS-2 scene within a digital image data granule	<b>A</b>	<b>D</b>	<b>NA</b>

**FINAL DRAFT**  
Created on 4/16/2002 9:07 PM

2.1.3.c.15	Locations of corrupted or invalid data within the digital image data granule	A	D	NA
2.1.3.c.16	Descriptions or characterizations of the corrupted or invalid data	A	D	NA
2.1.3.c.17	The sensor settings for variable sensor states at the time of data acquisition	D	D	NA
2.1.3.c.18	The date of data archival	D	D	NA
2.1.3.c.19	Identification of the facility, computer system, and software versions used to process and archive the digital image data.	D	D	NA
2.1.4	The LDCM shall generate and archive browse images for the archived, unprocessed LDCM digital image data.	T	D	NA
2.1.4.a	Browse Images shall be generated for each WRS-2 scene contained within the archived digital image data.		D	NA
2.1.4.b	The browse images shall provide a spatial resolution no coarser than 240 m.		T	NA
2.1.4.c	The browse images shall be composites of at least three bands that enable differentiation of clouds from land with at least 8 bits per display channel.		A	NA
2.2	<b>LDCM Data Products</b> For any of the data in the LDCM Active Archive, except where noted, the LDCM shall produce and distribute the following LDCM data products in accordance with the LDCM Data Policy, Attachment D to the LDCM RFP.	D		NA
2.2.1	<b>Level 0 LDCM Data Products</b> Level 0 LDCM Data Products shall consist of Level 0 Digital Image Data, Level 0 Ancillary Data, and Level 0 Metadata.	A	D	NA
2.2.1.a	The Level 0 LDCM Data Product shall provide all of the data required to produce the data products specified in Sections 2.2.2 and 2.2.3.	A	D	NA
2.2.1.b	The LDCM shall produce and distribute Level 0 LDCM Data Products for the data granules specified in Section 2.4 and in the formats specified in Section 2.5.	D	D	NA

**FINAL DRAFT**  
Created on 4/16/2002 9:07 PM

2.2.1.c	The LDCM shall produce Level 0 LDCM Data Products for any of the unprocessed LDCM digital image data in the LDCM Active Archive.	D	D	NA
2.2.1.1	<b>LDCM Level 0 Digital Image Data</b> Level 0 Digital Image Data shall consist of unprocessed LDCM digital image data produced in the			NA
2.2.1.1.a	data granules specified in Section 2.4	D	D	NA
2.2.1.1.b	formats specified in Section 2.5	D	D	NA
2.2.1.2	<b>LDCM Level 0 Ancillary Data</b> (header only)			
2.2.1.2.a	Level 0 Ancillary Data shall provide all of the ancillary data required to generate the products specified in Sections 2.2.2 and 2.2.3.	A	D	NA
2.2.1.2.b	The Level 0 Ancillary Data shall include, but not be limited to, the calibration coefficients and housekeeping data required to create Level 1 products, in metric engineering units.	A	D	NA
2.2.1.3	<b>LDCM Level 0 Metadata</b> (header only)			
2.2.1.3.a	Level 0 Metadata shall describe the associated Level 0 Digital Image Data and Level 0 Ancillary Data.	A		NA
2.2.1.3.b	Level 0 Metadata shall adhere to the Federal Geographic Data Committee (FGDC) standards for metadata.	D		NA
2.2.1.3.c	Level 0 Metadata shall include, but not be limited to:			NA
2.2.1.3.c.1	The WRS-2 path and row for each WRS-2 scene within a data product	D		NA
2.2.1.3.c.2	The acquisition date for the data product	D		NA
2.2.1.3.c.3	The acquisition start time and end time for the data product and the acquisition start time and end time for each of the WRS-2 scenes within the data product	D		NA

**FINAL DRAFT**  
Created on 4/16/2002 9:07 PM

<b>2.2.1.3.c.4</b>	Solar azimuth and zenith angles (in degrees, accurate to 3 decimal places) at the center of each WRS-2 scene within the data product at the date and time of data acquisition		<b>D</b>	<b>NA</b>
<b>2.2.1.3.c.5</b>	Identification of the satellite and sensor that acquired the digital image data	<b>D</b>		<b>NA</b>
<b>2.2.1.3.c.6</b>	Identification of the ground station that initially received the digital image data	<b>D</b>		<b>NA</b>
<b>2.2.1.3.c.7</b>	Identification of the data's path to the LDCM archive		<b>D</b>	<b>NA</b>
<b>2.2.1.3.c.8</b>	The spectral bands provided by the digital image data	<b>D</b>		<b>NA</b>
<b>2.2.1.3.c.9</b>	The geographic location of the corner points of the data product with an uncertainty of less than or equal to 250 meters (90% circular error), excluding terrain effects		<b>A</b>	<b>NA</b>
<b>2.2.1.3.c.10</b>	The geographic location of the corner points of each WRS-2 scene within the data product with an uncertainty of less than or equal to 250 meters (90% circular error), excluding terrain effects		<b>A</b>	<b>NA</b>
<b>2.2.1.3.c.11</b>	The geographic location of the center of each WRS-2 scene within the data product with an uncertainty of less than or equal to 250 meters (90% circular error), excluding terrain effects		<b>A</b>	<b>NA</b>
<b>2.2.1.3.c.12</b>	The percentage cloud cover for each WRS-2 scene the data product with an uncertainty of plus or minus 10%, 95% of the time		<b>A</b>	<b>NA</b>
<b>2.2.1.3.c.13</b>	The percentage cloud cover for each of the four quadrants of each WRS-2 scene within the data product with an uncertainty of plus or minus 10%, 95% of the time		<b>A</b>	<b>NA</b>
<b>2.2.1.3.c.14</b>	Data quality metrics for each WRS-2 scene within the data product	<b>A</b>	<b>D</b>	<b>NA</b>
<b>2.2.1.3.c.15</b>	Locations of corrupted or invalid data within the data product	<b>A</b>	<b>D</b>	<b>NA</b>
<b>2.2.1.3.c.16</b>	Descriptions or characterizations of the corrupted or invalid data	<b>A</b>	<b>D</b>	<b>NA</b>
<b>2.2.1.3.c.17</b>	The sensor settings for variable sensor states at the time of data acquisition	<b>D</b>	<b>D</b>	<b>NA</b>

**FINAL DRAFT**  
Created on 4/16/2002 9:07 PM

2.2.1.3.c.18	The date of data archival	D	D	NA
2.2.1.3.c.19	Identification of the facility, computer system, software, and software versions that generated the data product	D	D	NA
2.2.1.3.c.20	Date of product generation.		D	NA
2.2.2	<b>Level 1R LDCM Data Products</b> Level 1R LDCM Data Products shall consist of Level 1R Digital Image Data, Level 1R Ancillary Data, and Level 1R Metadata.	D		NA
2.2.2.a	The LDCM shall produce and distribute Level 1R LDCM Data Products for the data granules specified in Section 2.4 and in the formats specified in Section 2.5.	D		NA
2.2.2.b	The LDCM shall produce Level 1R LDCM Data Products for any of the unprocessed LDCM digital image data in the LDCM archive.	D		NA
2.2.2.1	<b>Level 1R Digital Image Data</b> (header only)			
2.2.2.1.a	Level 1R Digital Image Data shall provide radiometrically corrected digital image data consisting of digital values linearly scaled to at-aperture spectral radiance.	T		NA
2.2.2.1.b	The linear scale shall be constant for all the data from a particular spectral band	T		NA
2.2.2.2	<b>Level 1R Ancillary Data</b> The Level 1R Ancillary Data shall be identical in content to the Level 0 Ancillary Data for the corresponding Level 0 data product.	D		NA
2.2.2.3	<b>Level 1R Metadata</b> (header only)			
2.2.2.3.a	Level 1R Metadata shall describe the associated Level 1R Digital Image Data and Level 1R Ancillary Data.	D		NA
2.2.2.3.b	Level 1R Metadata shall adhere to the Federal Geographic Data Committee (FGDC) standards for metadata.	D		NA
2.2.2.3.c	Level 1R Metadata shall include, but not be limited to:			NA

**FINAL DRAFT**  
Created on 4/16/2002 9:07 PM

2.2.2.3.c.1	all of the items listed in Section 2.2.1.3	D		NA
2.2.2.3.c.2	The version of the calibration coefficients used to generate the Level 1R Digital Image Data	D		NA
2.2.2.3.c.3	The radiometric coefficients required to convert the digital values of the Level 1R digital image data to units of spectral radiance with the accuracy specified in Section 6.1.	T		NA
2.2.3	<b>Level 1Gs LDCM Data Products</b> Level 1Gs LDCM Data Products shall consist of Level 1Gs Digital Image Data and Level 1Gs Metadata.	D		NA
2.2.3.a	The LDCM shall produce and distribute Level 1Gs LDCM Data Products for the data granules specified in Section 2.4 and in the formats specified in Section 2.5.	D		NA
2.2.3.b	The LDCM shall produce Level 1Gs LDCM Data Products for any of the unprocessed LDCM digital image data in the LDCM archive.	D		NA
2.2.3.1	<b>Level 1Gs Digital Image Data</b> (header only)			
2.2.3.1.a	Level 1Gs Digital Image Data shall consist of radiometrically corrected digital image data resampled for registration to selectable cartographic projections, as specified in Section 2.3, referenced to the World Geodetic System 1984 (WGS84), G873 or current version.	T		NA
2.2.3.1.b	Image resampling shall be performed using selectable resampling methods, as specified in Section 2.3.2.	T		NA
2.2.3.1.c	The pixels of the Level 1Gs Digital Image Data shall be registered to the geodetic accuracy specified in Section 7.3.	A, T		NA
2.2.3.1.d	The digital values shall be linearly scaled to at-aperture spectral radiance.	T		NA
2.2.3.2	<b>Level 1Gs Metadata</b> Level 1Gs Metadata shall describe the associated Level 1Gs Digital Image Data.	D		NA
2.2.3.2.a	Level 1Gs Metadata shall adhere to the Federal Geographic Data Committee (FGDC) standards for metadata.	D		NA

**FINAL DRAFT**  
Created on 4/16/2002 9:07 PM

2.2.3.2.b	Level 1Gs Metadata shall include, but not be limited to:	D		NA
2.2.3.2.b.1	all of the items listed in Section 2.2.1.3	D		NA
2.2.3.2.b.2	The version of the calibration coefficients used to generate the Level 1Gs Digital Image Data	D		NA
2.2.3.2.b.3	The radiometric coefficients required to convert the digital values of the Level 1Gs digital image data to units of spectral radiance with the accuracy specified in Section 6.1	T		NA
2.2.3.2.b.4	The cartographic projection	D		NA
2.2.3.2.b.5	The cartographic projection parameters	D		NA
2.2.3.2.b.6	The current version of the WGS84 ordinate reference frame	D		NA
2.2.3.2.b.7	Identification of any supplementary data used to generate the Level 1Gs Digital Image Data	D		NA
2.2.3.2.b.8	Product corner points with the accuracy specified in Section 7.3		T	NA
2.2.3.2.b.9	User-selected processing parameters for the data products ordered.	D		NA
2.2.4	<b>Level 1Gp LDCM Data Products</b> Level 1Gp LDCM Data Products shall consist of Level 1Gp Digital Image Data and Level 1Gp Metadata.	D		NA
2.2.4.a	The LDCM shall produce and distribute Level 1Gp LDCM Data Products for the data granules specified in Section 2.4 and in the formats specified in Section 2.5.	D		NA
2.2.4.b	The LDCM shall produce Level 1Gp LDCM Data Products for any of the daylight, archived, unprocessed LDCM digital image data acquired over the fifty United States and the District of Columbia.	D		NA
2.2.4.c	<i>The LDCM will have the goal of producing Level 1Gp LDCM Data Products for any of the daylight, land LDCM digital image data in the LDCM archive.</i>	D		NA

**FINAL DRAFT**  
Created on 4/16/2002 9:07 PM

<b>2.2.4.1</b>	<b>Level 1Gp Digital Image Data</b> (header only)			
<b>2.2.4.1.a</b>	Level 1Gp Digital Image Data shall consist of radiometrically corrected digital image data resampled for registration to selectable cartographic projections, as specified in Section 2.3, referenced to the World Geodetic System 1984 (WGS84), G873 or current version.	<b>D</b>		<b>NA</b>
<b>2.2.4.1.b</b>	Image resampling shall be performed using selectable resampling methods, as specified in Section 2.3.2.	<b>D</b>		<b>NA</b>
<b>2.2.4.1.c</b>	The pixels of the Level 1Gp Digital Image Data shall be registered to the geodetic accuracy specified in Section 7.4.	<b>A, T</b>		<b>NA</b>
<b>2.2.4.1.d</b>	The digital values shall be linearly scaled to at-aperture spectral radiance.	<b>T</b>		<b>NA</b>
<b>2.2.4.2</b>	<b>Level 1Gp Metadata</b> Level 1Gp Metadata shall describe the associated Level 1Gp Digital Image Data.	<b>D</b>		<b>NA</b>
<b>2.2.4.2.a</b>	Level 1Gp Metadata shall adhere to the Federal Geographic Data Committee (FGDC) standards for metadata.	<b>D</b>		<b>NA</b>
<b>2.2.4.2.b</b>	Level 1Gp Metadata shall include, but not be limited to:	<b>D</b>		<b>NA</b>
<b>2.2.4.2.b.1</b>	all of the items listed in Section 2.2.1.3.	<b>D</b>		<b>NA</b>
<b>2.2.4.2.b.2</b>	The version of the calibration coefficients used to generate the Level 1Gp Digital Image Data	<b>D</b>		<b>NA</b>
<b>2.2.4.2.b.3</b>	The radiometric coefficients required to convert the digital values of the Level 1Gp digital image data to units of spectral radiance with the accuracy specified in section 6.1	<b>T</b>		<b>NA</b>
<b>2.2.4.2.b.4</b>	The cartographic projection	<b>D</b>		<b>NA</b>
<b>2.2.4.2.b.5</b>	The cartographic projection parameters	<b>D</b>		<b>NA</b>
<b>2.2.4.2.b.6</b>	The current version of the WGS84 ordinate reference frame	<b>D</b>		<b>NA</b>
<b>2.2.4.2.b.7</b>	Identification of any supplementary data used to generate the Level 1Gp Digital Image Data	<b>D</b>		<b>NA</b>

**FINAL DRAFT**  
Created on 4/16/2002 9:07 PM

2.2.4.2.b.8	Product corner points with the accuracy specified in Section 7.4		T	NA
2.2.4.2.b.9	User-selected processing parameters for the data products ordered.	D		NA
2.2.5	<b>Level 1Gt LDCM Data Products</b> Level 1Gt LDCM Data Products shall consist of Level 1Gt Digital Image Data and Level 1Gt Metadata. The LDCM shall	D		NA
2.2.5.a	produce and distribute Level 1Gt LDCM Data Products for the data granules specified in Section 2.4 and in the formats specified in Section 2.5.	D		NA
2.2.5.b	produce Level 1Gt LDCM Data Products for any of the daylight, archived, unprocessed LDCM digital image data acquired over the fifty United States and the District of Columbia	D		NA
2.2.5.c	<i>have the goal of producing Level 1Gt LDCM Data Products for any of the daylight, land LDCM digital image data in the LDCM archive.</i>	D		NA
2.2.5.1	<b>Level 1Gt Digital Image Data</b> (header only)			
2.2.5.1.a	Level 1Gt Digital Image Data shall consist of radiometrically corrected digital image data resampled for orthorectification and registration to selectable cartographic projections, as specified in Section 2.3, referenced to the World Geodetic System 1984 (WGS84), G873 or current version.	D		NA
2.2.5.1.b	Image resampling shall be performed using selectable resampling methods, as specified in Section 2.3.2.	D		NA
2.2.5.1.c	The pixels of the Level 1Gt Digital Image Data shall be registered to the geodetic accuracy specified in Section 7.5.	A	T	NA
2.2.5.1.d	The digital values shall be linearly scaled to at-aperture spectral radiance.	T		NA
2.2.5.2	<b>Level 1Gt Metadata</b> Level 1Gt Metadata shall describe the associated Level 1Gt Digital Image Data.	D		NA

**FINAL DRAFT**  
Created on 4/16/2002 9:07 PM

2.2.5.2.a	Level 1Gt Metadata shall adhere to the Federal Geographic Data Committee (FGDC) standards for metadata.	D		NA
2.2.5.2.b	Level 1Gt Metadata shall include, but not be limited to:	D		NA
2.2.5.2.b.1	all of the items listed in Section 2.2.1.3	D		NA
2.2.5.2.b.2	The version of the calibration coefficients used to generate the Level 1Gt Digital Image Data	D		NA
2.2.5.2.b.3	The radiometric coefficients require to convert the digital values of the Level 1Gt digital image data to units of spectral radiance with the accuracy specified in Section 6.1	T		NA
2.2.5.2.b.4	The cartographic projection	D		NA
2.2.5.2.b.5	The cartographic projection parameters	D		NA
2.2.5.2.b.6	The current version of the WGS84 ordinate reference frame	D		NA
2.2.5.2.b.7	Identification of any supplementary data used to generate the Level 1Gt Digital Image Data	D		NA
2.2.5.2.b.8	Product corner points with the accuracy specified in Section 7.5.		T	NA
2.2.5.2.b.9	User-selected processing parameters for the data products ordered.	D		NA
2.3	<b>Cartographic Registration</b> The Level 1Gs, Level 1Gp, and Level 1Gt LDCM Digital Image Data produced and distributed by the LDCM shall be registered to selectable cartographic projections by resampling the image data onto a regular grid in the projection space, with the output image grid aligned per user request to:	D		NA
2.3.a	Map projection grid north, or			NA
2.3.b	The nominal WRS-2 ground track			NA

**FINAL DRAFT**  
Created on 4/16/2002 9:07 PM

<b>2.3.1</b>	<b>Cartographic Projections</b> The LDCM Level 1Gs, Level 1Gp, and Level 1Gt products shall be registered to selectable cartographic projections including, but not limited to:	T		<b>NA</b>
<b>2.3.1.a</b>	Universal Transverse Mercator	T		<b>NA</b>
<b>2.3.1.b</b>	Lambert Conformal Conic	T		<b>NA</b>
<b>2.3.1.c</b>	Polar Stereographic	T		<b>NA</b>
<b>2.3.1.d</b>	Polyconic	T		<b>NA</b>
<b>2.3.1.e</b>	Transverse Mercator	T		<b>NA</b>
<b>2.3.1.f</b>	Oblique Mercator	T		<b>NA</b>
<b>2.3.1.g</b>	Space Oblique Mercator	T		<b>NA</b>
<b>2.3.1.h</b>	NAD83 State Plane	T		<b>NA</b>
<b>2.3.1.i</b>	Albers Equal Area	T		<b>NA</b>
<b>2.3.1.j</b>	Interrupted Goode Homolosine	T		<b>NA</b>
<b>2.3.1.k</b>	Mercator	T		<b>NA</b>
<b>2.3.1.l</b>	Equidistant Conic	T		<b>NA</b>
<b>2.3.2</b>	<b>Resampling Methods</b> The LDCM Level 1Gs, Level 1Gp, and Level 1Gt products shall be resampled into a selected cartographic projection system using customer-selectable resampling methods including:	T		<b>NA</b>
<b>2.3.2.a</b>	nearest neighbor	T		<b>NA</b>
<b>2.3.2.b</b>	bilinear interpolation	T		<b>NA</b>

**FINAL DRAFT**  
Created on 4/16/2002 9:07 PM

2.3.2.c	cubic convolution interpolation	T		NA
2.3.2.d	modulation transfer function compensation interpolation.	T		NA
2.3.3	<b>Resampled Grid Cell Size Characteristics</b> The LDCM Level 1Gs, Level 1Gp, and Level 1Gt products shall be resampled into a selected cartographic projection system using customer-specified grid cell (i.e., resampled output pixel) sizes, with the characteristics defined in the following subsections.			NA
2.3.3.1	<b>Selectable Resampled Grid Cell Sizes</b> The LDCM Level 1Gs, Level 1Gp, and Level 1Gt product grid cell sizes shall be independently selectable for the following band groups:	D		NA
2.3.3.1.a	standard reflective bands (bands 2 through 7)	D		NA
2.3.3.1.b	sharpening band (band 8)	D		NA
2.3.3.2	<b>Resampled Grid Cell Size Ranges</b> The LDCM Level 1Gs, Level 1Gp, and Level 1Gt product grid cell sizes shall be selectable with the minimum ranges specified in Table 2.3.3.2-1. Note: product throughput will be based upon the nominal grid cell sizes in Table 2.3.3.2-1.	T		NA
Table 2.3.3.2-1	<b>Resampled Grid Cell Sizes</b>	T		NA
2.3.3.3	<b>Resampled Grid Cell Size Increment</b> The LDCM Level 1Gs, Level 1Gp, and Level 1Gt product grid cell sizes shall be selectable in increments of 0.001 meters or smaller.	T		NA
2.4	<b>LDCM Data Product Granules</b> (header only)			
2.4.1	<b>WRS-2 Scenes</b> The LDCM shall be capable of producing and distributing Level 0, Level 1R, Level 1Gs, 1Gp, and Level 1Gt Data Products corresponding to the heritage Worldwide Reference System-2 (WRS-2) path/row scenes (185 x 180 km).		T	NA
2.4.2	<b>Sub-Scenes</b> (header only)			

# FINAL DRAFT

Created on 4/16/2002 9:07 PM

2.4.2.a	The LDCM shall produce and distribute at customer request Level 0, Level 1R, Level 1Gs, 1Gp, and Level 1Gt Data Products corresponding to sub-areas within the heritage WRS-2 path/row scenes.	D		NA
2.4.2.b	The smallest data product granule available from the LDCM shall be one-quarter of a WRS-2 scene.	D		NA
2.4.3	<b>Floating Sub-Interval Products</b> (Definition - Unprocessed LDCM digital image data acquired contiguously along an orbital path are herein referred to as a data interval.			
2.4.3.a	The LDCM shall produce and distribute at customer request Level 0, Level 1R, Level 1Gs, Level 1Gp, and Level 1Gt Data Products for contiguous sub-intervals within a data interval.	D		NA
2.4.3.b	The largest sub-interval Level 1R, Level 1Gs, Level 1Gp, and Level 1Gt data product available for the LDCM shall cover at least five WRS-2 scenes along an orbital path.	T		NA
2.4.3.c	The largest sub-interval available for Level 0 products for the LDCM shall cover at least 35 WRS-2 scenes along an orbital path.	T		NA
2.5	<b>LDCM Data Product Formats</b> (header only)			
2.5.1	<b>Level 0 and Level 1R LDCM Data Product Formats</b> The LDCM shall produce and distribute Level 0 and Level 1R LDCM Data Products including but not necessarily limited to the unencapsulated Hierarchical Data Format (HDF).	D		NA
2.5.2	<b>Level 1Gs, Level 1Gp, and Level 1Gt LDCM Data Product Formats</b> The LDCM shall produce and distribute Level 1Gs, Level 1Gp, and Level 1Gt LDCM Data Products in user selectable formats including, but not necessarily limited to:	D		NA
2.5.2.a	the unencapsulated Hierarchical Data Format (HDF)	D		NA
2.5.2.b	the Geographic Tagged Image File Format (GeoTIFF)	D		NA

**FINAL DRAFT**  
Created on 4/16/2002 9:07 PM

2.5.2.c	the FAST L7A format.	D		NA
2.6	<b>LDCM Data Product Compression</b> The LDCM shall produce and distribute uncompressed LDCM Data Products. Compressed data products may be offered as an option.	D		NA
2.7	<b>Data and Data Product Access and Availability</b> (header only)			
2.7.1	<b>LDCM Data Product Availability Time</b> The LDCM shall provide the capability to:			NA
2.7.1.a	Search the LDCM archive for archived, unprocessed LDCM digital image data within 48 hours of LDCM data acquisition by the LDCM sensor(s)		T	NA
2.7.1.b	Order LDCM Data Products within 48 hours of LDCM data acquisition by the LDCM sensor(s).		T	NA
2.7.2	<b>LDCM Data Shipping Time</b> (header only)			
2.7.2.1	<b>Small Orders</b> Subject to the data product generation and distribution capacity specified in Section 2.7.6, the LDCM shall ship orders less than or equal to 10 LDCM Data Products within two business days after the order or within two business days after payment for the order has been cleared, whichever is later	T		NA
2.7.2.2	<b>Large Orders</b> Subject to the data product generation and distribution capacity specified in Section 2.7.6, the LDCM shall ship orders of greater than 10 LDCM Data Products at a rate of at least 10 Products shipped per day, starting two business days after the order or after payment for the order has been cleared, whichever is later. Customers will have the option to delay shipping until a full order is available.	T		NA
2.7.3	<b>LDCM Data Access and Data Product Ordering</b> (header only)			
2.7.3.a	The LDCM shall provide the capability to search the archived LDCM data over the Internet on the basis of the metadata listed in 2.1.3.c.	D		NA

**FINAL DRAFT**  
Created on 4/16/2002 9:07 PM

2.7.3.b	The LDCM shall provide the capability to order LDCM Data Products from the results of searches.	D		NA
2.7.3.c	Data product search results, metadata, and browse images for a single digital image granule shall be provided for viewing within 60 seconds of user query initiation for 90% of the queries made over a local area network.	T		NA
2.7.3.1	<b>Metadata Access</b> The LDCM shall provide the capability to:			NA
2.7.3.1.a	view archived LDCM metadata over the Internet for the purpose of searching	D		NA
2.7.3.1.b	view the metadata within 48 hours of acquisition of the associated digital image data by the LDCM sensor(s).		T	NA
2.7.3.2	<b>Browse Image Access</b> The LDCM shall provide the capability to:			NA
2.7.3.2.a	view archived LDCM browse images over the Internet for the purpose of searching.	D		NA
2.7.3.2.b	view the browse images within 48 hours of acquisition of the associated digital image data by the LDCM sensor(s).		T	NA
2.7.4	<b>LDCM Data Product Ordering Mechanisms</b> The LDCM shall provide the capability to order LDCM Data Products by the following mechanisms:			NA
2.7.4.a	over the Internet	D		NA
2.7.4.b	telephone	D		NA
2.7.4.c	facsimile machine	D		NA
2.7.4.d	written request	D		NA
2.7.4.e	email request	D		NA
2.7.5	<b>LDCM Data Product Distribution</b> (header only)			
2.7.5.a	The LDCM shall distribute LDCM Data Products on standard physical media.	D		NA

**FINAL DRAFT**  
Created on 4/16/2002 9:07 PM

2.7.5.b	The LDCM shall electronically transmit LDCM Data Products at the request of the person ordering the products.	D		NA
2.7.6	<b>LDCM Data Product Generation and Distribution Capacity</b> The LDCM shall be capable of generating and distributing an average of 100 (over a 90 day period), with a peak capacity of 250, WRS-2 scene equivalents per day in any combination of data product types.	A, T		NA
2.8	<b>Algorithm and LDCM Data Product Documentation</b> (header only)			
2.8.1	<b>Archive and Product Generation Algorithms</b> used to produce the LDCM Data and Products listed in Sections 2.1 and 2.2 shall be documented, and made available to the extent allowable by U.S. export laws and regulations. The documented algorithms shall include, but not be limited to,	I		NA
2.8.1.a	algorithms applied to radiometric correction	I		NA
2.8.1.b	radiometric artifact correction	I		NA
2.8.1.c	geolocation	I		NA
2.8.1.d	geometric correction	I		NA
2.8.1.e	sampling or resampling for cartographic registration.	I		NA
2.8.2	<b>Compression Algorithms</b> Algorithms used for compression and decompression of unprocessed LDCM digital image data shall be documented, and made available to the extent allowable by U.S. export laws and regulations.	I		NA
2.8.3	<b>Product Specifications</b> The specifications of LDCM data products and formats shall be documented, with the documentation available publicly.	I		NA
2.9	<b>Short-Term and Long-Term LDCM Data Archives</b> (header only)			

## FINAL DRAFT

Created on 4/16/2002 9:07 PM

<b>2.9.1</b>	<b>Active Data Archival</b> (header only)			
<b>2.9.1.a</b>	The LDCM shall maintain the LDCM active archive for the life of the LDCM.	<b>D, A</b>		<b>NA</b>
<b>2.9.1.b</b>	The LDCM shall archive the data specified in Section 2.1 for the life of the LDCM.	<b>A</b>		<b>NA</b>
<b>2.9.1.c</b>	The LDCM shall produce and distribute the data products specified in Section 2.2 for the life of the LDCM.	<b>A</b>		<b>NA</b>
<b>2.9.2</b>	<b>Long-Term LDCM Data Archival</b> (header only)			
<b>2.9.2.a</b>	The LDCM shall provide a copy of all LDCM data, described in Section 2.1, procured or otherwise acquired by the U.S. Government under this contract, to the United States Geological Survey (USGS) Earth Resources Observation System (EROS) Data Center (EDC).	<b>D, A</b>		<b>NA</b>
<b>2.9.2.b</b>	The LDCM data, as described in Section 2.1, shall be delivered to the USGS EDC long-term archive within 48 hours after initial archiving.	<b>T</b>		<b>NA</b>
<b>3.0</b>	<b>LDCM Spatial Coverage and Temporal Resolution</b> The archived, unprocessed LDCM digital image data provides substantially cloud-free, sun-lit, multispectral digital image coverage of the Earth's land areas on a seasonal basis, as defined in the following sections.			<b>NA</b>
<b>3.1</b>	<b>Spatial Coverage</b> The LDCM shall be capable of obtaining unprocessed LDCM digital image data for every point on the Earth's continental and coastal surfaces between $\pm 81.8^\circ$ latitude.		<b>T</b>	<b>YES</b>
<b>3.1.1</b>	<b>LDCM Global Archive Coverage</b> This section includes requirements for coverage area, temporal frequency, and overall volume of data captured for the LDCM global archive(s), and does not include any requirement for International Cooperators.			<b>NA</b>

**FINAL DRAFT**  
Created on 4/16/2002 9:07 PM

3.1.1.1	<p><b>Daily LDCM Global Archive Coverage</b> The unprocessed LDCM digital image data captured into the LDCM active and long term archive(s) shall provide an average daily coverage of at least 250 full WRS-2 (see 2.4.1) land scenes per any 90 day period. WRS-2 land scenes are defined in the WRS Land Database, Revision 2.1, to include continental regions, coastal areas, islands, ice caps, and reefs.</p>	A	T	NO
3.1.1.2	<p><b>LDCM Global Archive Acquisition Strategy</b> The LDCM shall implement a WRS-2 scene acquisition strategy such that the distribution of acquisition priority scores from archived scenes during any 16 day cycle has an equal or higher mean and median compared to the distribution provided by the Landsat-7 Long Term Acquisition Plan (LTAP) and scheduler, where “acquisition priority scores” refers to the science acquisition priorities calculated by the LTAP, as defined in the Appendix to this specification.</p>	A	T	NA
3.1.1.3	<p><b>Acquisition Priority Updates</b> The LDCM shall update the LDCM acquisition strategy every 90 days, using base priorities and acquisition windows (defined in the Appendix to this specification) supplied by the government.</p>	D	A	NA
3.1.2	<p><b>Minimum Cross-Track Extent</b> The unprocessed LDCM digital image data stored in the LDCM archive shall have a minimum cross-track extent of 185 km.</p>		T	NO.
3.1.3	<p><b>WRS-2 Orientation</b> The unprocessed LDCM digital image data shall be acquired in accordance with the Worldwide Reference System 2 (WRS-2) grid, such that the swath center of the unprocessed LDCM digital image data shall be within 5 km of the center of the corresponding WRS-2 path.</p>	A	T	NO
3.2	<p><b>Special Acquisitions</b> (header only)</p>			

**FINAL DRAFT**  
Created on 4/16/2002 9:07 PM

3.2.1	<b>United States Coverage</b> Archived LDCM data shall provide coverage of the fifty United States and the District of Columbia and their coastal areas at least once every 16 days or less, regardless of cloud cover, subject to the solar zenith requirement 3.3.1.1.		T	NO
3.2.2	<b>High-Priority Target Coverage</b> The LDCM shall acquire and archive LDCM data for up to twelve of the 250WRS-2 scenes per day for high-priority targets of opportunity (e.g. natural disasters, volcanic eruptions, etc), which will be identified by the Government at least 24 hours prior to acquisition, and which may have individual requirements for predicted cloud cover.		T	NA
3.3	<b>Solar Illumination</b> The LDCM data archive shall be composed of both daylight and night data, consisting primarily of daylight LDCM data with a limited amount of nighttime coverage for specific targets, as defined in the following sections.	D		NA
3.3.1	<b>Global Daylight Coverage</b> (header only)			
3.3.1.1	<b>Solar Zenith Angle</b> LDCM data acquired in daylight for the LDCM archive shall be acquired when the solar zenith angle is less than 88°.		T	NA
3.3.1.2	<b>Local Solar Time</b> LDCM data collected along the equator shall be collected at 10 am (+/- 15 minutes), local solar time.	A	T	NA
3.3.2	<b>Night Images</b> (header only)			
3.3.2.a	The LDCM shall acquire and archive all bands for up to 25 of the 250 WRS-2 scenes at night during any 24-hour period for priority targets such as volcanic activity, calibration targets, and fires. Specific targets will be provided by the Government at least 24 hours in advance of acquisition.	A	T	NA
3.3.2.b	The LDCM shall be capable of acquiring up to 10 contiguous night WRS-2 scenes during any 24 hour period.	A, T		NA

**FINAL DRAFT**  
Created on 4/16/2002 9:07 PM

3.4	<b>Viewing Geometry; Maximum Viewing Zenith Angle</b> The LDCM data archive shall contain unprocessed LDCM digital image data acquired with viewing zenith angles less than or equal to 10°.		T	NA
4.0	<b>LDCM Spectral Bands</b> The LDCM shall acquire and archive multispectral digital image data for the spectral bands listed in Table 4.1-1.	D, A		
4.1.a	The full-width-half-maximum (FWHM) points of the relative spectral radiance response curve for each spectral band shall fall within the range of the minimum 50% lower band edge and the maximum 50% upper band edge as listed in Table 4.1-1.	A, T		NO
4.1.b	The bands shall be located so as to avoid atmospheric absorption features, where possible.	A, T		YES
Table 4.1-1	<b>Spectral bands and band widths</b>	T		NA
4.2	<b>Spectral Band Shape</b> (header only)			
4.2.1	<b>Spectral Flatness</b> (header only)			
4.2.1.1	<b>Flatness Between Band Edges</b> The system relative spectral radiance response between the lower band edge (lowest wavelength with 0.5 response) and the upper band edge (highest wavelength with 0.5 response) shall have the following properties:	T		NA
4.2.1.1.1	<b>Average Response</b> The average response shall be greater than 0.8.	T		NO
4.2.1.1.2	<b>Minimum Response</b> No value shall be below 0.4.	T		YES
4.2.1.2	<b>Flatness Between 80% response points</b> The system relative spectral radiance response between the minimum wavelength with a 0.8 response and the maximum wavelength with a 0.8 response point shall always exceed 0.7.	T		YES
4.2.2	<b>Out of Band Response</b> (header only)			

**FINAL DRAFT**  
Created on 4/16/2002 9:07 PM

4.2.2.a	The ratio of the integrated response beyond the 1% response points to the integrated response between the 1% response points shall be less than 2%. The integrated responses will be weighted by the solar exoatmospheric irradiance. The 1% response points are the points closest to the center wavelength where the response first drops to 1% of the peak response on each side of the center wavelength.	A, T		<b>YES</b>
4.2.2.b	Additionally the value of out of band response shall not exceed 0.1% at any wavelength more than 50 nm for all VNIR bands and 100 nm for all SWIR and sharpening bands from the corresponding 50% response band edge. If a red band is used for sharpening then Band 4 out of band requirements apply.	A, T		<b>YES</b>
4.2.3	<b>Edge Slope</b> (header only)			
4.2.3.a	The wavelength interval between the first 5% and the first 50% of peak response and the last 50% and the last 5% of peak response ranges shall not exceed the values in Table 4.2.3-1.	T		<b>YES</b>
4.2.3.b	The wavelength interval between the 1% response points and the corresponding 50% response band edge shall not exceed the values in Table 4.2.3-1.	T		<b>YES</b>
Table 4.2.3-1	<b>Edge Slope Intervals for LDCM bands</b>	T		
4.3	<b>Spectral Uniformity</b> The bandwidth shall vary by no more than $\pm 3\%$ across pixels within a band. Additionally see Section 6.2.3.			<b>??</b>
4.4	<b>Spectral Stability</b> Band center wavelengths and band edges shall not change by more $\pm 2$ nm over the expected life of the mission.	I, A, T		<b>??</b>
4.5	<b>Spectral Band Simultaneity</b> For any point within a single scene observed by the LDCM, the LDCM shall acquire data for all spectral bands within a two-minute period.	T	T	<b>YES</b>
5.0	<b>LDCM Spatial Resolution</b> (header only)			

**FINAL DRAFT**  
Created on 4/16/2002 9:07 PM

<b>5.1</b>	<b>Multispectral Ground Sample Distance</b> (header only)			
<b>5.1.a</b>	Unprocessed LDCM digital image data shall provide a pixel-to-pixel increment equivalent to a ground sampling distance (GSD) of 30 m or less across the WRS-2 scene for LDCM spectral bands 2, 3, 4, 5, 6, and 7.			<b>YES</b>
<b>5.1.b</b>	LDCM Level 1R digital image data shall provide a pixel-to-pixel increment equivalent to a ground sampling distance (GSD) of 30 m or less across the WRS-2 scene for LDCM spectral bands 2, 3, 4, 5, 6, and 7.			<b>YES</b>
<b>5.2</b>	<b>Sharpening Band Ground Sample Distance</b> (header only)			
<b>5.2.a</b>	Unprocessed LDCM digital image data shall provide a single sharpening band, LDCM spectral band 8, with a pixel-to-pixel increment equivalent to a GSD of 15 m or less across the WRS-2 scene.			<b>YES</b>
<b>5.2.b</b>	LDCM Level 1R digital image data shall provide a pixel-to-pixel increment equivalent to a GSD of 15 m or less across the WRS-2 scene for the single sharpening band, LDCM spectral band 8.			<b>YES</b>
<b>5.3</b>	<b>Edge Response</b> The mean relative edge response slope in the in-track and cross-track directions (mean of slope between 40%-60%) for Level 1R digital image data shall conform to the criteria described in the following subsections. <b>Note:</b> Table 5.3-1 lists the bands, their maximum allowable GSD, and the minimal edge slope. The edge response, in the context below, is the normalized response of the imaging system to an edge. That is, the edge response is normalized so that the mean minimum edge response is set to zero and the mean maximum response is set to 100%.	<b>A, T</b>		<b>NA</b>
<b>Table 5.3-1</b>	<b>GSD/Minimum Slope Specification</b>	<b>A, T</b>		

**FINAL DRAFT**  
Created on 4/16/2002 9:07 PM

5.3.1	<b>Standard Band Edge Response Slope</b> The mean relative edge response slope for LDCM spectral bands 2, 3, 4, 5, 6, and 7 (<30 m GSD) shall exceed 0.027/meter for Level 1R digital image data across the entire Field-of-View.	A, T		<b>NO/YES</b>
5.3.2	<b>Sharpening Band Edge Response Slope</b> The mean relative edge response slope for the sharpening band, LDCM spectral band 8 (<15 m GSD), shall exceed 0.054/meter for Level 1R digital image data across the entire Field-of-View.	A, T		<b>YES</b>
5.3.3	<b>Edge Response Overshoot</b> The overshoot of any edge response for all bands shall not exceed 5% for Level 1R digital image data.	A, T		<b>YES</b>
5.3.4	<b>Edge Response Uniformity</b> The mean relative edge response slope shall not vary by more than 10% in any band across the Field-of-View and by not more than 20% between LDCM spectral bands 2,3,4,5,6,and 7 for Level 1R digital image data.	A, T		<b>NO</b>
5.4	<b>Aliasing</b> (header only)			
5.4.1	<b>Level 1R Product Aliasing</b> The product of the mean relative edge response slope and the GSD shall be less than 1.0 for Level 1R digital image data for both the in-track and cross track directions.			<b>YES/NO</b>
5.4.2	<b>Level 1G Product Aliasing</b> The product of the mean relative edge response slope in Level 1G digital image data, resampled using the cubic convolution method, and the maximum GSD specified in Table 5.3-1 shall be less than 1.0 for both the in-track and cross track directions.			<b>NO</b>
5.5	<b>Stray Light Rejection and Internal Light Scattering</b> (header only)			
5.5.1	<b>Point Source Transmittance (PST)</b> For any detector in the sensor and for all bands, the normalized point source transmittance (PST) (peak point source response normalized to unity) shall be less than the values given in Table 5.5-1 for the corresponding off-field angles over the entire field-of-view of the system.	A, T		<b>NO</b>

**FINAL DRAFT**  
Created on 4/16/2002 9:07 PM

<b>Table 5.5-1</b>	<b>PST Specification</b>	<b>A, T</b>		
<b>5.5.2</b>	<b>Total Integrated Optical Scatter (TIS)</b> The total integrated scatter for 1 degree or greater for a point target imaged onto a detector in any band shall be less than 1%.	<b>A, T</b>		<b>NO</b>
<b>6.0</b>	<b>LDCM Radiometry</b> (header only)			
<b>6.1</b>	<b>Absolute Radiometric Accuracy</b> The digital values in a Level 1 data product shall be linearly scaled to at-aperture spectral radiance with an uncertainty less than or equal to 5% (1 sigma) with a goal of 3% (1 sigma) across the range of 0.3 Ltypical to 0.9 Lmax (Table 6.1-1) with all accuracies established relative to National Institute for Standards and Technology (NIST) standards.			<b>NO</b>
<b>Table 6.1-1</b>	<b>Radiance/Temperature Levels for Signal-to-Noise Ratio (SNR) Requirements and Saturation Radiances</b>	<b>A, T</b>	<b>T</b>	
<b>6.2</b>	<b>Radiometric Signal to Noise</b> (header only)			
<b>6.2.1</b>	<b>Pixel Signal-to-Noise Ratios (SNRs)</b> SNRs required for all LDCM Level 1 digital image data and for each spectral band are listed in Table 6.1-1 and 6.2.1-1.	<b>T</b>	<b>T</b>	<b>NA</b>
<b>6.2.1.a</b>	50% of the pixels shall meet or exceed these SNR values.	<b>T</b>	<b>T</b>	<b>YES</b>
<b>6.2.1.b</b>	99% of the pixels shall exceed 80% of these values.	<b>T</b>	<b>T</b>	<b>YES</b>
<b>Table 6.2.1-1</b>	<b>SNR Requirements and Goals</b>	<b>T</b>	<b>T</b>	
<b>6.2.2</b>	<b>Quantization Noise Limit</b> (header only)			
<b>6.2.2.1</b>	<b>Unprocessed LDCM Digital Image Data Quantization</b> The unprocessed LDCM digital image data SNR performance shall not be quantization noise limited, i.e. at zero radiance and above, system noise shall be greater than or equal to 0.5 Digital Number.			<b>YES</b>

**FINAL DRAFT**  
Created on 4/16/2002 9:07 PM

6.2.2.2	<b>LDCM Data Product Quantization</b> LDCM Level 0 and Level 1 digital image data SNR performance shall not be quantization noise limited, i.e. at zero radiance and above, system noise shall be greater than or equal to 0.5 Digital Number.			<b>YES</b>
6.2.3	<b>Pixel-to-Pixel Uniformity</b> For a uniform source above 2*Ltypical the standard deviation of the calibrated values across pixels within a line of Level 1R digital image data within a band shall not exceed 0.25% of the average radiance for bands 2-7 and 0.5% of the average radiance for band 8. Temporal noise may be averaged to verify compliance with this specification. <b>Note:</b> This requirement applies for target radiances with spectral characteristics as follows: the spectral radiance of the source used in pre-launch calibration, spectral radiance from bare soil as observed through a dry atmosphere, spectral radiance proportional to the exoatmospheric solar irradiance, and spectral radiance from a dense vegetation target as observed through a moist atmosphere (See Figure 6.2.3-1 and Top of Atmosphere Radiance Values , MODTRAN 4 Model table values, Reference d).	A, T	T	<b>NO</b>
6.2.4	<b>Coherent Noise</b> The magnitude of the autocorrelation of a dark (zero-radiance) scene, computed after subtraction of detector-by-detector direct current offset, and normalized to 1.0 at zero lag, shall not exceed 0.25 at any non-zero spatial lag.			<b>NO</b>
6.3	<b>Dynamic Range</b> The LDCM Level 0 and Level 1 digital image data shall cover, without saturating, signals up to the Lmax as shown in table 6.1-1. Note: For bands 2-8, this corresponds to the radiance reflected off of a Lambertian target of 100% reflectance illuminated by the sun at a solar zenith angle of 20°.	A, T	T	<b>NO</b>
6.4	<b>Polarization Sensitivity</b> The source of the data (excluding the thermal band) shall be insensitive to linear polarization, such that the polarization factor, defined as $PF = (I_{max} - I_{min}) / (I_{max} + I_{min})$ , is less than 0.05.	A, T		<b>YES</b>

# FINAL DRAFT

Created on 4/16/2002 9:07 PM

6.5	<b>Radiometric Stability</b> The LDCM Level 1 digital image data for radiometrically constant targets with radiances greater than or equal to Ltypical shall not differ by more than $\pm 1\%$ over any time up to 16 days nor by more than $\pm 2\%$ in any period between 16 days and five years.	T	T	<b>NO</b>
6.6	<b>Image Artifacts</b> (header only)			
6.6.1	<b>Bright Target Recovery</b> The unprocessed data in the archive shall be such that the recovery region around an image pixel which has been exposed to a radiance level of less than or equal to 1.5 times that of the source sensor's saturation level shall be contained within a 7 x 7 pixel region centered on the exposed pixel.	A, T	T	<b>NO</b>
6.6.2	<b>Pixel-to-Pixel Crosstalk</b> The crosstalk-induced artifacts in neighboring pixels caused by regions of pixels having radiance levels less than the saturation level and which are more than ten pixels away, shall not exceed 1%, in total, after radiometric correction.	A, T	T	<b>NO</b>
7.0	<b>LDCM Geometric Precision, Geolocation, and Cartographic Registration</b> (header only)			
7.1	<b>Band-to-Band Registration</b> Level 1G (radiometrically and geometrically corrected) data products shall exhibit band-to-band registration accuracy for targets at the Earth's surface as specified in the following sections. <b>Note:</b> Level 1G products that are created using the nearest neighbor resampling method are treated separately for purposes of band-to-band registration due to the inability to correct for sub-pixel effects when using this method.	A	T	<b>NA</b>

# FINAL DRAFT

Created on 4/16/2002 9:07 PM

7.1.1	<p><b>Level 1G Nearest Neighbor Product Band-to-Band Registration</b> Corresponding pixels from the digital images of the spectral bands in Level 1G data products created using nearest neighbor resampling, as specified in section 2.3.2.a, shall be co-registered with an uncertainty of 15 meters or less, with a goal of 3 meters or less, in the line and sample directions at the 90% confidence level for target areas within 100 meters of the WGS84 (G873 or current version) Earth ellipsoid surface.</p>		T	NA
7.1.2	<p><b>Level 1G Data Product Band-to-Band Registration</b> Corresponding pixels from the digital images of the spectral bands in Level 1G data products created using the resampling methods specified in sections 2.3.2.b through 2.3.2.d, shall be co-registered with an uncertainty of 4.5 meters or less, with a goal of 3 meters or less, in the line and sample directions at the 90% confidence level for target areas within 100 meters of the WGS84 (G873 or current version) Earth ellipsoid surface.</p>		T	NA
7.2	<p><b>Image-to-Image Registration</b> Two Level 1G data products of the same area, derived from data acquired on different dates, shall be capable of being co-registered with an uncertainty less than or equal to 0.5 pixel in the line and sample directions at the 90% confidence level when image-to-image correlation is applied to data from the same spectral band. This requirement applies to data from all spectral bands.</p>		T	NA
7.3	<p><b>Level 1Gs Product Geodetic Accuracy</b> (header only)</p>			

**FINAL DRAFT**  
Created on 4/16/2002 9:07 PM

7.3.1	<b>Level 1Gs Product Absolute Geodetic Accuracy</b> The pixels for targets at the Earth's topographic surface in the Level 1Gs data products shall be located relative to the WGS84 geodetic reference system, G873 or current version, with an uncertainty less than or equal to 65 meters (90% circular error) with a goal of 50 meters (90% circular error), excluding terrain effects. This specification applies to the horizontal error of ground control points measured in the 1Gs image, after compensation for control point height.		T	NA
7.3.2	<b>Level 1Gs Product Relative Geodetic Accuracy</b> The pixels for targets at the Earth's topographic surface in the Level 1Gs data products shall be located relative to the WGS84 geodetic reference system, G873 or current version, with an uncertainty less than or equal to 25 meters (90% circular error), excluding terrain effects, over an area of 180 km by 180 km, after the removal of constant offsets. This specification applies to the standard deviation of ground control points measured in the 1Gs image, after compensation for control point height.		T	NA
7.4	<b>Level 1Gp Product Geodetic Accuracy</b> The pixels for targets at the Earth's topographic surface in the Level 1Gp data products shall be located relative to the WGS84 geodetic reference system, G873 or current version, with an uncertainty less than or equal to 12 meters (90% circular error), excluding terrain effects.	A	T	NA
7.5	<b>Level 1Gt Product Geodetic Accuracy</b> The pixels for targets at the Earth's topographic surface in the Level 1Gt orthorectified data products shall be located relative to the WGS84 geodetic reference system, G873 or current version, with an uncertainty less than or equal to 12 meters (90% circular error), including compensation for terrain effects.		T	NA
8.0	<b>LDCM Thermal Band Option Requirements</b> (header only)			
8.1	<b>LDCM Data and Data Products</b> The requirements of Section 2 shall apply to the thermal band.			NA

**FINAL DRAFT**  
Created on 4/16/2002 9:07 PM

<b>8.1.1</b>	<b>Resampled Grid Cell Size Characteristics for Thermal Bands</b> The LDCM Level 1Gs, Level 1Gp, and Level 1Gt product thermal bands shall be resampled into a selected cartographic projection system using customer-specified grid cell (i.e., resampled output pixel) sizes, with the characteristics defined in the following subsections.	<b>D</b>		<b>NA</b>
<b>8.1.1.1</b>	<b>Selectable Resampled Grid Cell Sizes for Thermal Bands</b> The LDCM Level 1Gs, Level 1Gp, and Level 1Gt product grid cell sizes shall be independently selectable for the following band group:	<b>D</b>		<b>NA</b>
<b>8.1.1.1.a</b>	Thermal bands (bands 10, 11)	<b>D</b>		<b>NA</b>
<b>8.1.1.2</b>	<b>Resampled Grid Cell Size Range for Thermal Bands</b> The LDCM Level 1Gs, Level 1Gp, and Level 1Gt product thermal band grid cell sizes shall be selectable with the minimum range specified in Table 8.1.1.2-1. Note: product throughput will be based upon the nominal grid cell size in Table 8.1.1.2-1.	<b>T</b>		<b>NA</b>
<b>Table 8.1.1.2-1</b>	<b>Resampled Grid Cell Sizes for Thermal Bands</b>	<b>T</b>		<b>NA</b>
<b>8.1.1.3</b>	<b>Resampled Grid Cell Size Increment for Thermal Bands</b> The LDCM Level 1Gs, Level 1Gp, and Level 1Gt product grid cell sizes shall be selectable in increments of 0.001 meters or smaller.	<b>T</b>		<b>NA</b>
<b>8.2</b>	<b>LDCM Spatial Coverage and Temporal Resolution</b> The requirements of Section 3 shall apply to the thermal band.			<b>NA</b>
<b>8.3</b>	<b>LDCM Thermal Spectral Bands</b> The LDCM shall acquire and archive data for the thermal bands listed in Table 8.3-1.	<b>D</b>		<b>NA</b>
<b>8.3.1</b>	<b>Thermal Spectral Band Widths</b> The FWHM points of the relative spectral radiance response curve for each band shall fall within the range of the minimum 50% lower band edge and the maximum 50% upper band edge as listed in Table 8.3-1.	<b>T</b>		<b>NA</b>
<b>Table 8.3-1</b>	<b>Thermal Spectral Bands and Bandwidths</b>	<b>T</b>		<b>NA</b>

**FINAL DRAFT**  
Created on 4/16/2002 9:07 PM

<b>8.3.2</b>	<b>Spectral Characteristics</b> (header only)			
<b>8.3.2.1</b>	<b>Spectral Flatness</b> (header only)			
<b>8.3.2.1.1</b>	<b>Flatness Between Band Edges</b> The system relative spectral radiance response between the lower band edge (lowest wavelength with 0.5 response) and the upper band edge (highest wavelength with 0.5 response) shall have the following properties:	<b>T</b>		<b>NA</b>
<b>8.3.2.1.1.1</b>	<b>Average Response</b> The average response shall be greater than 0.8.	<b>T</b>		<b>NA</b>
<b>8.3.2.1.1.2</b>	<b>Minimum Response</b> No value shall be below 0.4.	<b>T</b>		<b>NA</b>
<b>8.3.2.1.2</b>	<b>Flatness Between 80% response points</b> The system relative spectral radiance response between the minimum wavelength with a 0.8 response and the maximum wavelength with a 0.8 response point shall always exceed 0.7.	<b>T</b>		<b>NA</b>
<b>8.3.2.2</b>	<b>Out of Band Response</b> The ratio of the integrated response beyond the 1% response points to the integrated response between the 1% response points shall be less than 2% between 3000 and 20000 nm and less than 0.5% below 3000 nm. The integrated responses will be weighted by the radiance from a 300k blackbody summed with the radiance from a Lambertian surface of 100% reflectance illuminated by the sun at a zenith angle of 30°. The 1% response points are the points closest to the center wavelength where the response first drops to 1% of the peak response on each side of the center wavelength.			<b>NA</b>
<b>8.3.2.3</b>	<b>Edge Slope</b> (header only)			
<b>8.3.2.3.a</b>	The wavelength interval between the first 5% and the first 50% of peak response and the last 50% and the last 5% of peak response ranges shall not exceed the values in Table 8.3.2.3-1.	<b>T</b>		<b>NA</b>

**FINAL DRAFT**  
Created on 4/16/2002 9:07 PM

<b>8.3.2.3.b</b>	The wavelength interval between the 1% response points and the corresponding 50% response band edge shall not exceed the values in Table 8.3.2.3-1.	T		<b>NA</b>
<b>Table 8.3.2.3-1</b>	<b>Edge Slope Intervals for LDCM Thermal bands</b>	T		<b>NA</b>
<b>8.3.2.4</b>	<b>Spectral Uniformity</b> The bandwidth shall vary by no more than $\pm 3\%$ across pixels within a band. Additionally see Section 8.5.2.3.			<b>NA</b>
<b>8.3.2.5</b>	<b>Spectral Stability</b> Band center wavelengths and band edges shall not change by more $\pm 20$ nm over the expected life of the mission.	I, A, T		<b>NA</b>
<b>8.3.2.6</b>	<b>Spectral Band Simultaneity</b> (header only)			
<b>8.3.2.6.a</b>	For any point within a single scene observed by the LDCM, the LDCM shall acquire data for all spectral bands within a two-minute period.		T	<b>NA</b>
<b>8.3.2.6.b</b>	The data for the two thermal bands shall be acquired within 10 seconds of each other.		T	<b>NA</b>
<b>8.4</b>	<b>LDCM Thermal Spectral Band Spatial Resolution</b> (header only)			
<b>8.4.1</b>	<b>Thermal Bands Ground Sample Distance</b> (header only)			
<b>8.4.1.a</b>	Unprocessed LDCM digital image data shall provide a pixel-to-pixel increment equivalent to a GSD 120m or less for the thermal bands across the WRS-2 scene.		T	<b>NA</b>
<b>8.4.1.b</b>	LDCM Level 1R digital image data shall provide a pixel-to-pixel increment equivalent to a GSD 120m or less for the thermal bands across the WRS-2 scene.		T	<b>NA</b>
<b>8.4.2</b>	<b>Thermal Band Edge Response Slope</b> The mean relative edge response slope for the thermal bands ( $< 120\text{m}$ ), shall exceed 0.006/meter for Level 1R digital image data across the entire Field-of-View. See Table 8.4.2-1.	A, T		<b>NA</b>
<b>Table 8.4.2-1</b>	<b>Thermal Band Edge Response Slope</b>	A, T		<b>NA</b>

**FINAL DRAFT**  
Created on 4/16/2002 9:07 PM

8.4.3	<b>Edge Response Overshoot and Aliasing</b> The requirements of 5.3.3 and 5.4 shall apply to the thermal bands.			NA
8.4.4	<b>Thermal Band Edge Response Uniformity</b> The mean relative edge response slope shall not vary by more than 10% in any band across the Field-of-View and by not more than 20% between the LDCM spectral bands 10 and 11 (thermal bands) for Level 1R digital image data.	A, T		NA
8.5	<b>LDCM Thermal Spectral Band Radiometry</b> (header only)			
8.5.1	<b>Absolute Radiometric Accuracy</b> The digital values in a Level 1 data product shall be linearly scaled to at-aperture spectral radiance with an uncertainty less than or equal to 2%(1 sigma) with a goal of 1% (1 sigma) across the range of radiances corresponding to 240K to 330K blackbodies with all accuracies established relative to NIST standards.			NA
8.5.2	<b>Radiometric Precision</b> (header only)			
8.5.2.1	<b>Pixel Noise Equivalent Delta Temperatures</b> Noise Equivalent Delta Temperatures (NEDT) required for LDCM Level 1 digital image data and for each thermal band are listed in Table 8.5.2.1-1 and 8.5.2.1-2. 50% of the pixels shall be less than or equal to these NEDT values, 99% of the pixels shall be less than or equal to 1.2 times these values.	A	T	NA
Table 8.5.2.1-1	<b>Temperatures for Noise and Saturation for Thermal Bands</b>	A	T	NA
Table 8.5.2.1-2	<b>Noise Equivalent Delta Temperatures for Thermal Bands</b>	A	T	NA
8.5.2.2	<b>Quantization Noise Limit</b> The requirements of Section 6.2.2 shall apply to the thermal bands.			NA

# FINAL DRAFT

Created on 4/16/2002 9:07 PM

8.5.2.3	<b>Pixel-to-Pixel Uniformity</b> For a uniform source above the radiance corresponding to a blackbody temperature of 240K, the standard deviation of the calibrated values across pixels within a line of LDCM Level 1R digital image data within a band shall not exceed 0.5% (0.25% goal) of the average radiance. This requirement applies for spectral radiances from 240K to 340K blackbody sources. Temporal noise may be averaged to verify compliance with this specification.	A, T		NA
8.5.2.4	<b>Coherent Noise</b> The requirements of Section 6.2.4 shall apply to the thermal bands.			NA
8.5.3	<b>Dynamic Range</b> The dynamic range of the LDCM Level 0 and Level 1 digital image data shall be from the noise floor up to the TMAX as shown in Table 8.5.2-1. The equivalent blackbody temperatures of the noise floors of bands 10 and 11 are 143K at the required NEDT (133K at the goal NEDT) and 133K at the required NEDT (126K at the goal NEDT), respectively.	A, T		NA
8.5.4	<b>Radiometric Stability</b> The radiometrically calibrated LDCM Level 1 digital image data for radiometrically constant targets with radiances greater than or equal to the radiance of a 240K blackbody, shall not differ by more than $\pm 0.5\%$ over any time up to 16 days nor by more than $\pm 1\%$ in any period between 16 days and five years.	A, T		NA
8.5.5	<b>Image Artifacts</b> The requirements of Section 6.6 shall apply to the thermal bands.			NA
8.6	<b>LDCM Geometric Precision, Geolocation, and Cartographic Registration</b> (header only)			
8.6.1	<b>Band-to-Band Registration</b> Level 1G (radiometrically and geometrically corrected) data products shall exhibit band-to-band registration accuracy for targets at the Earth's surface as specified in the following sections.	A	T	NA

**FINAL DRAFT**  
Created on 4/16/2002 9:07 PM

8.6.1.1	<b>Level 1G Nearest Neighbor Product Band-to-Band Registration</b> Corresponding pixels from the digital images of the spectral bands in Level 1G data products created using the nearest neighbor resampling method, as specified in section 2.3.2.a, shall be co-registered with an uncertainty as specified in Table 8.6-1, in the line and sample directions at the 90% confidence level for target areas within 100 meters of the WGS84 (G873 or current version) Earth ellipsoid surface.		T	NA
Table 8.6-1	<b>Level 1G Nearest Neighbor Band Registration Requirements</b>		T	NA
8.6.1.2	<b>Level 1G Data Product Band-to-Band Registration</b> Corresponding pixels from the digital images of the spectral bands in Level 1G data products created using the resampling methods specified in sections 2.3.2.b through 2.3.2.d shall be co-registered with an uncertainty as specified in Table 8.6-2, in the line and sample directions at the 90% confidence level for target areas within 100 meters of the WGS84 (G873 or current version) Earth ellipsoid surface.		T	NA
Table 8.6-2	<b>Level 1G Band Registration Requirements</b>		T	NA
8.6.2	<b>Thermal Spectral Band Registration and Geodetic Accuracy</b> The requirements of Section 7.2-7.5 shall apply to the thermal bands.			NA
9.0	<b>LDCM Optional Reflective Bands</b> (header only)			
9.1	<b>LDCM Data and Data Products</b> The requirements of Section 2 shall apply to the optional reflective bands.			NA
9.1.1	<b>Resampled Grid Cell Size Characteristics for Optional Reflective Bands</b> The LDCM Level 1Gs, Level 1Gp, and Level 1Gt product optional reflective bands shall be resampled into a selected cartographic projection system using customer-specified grid cell (i.e., resampled output pixel) sizes, with the characteristics defined in the following subsections.			NA

# FINAL DRAFT

Created on 4/16/2002 9:07 PM

9.1.1.1	<b>Selectable Resampled Grid Cell Sizes for Optional Reflective Bands</b> The LDCM Level 1Gs, Level 1Gp, and Level 1Gt product grid cell sizes shall be independently selectable for the following band groups:	D		NA
9.1.1.1.a	coastal/aerosol band (band 1)	D		NA
9.1.1.1.b	the cirrus band (band 9)	D		NA
9.1.1.2	<b>Resampled Grid Cell Size Ranges</b> The LDCM Level 1Gs, Level 1Gp, and Level 1Gt product optional reflective band grid cell sizes shall be selectable with the minimum ranges specified in Table 9.1.1.2-1. Note: product throughput will be based upon the nominal grid cell sizes in Table 9.1.1.2-1.	T		NA
Table 9.1.1.2-1	<b>Resampled Grid Cell Sizes</b>	T		NA
9.1.1.3	<b>Resampled Grid Cell Size Increment</b> The LDCM Level 1Gs, Level 1Gp, and Level 1Gt product grid cell sizes shall be selectable in increments of 0.001 meters or smaller.	T		NA
9.2	<b>LDCM Spatial Coverage and Temporal Resolution</b> The requirements of Section 3 shall apply to the optional reflective bands.			NO
9.3	<b>LDCM Spectral Bands</b> The LDCM shall acquire and archive data for the optional reflective bands listed in Table 9.3.1-1.			NA
9.3.1	<b>Reflective Bands and Band Width</b> The full-width-half-maximum (FWHM) points of the relative spectral radiance response curve for each spectral band shall fall within the range of the minimum 50% lower band edge and the maximum 50% upper band edge as listed in Table 9.3.1-1.			YES
Table 9.3.1-1	<b>Reflective bands and band widths</b>	A, T		
9.3.2	<b>Spectral Characteristics</b> (header only)			
9.3.2.1	<b>Spectral Flatness</b> (header only)			

**FINAL DRAFT**  
Created on 4/16/2002 9:07 PM

<b>9.3.2.1.1</b>	<b>Flatness Between Band Edges</b> The system relative spectral radiance response between the lower band edge (lowest wavelength with 0.5 response) and the upper band edge (highest wavelength with 0.5 response) shall have the following properties:	T		
<b>9.3.2.1.1.1</b>	<b>Average Response</b> The average response shall be greater than 0.8.	T		<b>YES</b>
<b>9.3.2.1.1.2</b>	<b>Minimum Response</b> No value shall be below 0.4.	T		<b>YES</b>
<b>9.3.2.1.2</b>	<b>Flatness Between 80% response points</b> The system relative spectral radiance response between the minimum wavelength with a 0.8 response and the maximum wavelength with a 0.8 response point shall always exceed 0.7.	A, T		<b>YES</b>
<b>9.3.2.2</b>	<b>Out of Band Response</b> (header only)			
<b>9.3.2.2.a</b>	The ratio of the integrated response beyond the 1% response points to the integrated response between the 1% response points shall be less than 2%. The integrated responses will be weighted by the solar exoatmospheric irradiance. The 1% response points are the points closest to the center wavelength where the response first drops to 1% of the peak response on each side of the center wavelength.	A, T		<b>YES</b>
<b>9.3.2.2.b</b>	Additionally, the value of out of band response shall not exceed 0.1% at any wavelength more than 50 nm from the corresponding 50% response band edge.	A, T		<b>YES</b>
<b>9.3.2.3</b>	<b>Edge Slope</b> (header only)			
<b>9.3.2.3.a</b>	The wavelength interval between the first 5% and the first 50% of peak response and the last 50% and the last 5% of peak response ranges shall not exceed the values in Table 9.3.2.3-1.	A, T		<b>YES</b>
<b>9.3.2.3.b</b>	The wavelength interval between the 1% response points and the corresponding 50% response band edge shall not exceed the values in Table 9.3.2.3-1.	A, T		<b>YES</b>
<b>Table 9.3.2.3-1</b>	<b>Edge Slope Intervals for LDCM optional reflective bands</b>	A, T		<b>NA</b>

**FINAL DRAFT**  
Created on 4/16/2002 9:07 PM

<b>9.3.2.4</b>	<b>Spectral Uniformity</b> The bandwidth shall vary by no more than $\pm 3\%$ across pixels within a band. Additionally see section 9.5.2.3.			<b>??</b>
<b>9.3.2.5</b>	<b>Spectral Stability</b> Band center wavelengths and band edges shall not change by more $\pm 2$ nm over the expected life of the mission.	<b>A, T</b>		<b>??</b>
<b>9.3.2.6</b>	<b>Spectral Band Simultaneity</b> For any point within a single scene observed by the LDCM, the LDCM shall acquire data for all spectral bands within a two-minute period.	<b>A, T</b>		<b>YES</b>
<b>9.4</b>	<b>LDCM Spatial Resolution</b> (header only)			
<b>9.4.1</b>	<b>Ground Sample Distance</b> (header only)			
<b>9.4.1.1</b>	<b>Coastal/Aerosol Band Ground Sample Distance</b> (header only)			
<b>9.4.1.1.a</b>	Unprocessed LDCM digital image data shall provide a pixel-to-pixel increment equivalent to a ground sampling distance (GSD) of 30 m or less across the WRS-2 scene for LDCM spectral band 1 (refer to Table 9.3.1-1).		<b>T</b>	<b>YES</b>
<b>9.4.1.1.b</b>	LDCM Level 1R digital image data shall provide a pixel-to-pixel increment equivalent to a ground sampling distance (GSD) of 30 m or less across the WRS-2 scene for LDCM spectral band 1 (refer to Table 9.3.1-1).		<b>T</b>	<b>YES</b>
<b>9.4.1.2</b>	<b>Cirrus Band Ground Sample Distance</b> (header only)			
<b>9.4.1.2.a</b>	Unprocessed LDCM digital image data shall provide a pixel-to-pixel increment equivalent to a GSD 120 m or less across the WRS-2 scene for LDCM spectral band 9 (refer to Table 9.3.1-1).		<b>T</b>	<b>NA</b>
<b>9.4.1.2.b</b>	LDCM Level 1R digital image data shall provide a pixel-to-pixel increment equivalent to a GSD 120 m or less across the WRS-2 scene for LDCM spectral band 9 (refer to Table 9.3.1-1).		<b>T</b>	<b>NA</b>

**FINAL DRAFT**  
Created on 4/16/2002 9:07 PM

9.4.2	<b>Edge Response</b> The mean relative edge response slope in the in-track and cross-track directions (mean of slope between 40%-60%) for Level 1R digital image data shall conform to the criteria described in the following subsections. <b>Note:</b> Table 9.4.2-1 lists the bands, their maximum allowable GSD, and the minimal edge slope. The edge response, in the context below, is the normalized response of the imaging system to an edge. That is, the edge response is normalized so that the mean minimum edge response is set to zero and the mean maximum response is set to 100%.	A, T		
Table 9.4.2-1	<b>GSD/Minimum Slope Specification</b>	A, T		
9.4.2.1	<b>Coastal/Aerosol Band Edge Response Slope</b> The mean relative edge response slope for the coastal/aerosol band, LDCM spectral band 1 (< 30 m), shall exceed 0.027/meter for Level 1R digital image data across the entire Field-of-View.	A, T		<b>YES</b>
9.4.2.2	<b>Cirrus Band Edge Response Slope</b> The mean relative edge response slope for the cirrus band, LDCM spectral band 9 (< 120 m), shall exceed 0.006/meter for Level 1R digital image data across the entire Field-of-View.	A, T		<b>NA</b>
9.4.3	<b>Edge Response Overshoot, Aliasing, and Stray Light Rejection</b> The requirements of 5.3.3, 5.4, and 5.5 shall apply to the optional reflective bands.			<b>NO</b>
9.4.4	<b>Band 1 Edge Response Uniformity</b> The mean relative edge response slope shall not vary by more than 10% in any band across the Field-of-View and by not more than 20% between LDCM spectral bands 1,2,3,4,5,6,and 7 for Level 1R digital image data.	A, T		<b>YES</b>
9.5	<b>LDCM Radiometry</b> (header only)			

**FINAL DRAFT**  
Created on 4/16/2002 9:07 PM

<b>9.5.1</b>	<b>Absolute Radiometric Accuracy</b> The digital values in a Level 1 data product shall be linearly scaled to at-aperture spectral radiance with an uncertainty less than or equal to 5% (1 sigma) with a goal of 3% (1 sigma) across the range of 0.3 L typical to 0.9 L max (Table 9.5.1-1), with all accuracies established relative to National Institute for Standards and Technology (NIST) standards.			<b>NO</b>
<b>Table 9.5.1-1</b>	<b>Radiance Levels for SNR Requirements and Saturation Radiances</b>	<b>A, T</b>	<b>T</b>	
<b>9.5.2</b>	<b>Radiometric Precision</b> (header only)			
<b>9.5.2.1</b>	<b>Pixel Signal-to-Noise Ratios</b> Signal to noise ratios required for LDCM Level 1 digital image data and for each spectral band are listed in Table 9.5.1-1 and 9.5.2-1.	<b>T</b>	<b>T</b>	
<b>9.5.2.1.a</b>	50% of the pixels shall meet or exceed these SNR values.	<b>T</b>	<b>T</b>	<b>YES</b>
<b>9.5.2.1.b</b>	99% of the pixels shall exceed 80% of these values.	<b>T</b>	<b>T</b>	<b>YES</b>
<b>Table 9.5.2-1</b>	<b>SNR Requirements and Goals</b>	<b>T</b>	<b>T</b>	
<b>9.5.2.2</b>	<b>Quantization Noise Limit</b> The requirements of Section 6.2.2 shall apply to the optional reflective bands.			<b>YES</b>
<b>9.5.2.3</b>	<b>Pixel-to-Pixel Uniformity</b> The requirements of Section 6.2.3 for bands 2-7 shall apply to the optional reflective bands.			<b>NO</b>
<b>9.5.2.4</b>	<b>Coherent Noise</b> The requirements of Section 6.2.4 shall apply to the optional reflective bands.			<b>NO</b>
<b>9.5.3</b>	<b>Dynamic Range</b> The LDCM Level 0 and Level 1 digital image data shall cover, without saturating, signals up to the L max as shown in Table 9.5.1-1. <b>Note:</b> For band 1, this corresponds to the radiance reflected off of a Lambertian target of 100% reflectance illuminated by the sun at a solar zenith angle of 20°.	<b>A, T</b>		<b>YES</b>

**FINAL DRAFT**  
Created on 4/16/2002 9:07 PM

9.5.4	<b>Polarization Sensitivity, Radiometric Stability, and Image Artifacts</b> The requirements of Section 6.4, 6.5, and 6.6 shall apply to the optional reflective bands			<b>NO</b>
9.6	<b>LDCM Geometric Precision, Geolocation, and Cartographic Registration</b> (header only)			
9.6.1	<b>Level 1G Nearest Neighbor Product Band-to-Band Registration</b> Corresponding pixels from the digital images of the spectral bands in Level 1G data products created using the nearest neighbor resampling method, as specified in section 2.3.2.a, shall be co-registered with an uncertainty as specified in Table 9.6.1-1, in the line and sample directions at the 90% confidence level for target areas within 100 meters of the WGS84 (G873 or current version) Earth ellipsoid surface.	A	T	<b>NA</b>
Table 9.6.1-1	<b>Level 1G Nearest Neighbor Band Registration Requirements</b>		T	<b>NA</b>
9.6.2	<b>Level 1G Data Product Band-to-Band Registration</b> Corresponding pixels from the digital images of the spectral bands in Level 1G data products created using the resampling methods specified in sections 2.3.2.b through 2.3.2.d shall be co-registered with an uncertainty as specified in Table 9.6.2-1, in the line and sample directions at the 90% confidence level for target areas within 100 meters of the WGS84 (G873 or current version) Earth ellipsoid surface.		T	<b>NA</b>
Table 9.6.2-1	<b>Level 1G Band Registration Requirements</b>		T	<b>NA</b>
9.6.3	<b>Registration and Geodetic Accuracy</b> The requirements of Sections 7.2 through 7.5 shall apply to the optional reflective bands.			<b>NA</b>

## **Appendix B: Stray Light Analysis and Impact on Flight Data**

### *INTRODUCTION*

The stray light of the ALI may be divided into three components: mirror scatter, black paint scatter, and filter scatter. The mirror and black paint scatter affect large regions (>3 degrees) and will be discussed first. The filter scatter affects much smaller regions (<0.25 degrees) and is discussed later.

### *MIRROR AND BLACK PAINT SCATTER*

A significant portion of ALI stray light is the result of scatter from the primary and tertiary mirrors. The ALI optical fabrication priorities were to first produce mirrors with correct figuring to achieve the required image sharpness over the full 15 x 1.3 degree field of view. Mirror finish was lower on the priority list. The SiC mirrors produced by SSG Inc. for the ALI were of excellent figure quality but constrained by EO-1 programmatic considerations (budget, schedule) in obtaining optimum BRDF performance [B-1,B-2]. Based on mirror BRDF measurements performed by SSG Inc. and Schmitt Measurement Systems and analysis by Lambda Research Corp. [B-3], the EO-1 SiC mirrors did not meet the EO-1 adopted Landsat 7 specification for scattered light. It was concluded by the EO-1 project office [B-1,B-2] that the ALI telescope mirror surface quality was reasonably good and comparable to other Earth sensing instruments and that the full set of NMP technology validation objectives for ALI were realizable without additional mirror polishing. Lincoln Laboratory proceeded with integrating the ALI and performed a thorough instrument system calibration.

A separate NASA funded technology program was conducted by SSG Inc., which demonstrated component level BRDF consistent with the Landsat 7 stray light specification. Silicon clad SiC aspheric optics and uncoated SiC flat optical surfaces were demonstrated to have BRDF, which met all requirements. These demonstrations units also included a full scale ALI spare primary mirror, which was processed after the flight telescope had been delivered.

### *STRAY LIGHT MODELING*

A methodology for assessing the effect of telescope stray light on the measurement of scene radiance was developed. It was based on a generalization of the Stray Light Analysis Report No. 3 by Lambda Research [B-3]. The analysis also included the effects of the reflective baffle, which defined the aperture stop, at the secondary mirror. The black paint used on the baffle was Aeroglaze Z- 306. The stray light contribution from this effect amounted to 1%. The results provide a useful and simple tool for estimating the effects of stray light.

Assumptions:

1. The scene geometry is the same as for the Landsat specification, consisting of a large annular background region surrounding a small circular target region.
2. The scattered background radiance falling into the target region is due to both mirror scatter [B-3] and scatter from the reflective baffle. The major contribution from mirror scatter comes from approximately 3 degrees around the target region. The contribution from the black reflective baffle is defined as 1% of a 3 degree background region, centered on the target.
3. The fraction of background radiance falling into the target region is a constant.

**FINAL DRAFT**  
Created on 4/16/2002 9:07 PM

4. The fraction of target radiance that is scattered out is also a constant and is the total integrated scatter (TIS) from the referenced report.
5. The radiometric calibration is based on a very low spatial frequency standard, e.g., a large extended near field source.

Definitions:

- $L_B$  = The true background radiance
- $L_B^*$  = The estimated background radiance
- $L_T$  = The true target radiance
- $L_T^*$  = The estimated target radiance
- $\Delta L_T$  = The uncalibrated target radiance error due to the telescope stray light
- $\Delta L_B$  = The calibrated background radiance error due to the telescope stray light
- $\sigma_B$  = The fraction of background radiance falling into any target region
- $\sigma_T$  = The total fraction of radiance that is scattered from any portion of the scene

The resulting radiance errors are:

$$\Delta L_B = L_B^* - L_B = 0$$

$$\Delta L_T = L_T^* - L_T = [\sigma_B / (1 - \sigma_T + \sigma_B)] [L_B - L_T]$$

$$\Delta L_T / L_T = \varepsilon [L_B / L_T - 1.]$$

Table B-1: Stray Light Parameters

Band	$\sigma_T$ (%)	$\sigma_B$ (%)	$\varepsilon$ (%)
Pan	6.5	3.6	3.5
MS-1	15.5	7.6	8.3
MS-2	10.9	5.5	5.8
MS-3	7.6	4.1	4.2
MS-4	4.4	2.7	2.7
MS-5	0.9	1.3	1.3
MS-7	0.5	1.2	1.2

Stray light may be an issue for measurements on dark scenes near very large and very bright regions and conversely for small bright scenes surrounded by large dark regions. This is especially true at the shorter wavelengths. The on-orbit effects of stray light on the ALI have been quantified and the results are summarized in this Appendix.

*ON-ORBIT STRAY LIGHT CHARACTERIZATION*

Two types of data have been used to characterize the ALI stray light performance: limb scans and nominal Earth scenes containing uniform regions. The limb scans were used to evaluate the off-axis scatter of the ALI mirrors and

black paint. The Earth scene data were compared to Landsat 7 ETM+ and ground truth data to evaluate the impact of stray light for a variety of scene contrasts.

### Limb Scan Observations

The off-axis stray light characteristics of the ALI have been investigated by scanning the Earth's limb across the telescope field of view. Four limbs scans were performed in 2001, scanning in the +pitch, -pitch, +roll, -roll directions. For each observation, the instrument begins collecting data with the Earth completely filling the ALI FOV. The instrument is then pitched or rolled until the Earth's limb is 50° off-axis and the ALI is viewing deep space. A plot of an individual detector's response over time traces the transition from Earth observing to space observing events. The Earth limb profile for a +roll scan as viewed by detector 100 for Band 3 is depicted in Figure B-1.

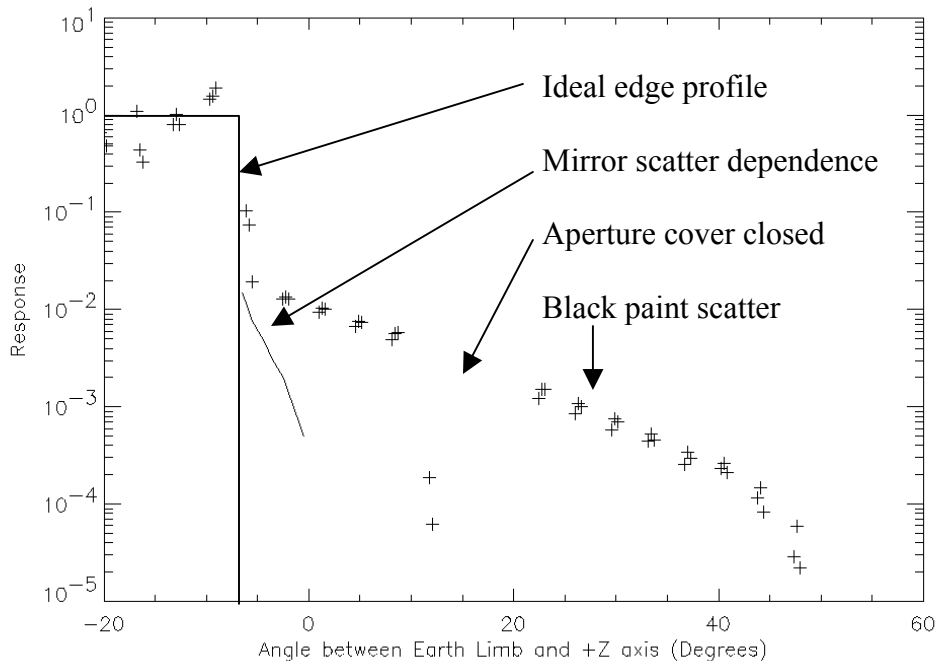


*Figure B-1: Earth limb scan history for detector 100, Band 3.*

The Earth's limb is located at the -7° position (angle of the detector FOV relative to the boresight). An instrument with zero stray light effects will observe a limb profile that is the product the limb's natural illumination falloff with altitude and the instrument edge spread function. An idealized edge profiles (step function) is overlaid in Figure B-1. The effects of stray light are evident for angles up to 40 degrees off-axis. Also overlaid in Figure B-1 is the expected ideal profile for the ALI based on the stray light analysis of the mirrors conducted by Lambda Research Corporation [B-3]. Clearly, the expected falloff due to stray light effects from the mirrors alone does not match the observed profile. This data confirms the effects of scatter from the Z306 black paint inside of the telescope. These data are also useful for they define the angular dependency of all ALI stray light sources in the +pitch, -pitch, + roll,

# FINAL DRAFT

Created on 4/16/2002 9:07 PM

and - roll directions. Finally, the effect of the black paint (1%) is equivalent to that of the mirror scatter for small angles but is the dominant source of stray light for larger angles.

## Earth Observations

The impact of stray light for typical Earth scenes and the validity of the stray light model discussed previously have been evaluated by comparing diffuse scenes as seen by the ALI, the Landsat 7 ETM+, and ground truth data. EO-1 and Landat 7 are flying in formation, allowing for data from the same scene to be collected by the ALI and ETM+ with only a one-minute separation. The ground truth data are collected during both observations.

For the comparison, the radiance of a spatially uniform region of a scene is extracted from the ALI, ETM+, and ground truth data. The ratios of the ALI data to similar ETM+ data (bands 1, 2, 3, 5) and ground truth data are then plotted as a function of the *radiance ratio*,  $t/b$ . The *radiance ratio* is calculated from the ETM+ data and is defined as the ratio of the mean target radiance to the mean background radiance, defined by a circle  $3^\circ$  in radius and centered on the target region. In this context, the *radiance ratio* is defined as the *true* contrast of the region being evaluated for stray light effects.

The predicted impact of stray light on the ALI data as a function of  $t/b$  for Band 3 is provided in Figure B-2. For regions where the target radiance is greater than the background radiance, the expected stray light error is  $-3\%$  and is dominated by the effect of light being scattered out of the target region into the surrounding background region due to the effects of total integrated scatter. For targets whose radiance is much lower than the mean background radiance, the impact of stray light is the result of light being scattered from the bright background into the dim target regions.

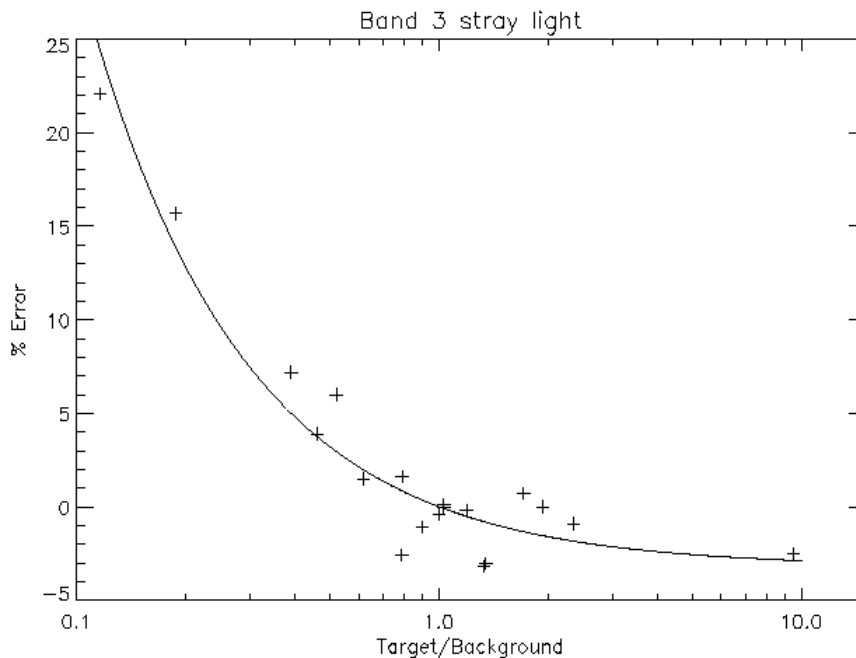


Figure B-2: Stray light model and flight data for Band 3.

# FINAL DRAFT

Created on 4/16/2002 9:07 PM

Also plotted in Figure B-2 is the result of an ALI, ETM+, and ground truth comparison for scenes containing a variety of  $t/b$  values. The scenes used for this analysis included Maricopa, Arizona, Suez Canal, Antarctic Ross Ice Shelf, Cuprite, Nevada, Barreal Blanco, Argentina, and the San Francisco Salt Ponds.

The model and data agree qualitatively and indicate a substantial rise in the expected radiometric error for targets with low radiance ratios for this band (3). This analysis was extended to also assess the effects of stray light for Bands 1, 2, 5 and 7 (these ALI bands are very similar to the corresponding ETM+ bands). The results for Bands 1, 2, and 3 are shown in Figure B-3. The derived values of the scattering parameter  $\epsilon$ , for all the bands, are summarized in Table B-2.

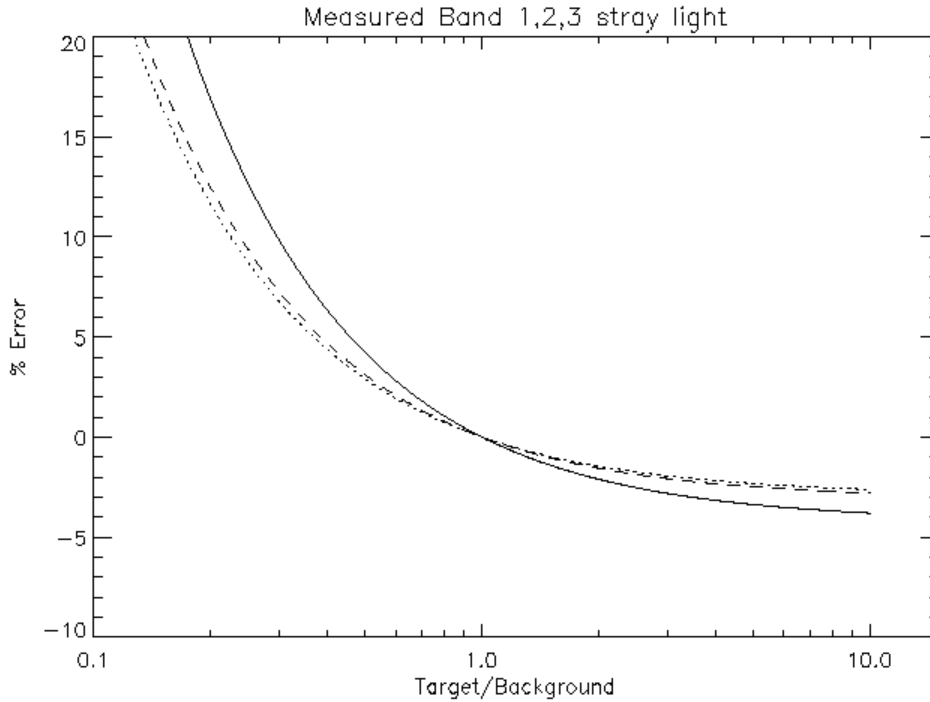


Figure B-3: Effects of stray light for bands 1 (solid), 2 (dotted), 3 (dashed). These results have been derived by fitting the stray light model to flight data.

Table B-2: Radiance errors derived from the stray light model and flight data.

Band	Radiance Error $\epsilon$ (%) Theoretical	Radiance Error $\epsilon$ (%) Measured
1	8.3	4.2
2	5.8	2.9
3	4.2	3.1
4	2.7	-

# FINAL DRAFT

Created on 4/16/2002 9:07 PM

5	1.3	<1.0
7	1.2	<1.0

The SWIR stray light data suggest little impact for all radiance ratios  $t/b > 0.75$ . However, it must be noted that the stray light analysis could not be extended below  $t/b = 0.75$  due to the large scatter in the ALI and ETM+ data as a result of low signal in these bands. Significant error due to stray light is expected and observed for SWIR data with  $t/b < 0.75$  (e.g. small lakes). The data and model also indicate an increasing effect of stray light with decreasing wavelength, particularly for  $t/b < 1.0$ . However, the flight data suggest the magnitude of the stray light impact is less than predicted by the model for the VNIR bands (Table B-2).

## IMPACT ON FLIGHT DATA

In principle, the effects of stray light on a particular target could be assessed if the radiance ratio for the target was known. However, the effects of large off-axis scattering by the black paint on the interior of the telescope cavity can be problematic in some instances. As an example of the utility of the stray light model and the effects of the black paint scatter, a scene of the West Coast of Africa is shown in Figure B-4.

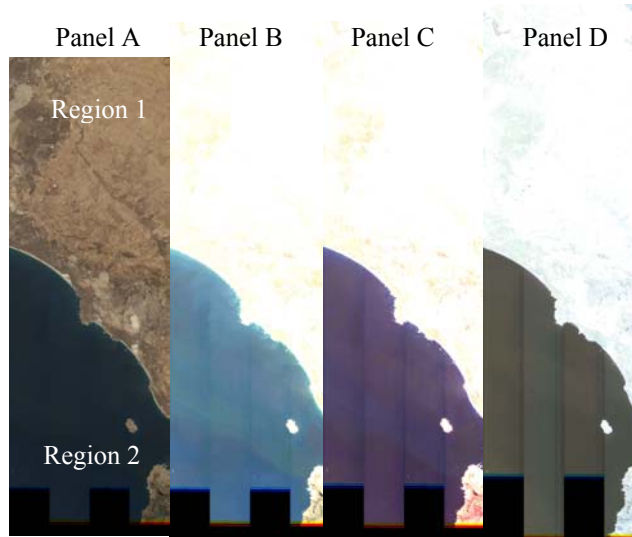


*Figure B-4: Stray light impact example for West Coast, Africa scene. The effects of black paint scatter in the water is evident in the enhanced images in panels B, C, D.*

Panel A is a true-color, Band 321, image that has been radiometrically calibrated. Regions 1 and 2 have radiance ratios near 1.0 and so the predicted radiometric error due to stray light is minimal. Panels B, C, and D are three-color images defined by bands 321, 432, and 755p respectively. These images have been stretched to enhance the region

## FINAL DRAFT

Created on 4/16/2002 9:07 PM

of water off the African coast. Although the radiometric model predicts minimal stray light in this region, clear 3-10% SCA-to-SCA banding is evident. The stray light effects observed off the African coast are the result of large off-axis angle scattering of the in-land region photons off the black-paint behind the secondary mirror. To properly account for this effect, a second background region, extending more than ten degrees, would be needed. Since the ALI field of view is only 3 degrees, an independent measure of the extended background radiance is required.

Finally, it should be noted that extended off-axis scattering by the black paint only becomes problematic for large regions with relatively low radiances. This is because the scattering effect of the paint is approximately 1% of the mean of the extended background. For small regions ( $< 3^\circ$ ) the model discussed above is appropriate. For larger regions, the effects of the black paint scatter are small if the target radiance approaches or exceeds the extended background radiance. However, for large regions with low radiance levels (e.g. water) and a relatively high, extended background radiance (e.g. land, clouds, ice), the  $3^\circ$  assumption for the background region breaks down and the 1% scatter effect of the black paint becomes significant.

### *FILTER SCATTER*

Evidence for a third source of stray light manifests itself as a 1% *echo* or *ghost* following the primary image for Bands 5p, 5, and 7. This artifact is clearly observed in lunar calibration and lava flow data.

#### Lunar Calibration

During an ALI lunar calibration, the Moon is scanned in each of the four sensor chip assemblies or SCAs. Figure B-5 depicts the raster scanning technique used during a typical lunar observation. Figure B-6 is a photo of the ALI SCA module with the scan path of the moon overlaid.

Lunar images, created from each of the ten ALI bands for SCA 1, are shown in Figure B-7. After stretching the image and zeroing the main lunar image, any residual stray light effects are revealed (Figure B-8). Clearly, an elongated secondary image of the Moon is observed after the primary image in Band 5p, 5, and 7. Another ghost image is also seen prior to the image for Band 1p. No obvious ghosting effects are seen in the VNIR bands.

The characteristics of the lunar ghost are:

1. Observed for Bands 1p, 4, 4p, 5p, 5, 7
2. Restricted to in-track only
3. Band 1p effect on opposite side of the SWIR effects
4. Always occur after the main image
5. Band 7 ghost 62 frames long
6. Band 5 ghost 44 frames long
7. Band 5p ghost 18 frames long
8. Ghost intensities are ~1% of the average Lunar brightness

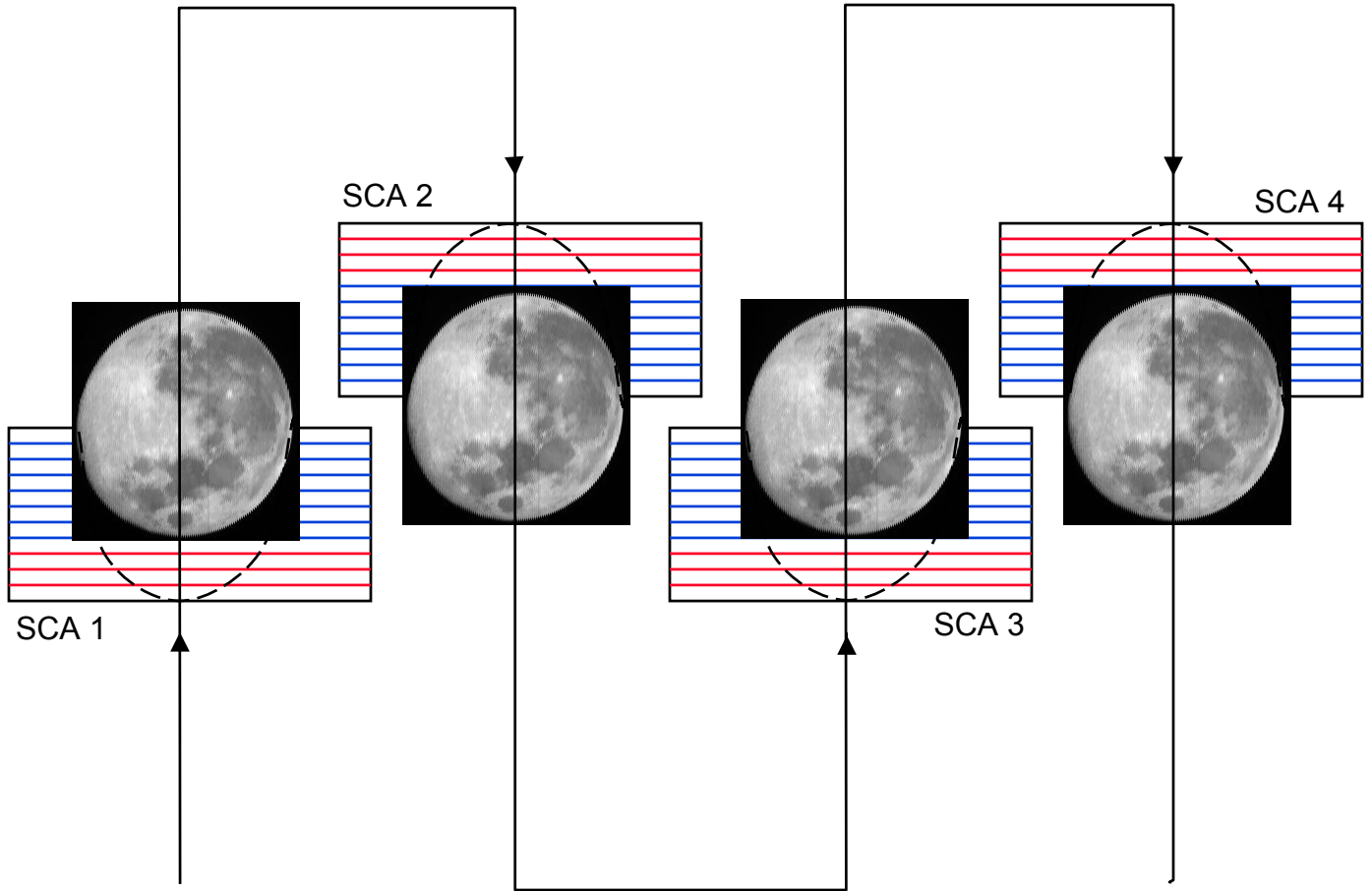
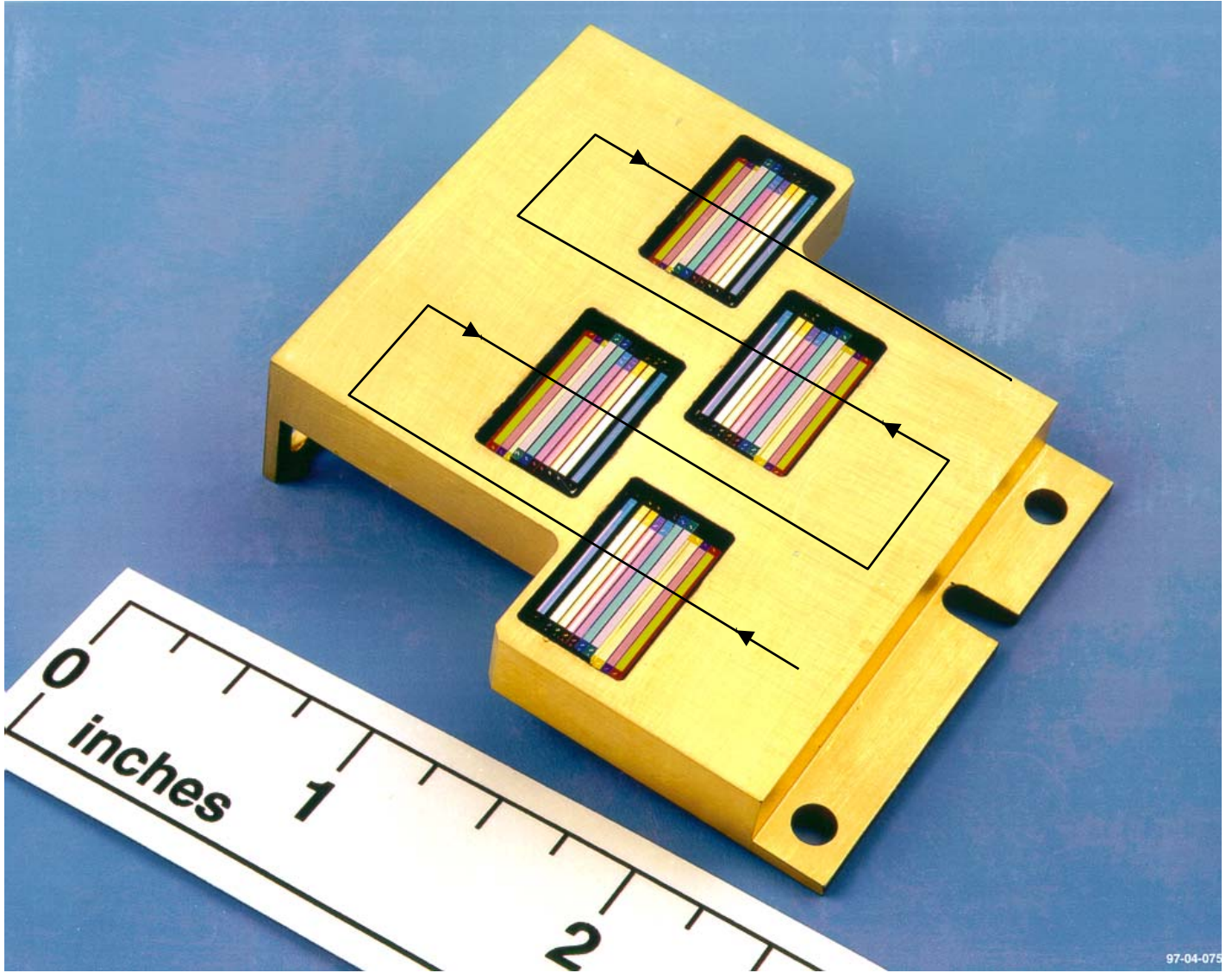
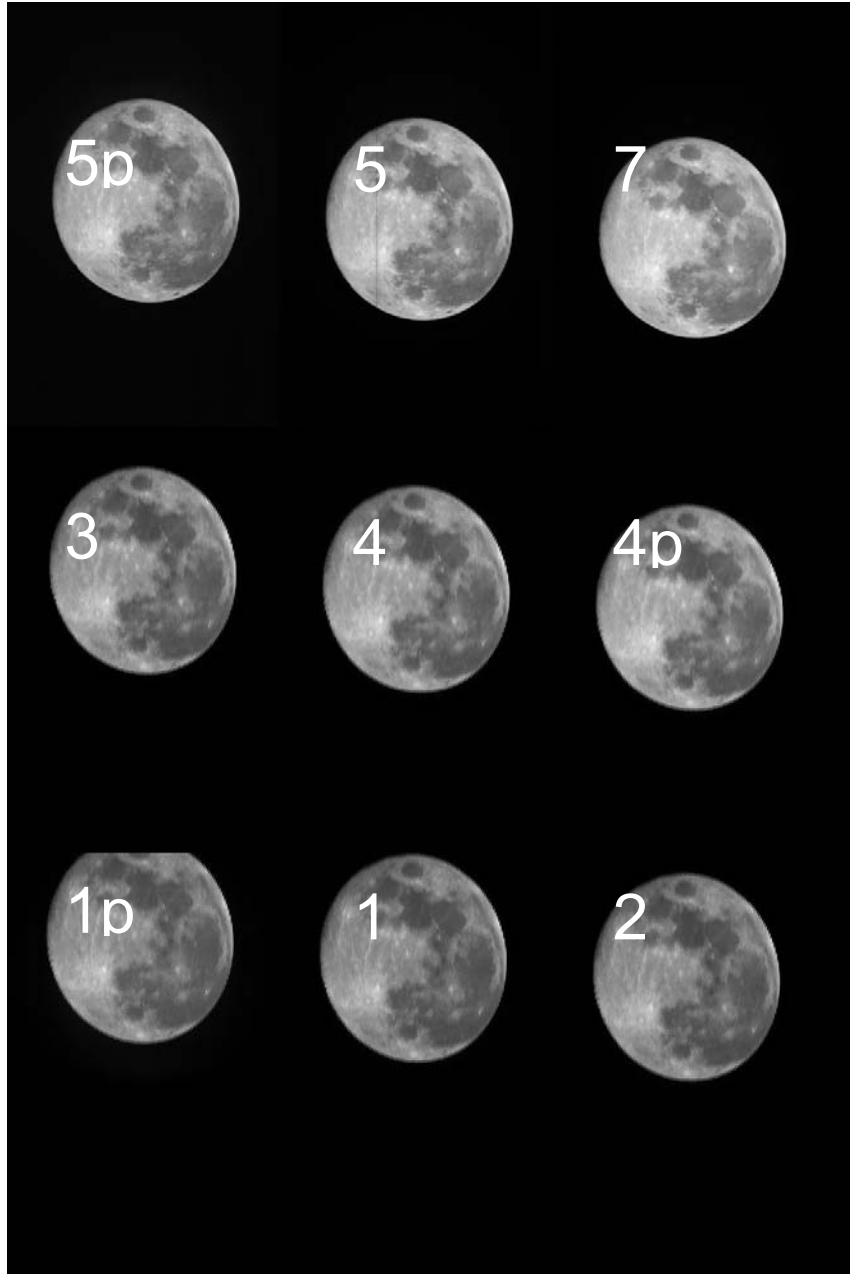


Figure B-5: Raster scan for a typical ALI Lunar calibration.



*Figure B-6: Direction of a typical Lunar calibration scan on the SCA module.*



*Figure B-7: Images of the moon from a typical Lunar calibration.*

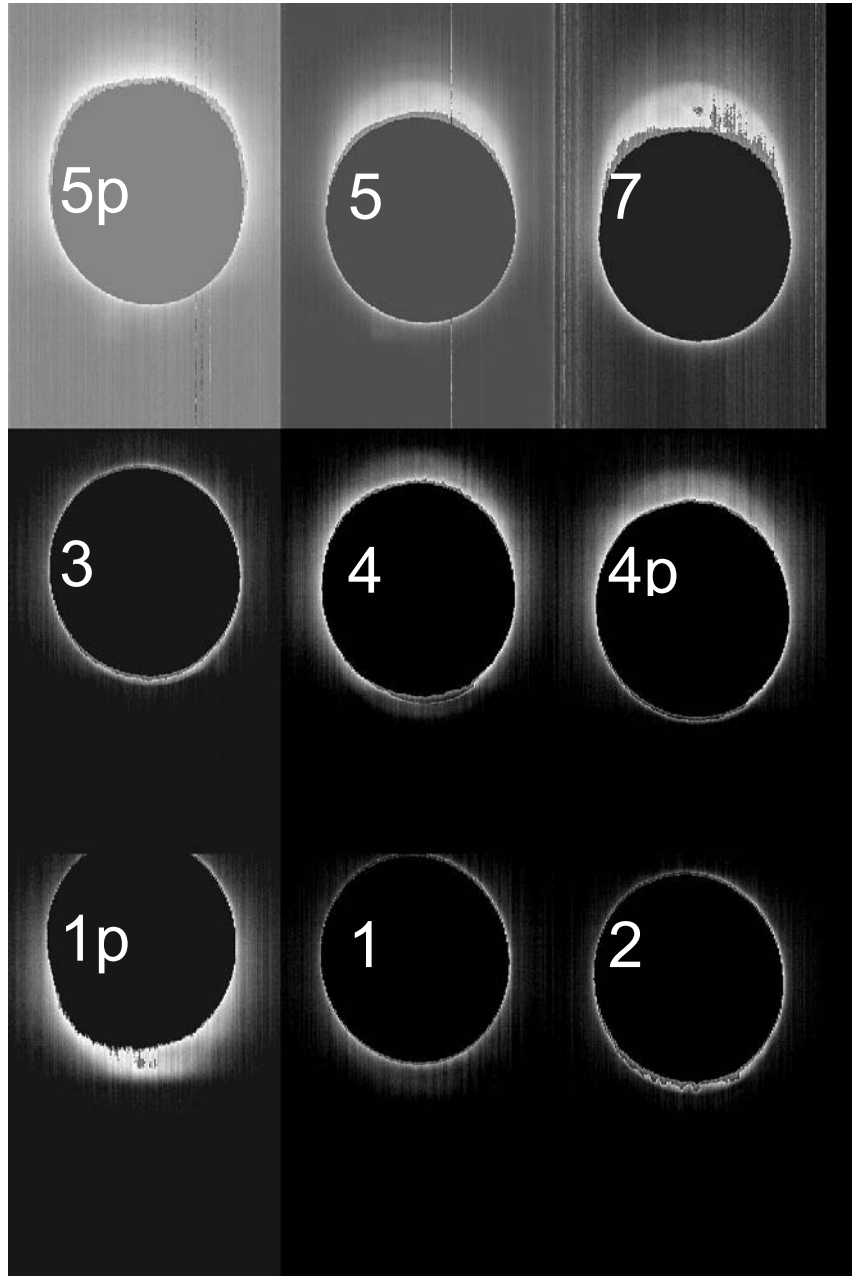


*Figure B-8: Stretched images from a typical Lunar calibration.*

## FINAL DRAFT

Created on 4/16/2002 9:07 PM

### Lava Flow Observation

Ghost images have also been observed in the Mount Etna observation on 203091955. During this observation, active lava flows were visible and observed by the instrument. These flows are highly luminous and saturate the ALI in Bands 5 and 7. Additionally, ghost images appear after the primary lava flow images and are observed in Bands 5p, 5, and 7.

Figure B-9 provides an example of the lava flow ghost images for Band 7. The characteristics of the lava flow ghosts are :

1. Observed for Bands 5p, 5, 7
2. Restricted to in-track only
3. Always occurs after the main image
4. Odd and even pixels appear shifted by 15 frames within the ghost image
5. Band 7 ghost 53-65 frames long
6. Band 5 ghost 43 frames long
7. Band 5p ghost 14-23 frames long

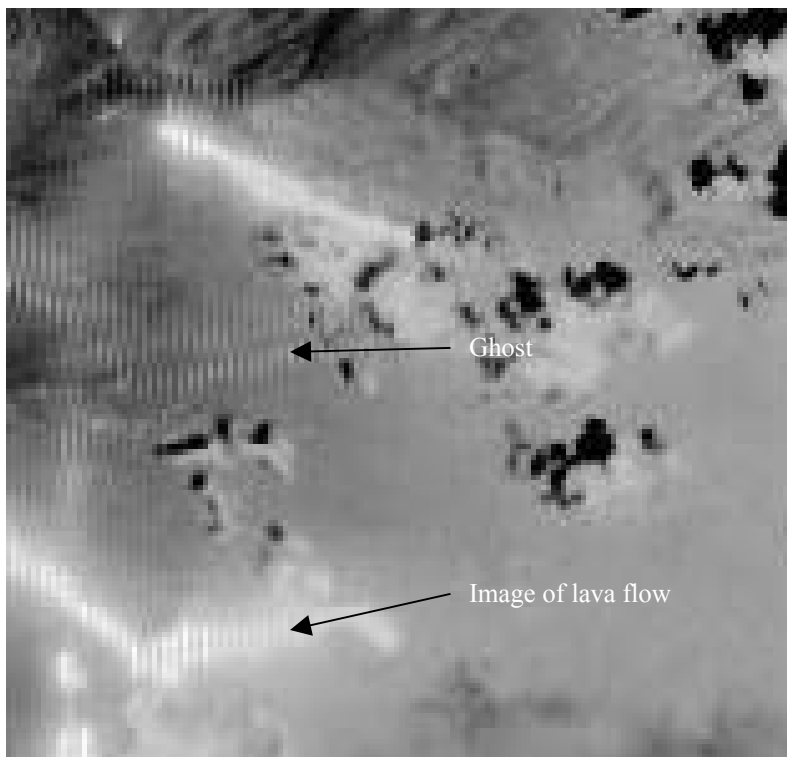


Figure B-9: Ghosting effects observed in Mount Etna lava flows (Band 7).

## Ghost Generation Model

The current ghost generation model is based on the scatter of light, at the interface of the VNIR and SWIR filter blocks located directly above the detector arrays, onto the SWIR filters. Figure B-10 provides a cross-section of the focal plane filters and indicates the ghost generation scattering point.

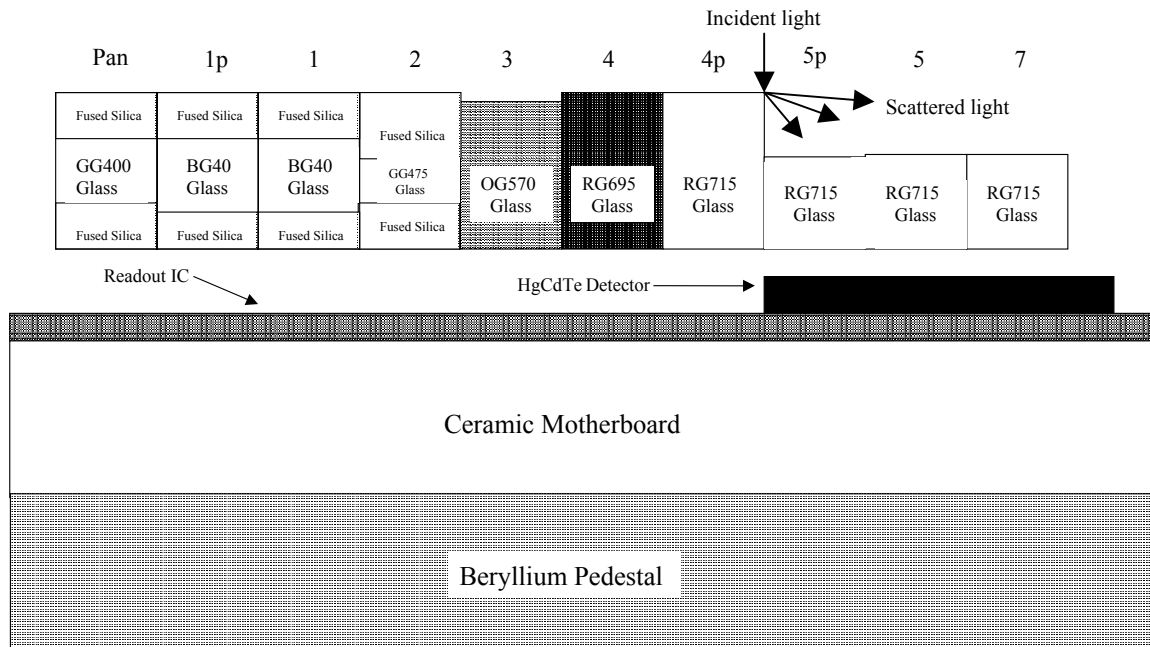


Figure B-10: Cross section of ALI SCA. The ghost generation model assumes light is scattered from the discontinuity at the boundary between the VNIR and SWIR filter assemblies.

When considering the observed lunar calibration ghost, it is useful to separate the imaging processes into separate components (Figure B-11). Initially, the image of the moon is projected onto the SWIR filter surfaces prior to being imaged by the VNIR arrays. No portion of the image of the lunar disk intersects the VNIR/SWIR filter boundary and no scattering occurs. Once the image reaches the VNIR/SWIR filter interface and the VNIR bands begin to record the image of the moon, a portion of the disk intersects the filter boundary, and in-track scattering occurs. However, as long as the portion of the lunar image intersecting the boundary is less than the width of the image intersecting the SWIR arrays the scattered image will overlap the lunar disk image and no obvious ghost will appear. This ghosting effect will add a 1% uncertainty to the primary lunar image. Once, the extent of the lunar image interacting with the filter boundary exceeds the portion of the lunar image intersecting the SWIR arrays and the scattered light 'spills over' to the region outside the lunar limb and the ghost image begins to appear. However, the

## **FINAL DRAFT**

Created on 4/16/2002 9:07 PM

extent of the cross-track width of the ghost is limited to the extent of the lunar image intersecting the filter boundary. The ghost image will continue to develop, appearing to trace the lunar limb, until the down-track image of the moon passes the VNIR.SWIR filter boundary.

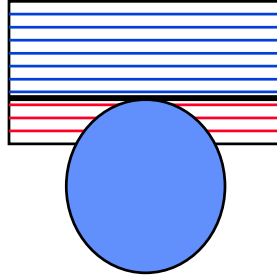
The generation of lava flow ghost images also relies on the in-track scattering of an image at the VNIR/SWIR filter boundary (Figure B-12). Initially, the image of the flow is constrained to be within the SWIR filter region and no scattering occurs. However, once the flow image begins to intersect the boundary, light is scattered back into the SWIR filter region. If the scattered light cross-track dimension exceeds the image of the flow within the SWIR bands, a ghost effect appears. In this manner, the intricate structure of the flow will be 'traced' in the down-track SWIR data as it did in the lunar data.

The ghost model, as defined above, predicts several characteristics that should be observable in the lunar and lava flow data. One of the key predictions is that the Band 7 ghost should be the largest and be 3 times that of Band 5p and 1.5 times that of Band 5. Additionally, odd and even detectors for each band should be illuminated simultaneously by the scattered light, resulting in an odd-even effect in reconstructed images. Both of these effects are observed in the lunar and lava flow data. All of the ghost model predictions are listed in Table B-3, along with the status of the verification in the ALI data.

**FINAL DRAFT**  
Created on 4/16/2002 9:07 PM

Position

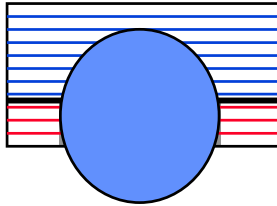
Limb approaches boundary



Results

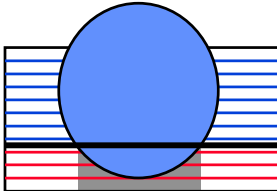
Reflections begin but are contained within the lunar image. No ghosting observed.

Intersection of image with boundary exceeds intersection of image with Band 7 array.



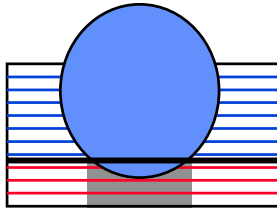
Reflections begin to exceed lunar image for Band 7 - Ghost image begins near center of lunar image for this band. Constrained to width of lunar image.

Limb crosses Band 7



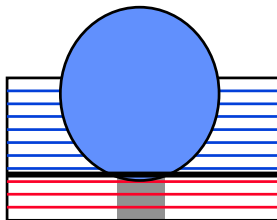
True image for Band 7 ending. Ghost for Band 7 reducing in cross-track to extent of lunar image intersecting with boundary.

Limb crosses Band 5



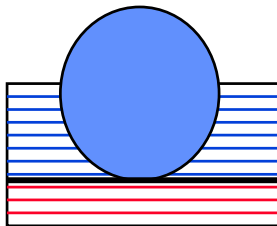
True image for Band 5 ending. Ghost for all SWIR bands restricted to extent of lunar image intersecting with boundary.

Limb crosses Band 5p



True image for Band 5p ending. Ghost for all SWIR bands restricted to extent of lunar image intersecting with boundary.

Limb crosses



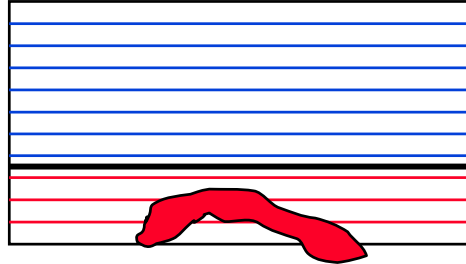
All reflections end. No ghosting observed.

*Figure B-11: Generation of Lunar ghosts by scattering off the VNIR/SWIR filter boundary.*

Position

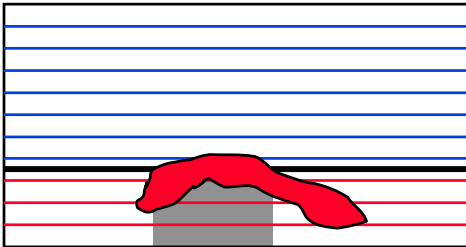
Results

Lava flow approaches boundary.



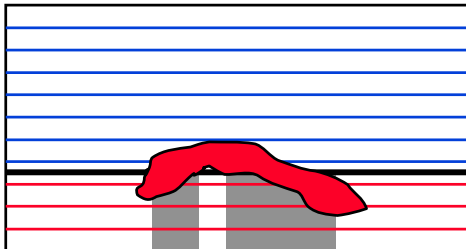
No reflections. No ghosting observed.

Lava flow image begins to cross boundary.



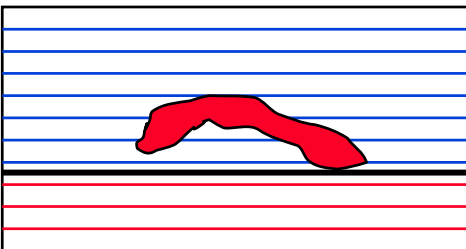
Reflections begin but are constrained to that part of the flow image interacting with the boundary.

One-half of flow beyond boundary.



Reflections continue but vary according to that part of the flow image interacting with the boundary, creating a "reflected image" of the flow.

Lava flow exits boundary.



All reflections end. No ghosting observed.

Figure B-12: Generation of lava flow ghosts by scattering off the VNIR/SWIR filter boundary.

# FINAL DRAFT

Created on 4/16/2002 9:07 PM

Table B-3: Ghost generation model predictions.

Prediction	Status
Band 7 ghost 3x that of Band 5p	Confirmed – lunar/lava
Band 7 ghost 1.5x that of Band 5	Confirmed – lunar/lava
Ghost will appear after primary image and will be limited to in-track	Confirmed lunar/lava
Ghosts will appear to trace primary image's spatial signature	Confirmed – lunar/lava
No ghosts will occur in the VNIR	Confirmed – lunar/lava
Odd/Even effects will occur in the reconstructed image	Confirmed – lunar/lava
Lunar ghost will occur before the primary image if the lunar scan direction is reversed	Unconfirmed - Special lunar calibration scheduled (April 2002)
Ghosts will occur before the primary image for SCA 1 and 3 for normal DCEs	Unconfirmed – Special image of a flare a night for SCA 3 and 4 scheduled (April 2002)

## Discussion

The ghost image effects observed in the ALI lunar are approximately 1% of the mean lunar irradiance. The model developed to account for this effect predicts all data should have this effect to some degree. The impact of this effect will depend on the local SWIR contrast within a scene. For flat scenes with large diffuse regions, no radiometric impact will occur due to focal plane ghosting. This is because a uniform diffuse scene, which included the effects of ghosting, was used to calibrate the ALI in the laboratory. For other scenes with varying local contrast, the impact on the ALI absolute radiometry will be based on the ratio of the radiance impinging on the filter boundary to the radiance falling on the SWIR arrays from the scene. If the boundary radiance is small or equivalent to the scene radiance, the impact on the scene radiometry is minor. This is the case for the lunar observation when the intersection of the lunar disk with the boundary is smaller than the intersection of the image with the SWIR arrays. However, as the radiance falling on the boundary regions exceeds the radiance on the SWIR arrays, the impact on the absolute radiometry of a scene grows. The extreme cases of this are the lunar and lava flow ghosts. In the lunar image case, the irradiance of the lunar disk is infinitely greater than that of deep space, and an obvious ghost appears. For the lava flows, the radiance of the lava is much greater (saturates ALI detectors) than the surrounding terrain, resulting in the ghost images.

Although the ghost model does account for the observed SWIR effects, it does not explain the ghost observed in Band 1p. However, the reversal of the ghost to occur before the primary image indicated a different mechanism and requires further investigation. No resources have been used to investigate the Band 1p ghost at this time, but it is tempting to attribute the observed effect to a scatter off the bezel surrounding the SCA in much the same manner as was done for the VNIR/SWIR filter boundary described above.

## FINAL DRAFT

Created on 4/16/2002 9:07 PM

If the ghost generation model is correct, this effect can be removed by manufacturing the ALI filter arrays such that no filter boundary occurs between filters. However, care must be taken to preserve the focus of the instrument when aligning filters with different indices of refraction.

### *Conclusion*

The EO-1 Advanced Land Imager stray light from the telescope mirrors and black paint has been characterized on orbit using Earth limb scans and by comparing flight data to ETM+ and ground truth data. The stray light model for these components agrees qualitatively with the flight data for off-axis angles  $< 3^\circ$ . The stray light component caused by the black paint lining the inside of the telescope is the dominant source of stray light for larger off-axis angles and is difficult to assess using only ALI data.

Another stray light generation model, based on the scattering of incident light off the boundary between the VNIR and SWIR filter assemblies, has also been developed and is consistent with ghosting or echo effects observed in the SWIR bands in Lunar and lava flow observations.

For scenes with high contrast (e.g. coastlines, lakes in snow covered areas, mostly cloudy scenes over water) the impact of stray light on the ALI radiometry may become significant. It is therefore recommended that scientific inferences, developed using high contrast ALI data, should be carefully evaluated for stray light effects.

### *References*

[B-1] [eo1.gsfc.nasa.gov/Technology/StrayLightIssues.html](http://eo1.gsfc.nasa.gov/Technology/StrayLightIssues.html)

[B-2] "Report and Recommendations from EO-1 ALI SiC Optics Performance Workshop", May 29, 1998, found at [eo1.gsfc.nasa.gov/Technology/StrayLightIssues.html](http://eo1.gsfc.nasa.gov/Technology/StrayLightIssues.html)

[B-3] "Stray Light Analysis Report No. 3" - prepared by Lambda Research Corporation, Littleton, MA 01460-4400, May 4, 1998

## Appendix C: Focal Plane Contamination

### *Introduction*

Contamination of the focal plane by an unknown substance was recognized in October 1998 during the characterization and calibration of the Advanced Land Imager at Lincoln Laboratory. This contaminant may be completely eliminated by raising the temperature of the focal plane to above 260 K. Prior to launch, several bake outs occurred in an attempt to eliminate the source of the contaminant. In January 1999, the entire instrument was baked out at 303 K while under vacuum for one week and then later for an additional two days. The focal plane was baked out for three hours at 273 K in October 1999 and for one day at 273 K in July 2000 during spacecraft thermal vacuum testing at Goddard Space Flight Center.

In the event that on-orbit bake outs would become necessary, an additional heater was added to the focal plane radiator in February 1999. This heater, along with others on the instrument, will raise the temperature of the focal plane to 270 K in the space environment.

### *Detection*

The monitoring of contaminant deposition on the ALI focal plane during ground testing and on-orbit is performed using the internal reference lamps mounted on the telescope metering truss (Figure C-1). These lamps provide three levels of stable, repeatable reference illumination of the focal plane. However, because the internal reference lamp assembly has a much higher f-number (40) compared to the telescope (7.5), the assembly acts as a microscope for detecting contamination effects. This magnification must be considered when assessing the impact of focal plane contamination on image quality and radiometry. Generally, any apparent spatial variations caused by focal plane contamination should be reduced by a factor of 4 when applied to imagery collected on-orbit.

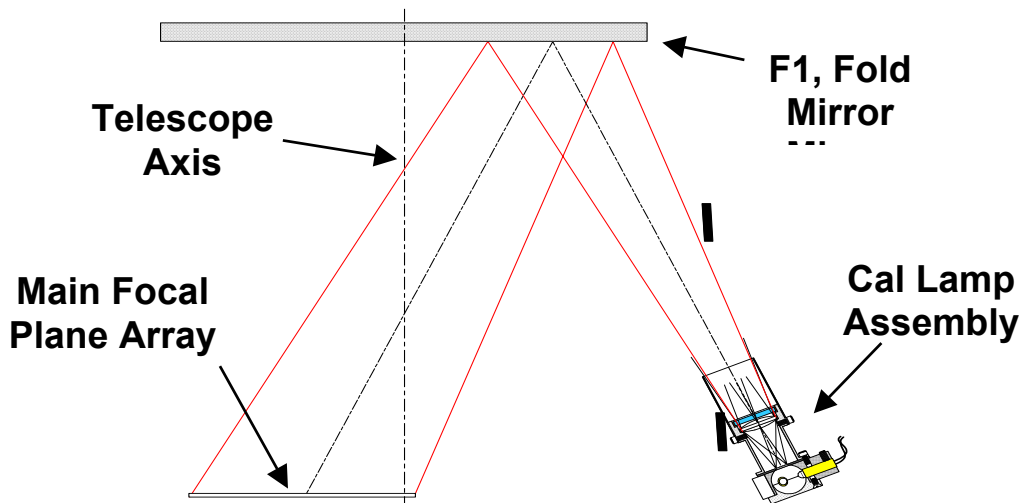


*Figure C-1: Illumination of the ALI focal plane using the internal reference lamp assembly.*

The first step in detecting contaminants is to collect data using the internal reference lamp assembly when the focal plane is considered 'clean'. The dark current subtracted response of the focal plane for each band using the clean

## FINAL DRAFT

Created on 4/16/2002 9:07 PM

data is considered the baseline. Data is then collected once per day over a period of interest. All data are then divided by the baseline data, and the mean and standard deviations of the ratio are then computed for each band. The mean and standard deviations are considered figures of merit for focal plane contamination. If the reference lamps and focal plane are stable, and if no contamination occurs, the mean of the ratios for each day should be unity and the standard deviations should be equivalent to the noise of the detectors.

### *Location of Contamination*

The location of ALI contamination has been identified as the top surfaces of the spectral filters overlaying the focal plane detectors. A CCD camera was placed at the focus of a collimator and images of the filter surfaces were obtained. The left side of Figure C-2 shows a portion of the focal plane filters during a period when contamination had been detected. The image on the right is of the same portion of the filter after the instrument had been baked out. Clearly, a residue had formed on the surface of the filters during contamination build-up. Additionally, all evidence of the residue has been eliminated as a result of the bake out. This conclusion is supported by the levels of post-bake out data returning to baseline levels once the focal plane had been cooled to 220 K.

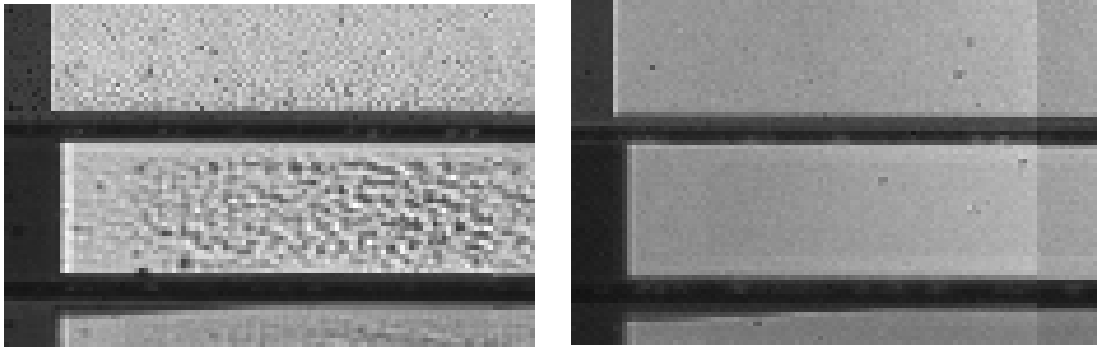


*Figure C-2: Image of a portion of the top surface of the focal plane filters when contaminated (left) and after a bake out (right).*

### *Characteristics*

Focal plane contamination appears in three forms: pixel-to-pixel variation, mean level shifts, and bowing. Pixel-to-pixel variation refers to an apparent random shifting in individual detector responses either above or below the original reference values. As deposition continues, the pixel-to-pixel variations increase and the standard deviations between observations increase.

Another characteristic of contamination is a mean level shift. This refers to the gradual shift of the apparent mean level response of an SCA as contaminants are accumulated on the filter surfaces. This shift usually lowers the mean level of the pixel response curve. However, in some instances, higher mean levels have been observed.

Bowing is also observed in cases of significant focal plane contamination. As an SCA becomes contaminated, the mean apparent response of the detectors may change as a function of detector position. Detectors near the edges of

# FINAL DRAFT

Created on 4/16/2002 9:07 PM

SCAs have a larger change in apparent response, relative to those near the middle of the SCA, resulting in a bowing appearance for some bands.

Figure C-3 depicts history of focal plane contamination for Band 4 for two periods. The left column shows rapid contamination of the focal plane over a six data period. Clearly evident are the effects of pixel-to-pixel variations, as well as mean level shifting and bowing. The right column shows a significantly reduced contaminant build-up after the first instrument bake out at Lincoln Laboratory.

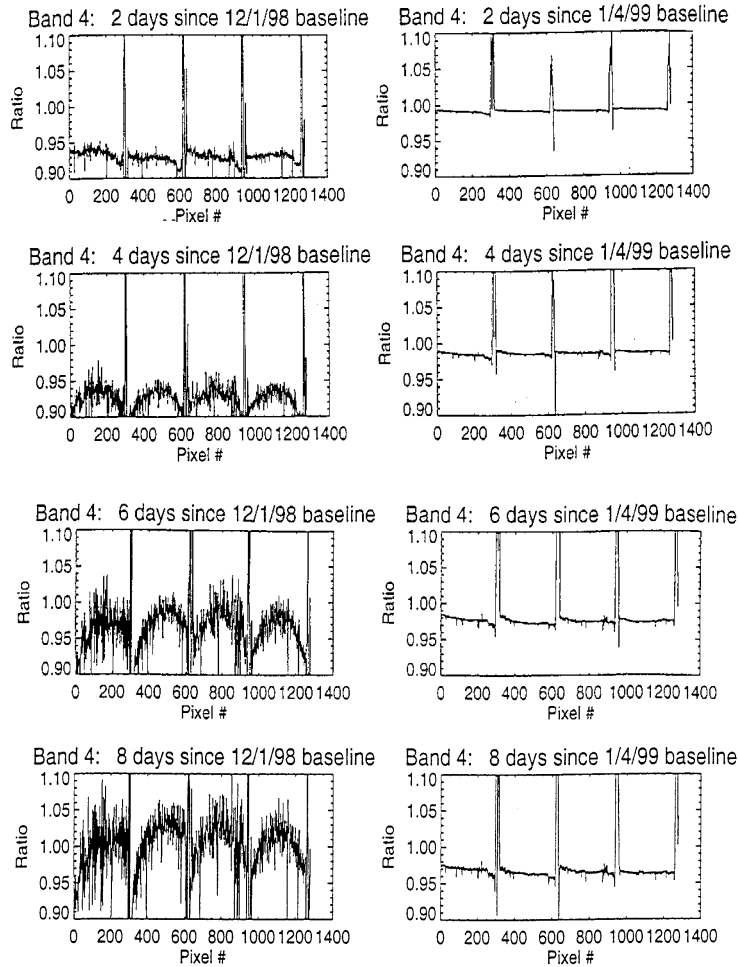


Figure C-3: History of focal plane contamination for two periods during instrument characterization at Lincoln Laboratory.

# FINAL DRAFT

Created on 4/16/2002 9:07 PM

## On-orbit Monitoring

Contamination on orbit has been monitored using the internal reference lamps. Figures C-4 through C-7 provide a history of focal plane contamination since launch for the panchromatic band. Figures C-4 and C-5 depict the mean and standard deviation of the ratio of lamp data collected for each day relative to the December 1, 2000 data. As is clearly evident, significant contamination build-up was observed during the first 30 days on orbit. However, once the bakeout frequency was increased to once every six days, the amount of contamination was significantly restricted. Figures C-6 and C-7 depict the mean and standard deviations as above, but only for the fourth day after each bakeout. As can be seen, the rate of contamination build-up significantly decreased over the first 15 bakeout periods. Since then, the bakeout frequency has decreased to once every 10 days.

Contamination build-up on the focal plane will continue to be monitored for the duration of the EO-1 mission and the bakeout frequency will be adjusted to maintain radiometric effects below 1%.

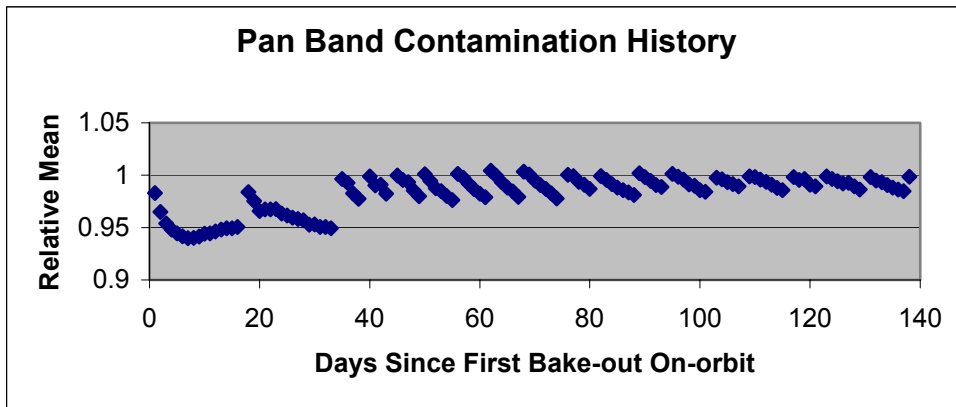


Figure C-4: Pan Band on-orbit contamination history.

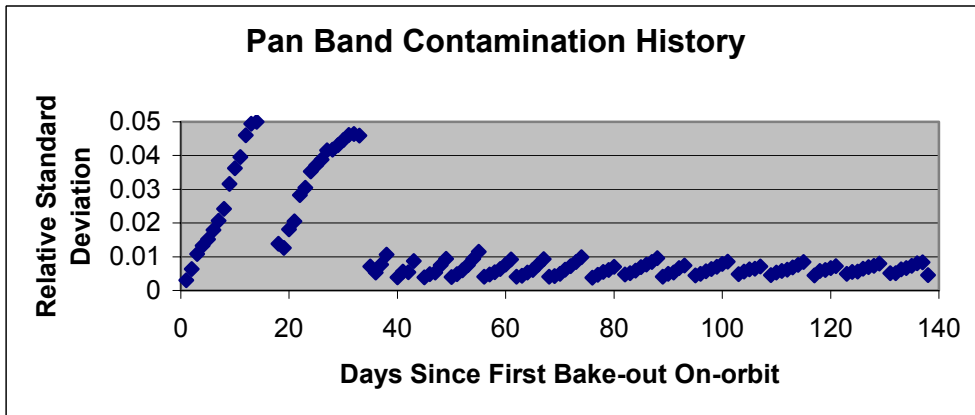


Figure C-5: Pan Band on-orbit contamination history.

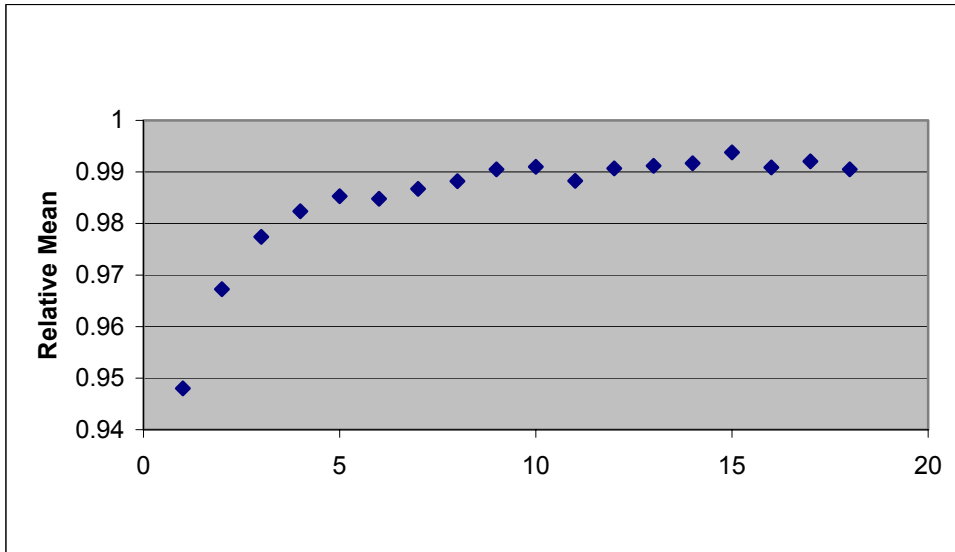


Figure C-6: Pan Band on-orbit contamination history.

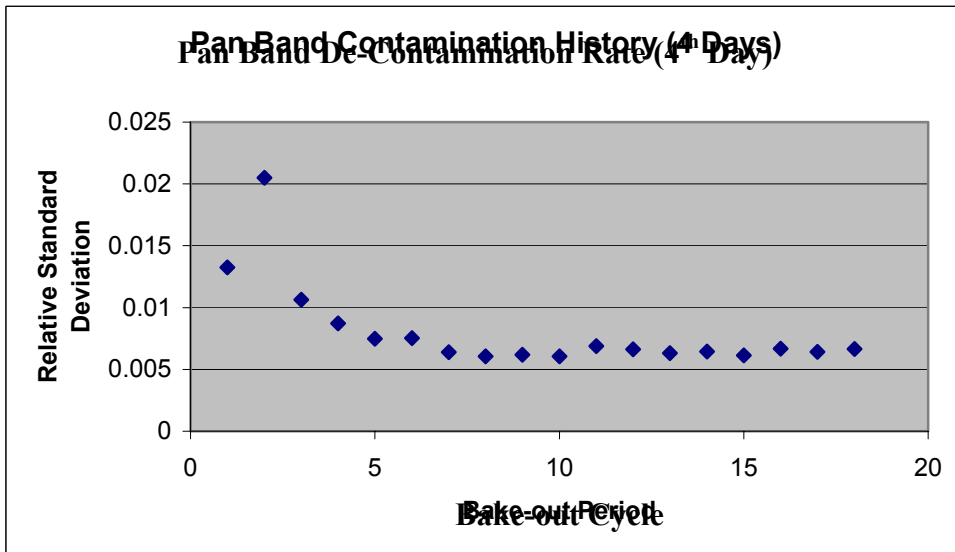


Figure C-7: Pan Band on-orbit contamination history.

## **FINAL DRAFT**

Created on 4/16/2002 9:07 PM

### *Discussion*

Much information pertaining to the contamination of the Advanced Land Imager focal plane has been obtained during ground testing between October 1998 and November 2001. The contaminant appears to condense on the surfaces of the spectral filters lying above the detectors when the focal plane is operated at 220K. However, once the focal plane is warmed above 260 K the contaminant 'boils off' and detector responses return to baseline levels. This implies that mirror surfaces, maintained above 273 K at all times, will not collect contaminants during ground testing or during orbital operations.

Although the source of the contamination is not known, the leading suspect is the black paint (Z306) coating the inside of the telescope to reduce stray light. Bake out of the telescope surround structure was limited to 70 hours and it is possible that residual outgassing of the paint may be sticking onto the filter surfaces when the focal plane is cold.

Finally, on-orbit bakeouts have proven effective in removing the contaminant from the filter surfaces.

## **Appendix D: Leaky Detector Analysis and Correction**

The Earth Observing-1 Advanced Land Imager focal plane contains two leaky detectors (1149 of Band 2 and 864 of band 3), which were initially discovered during ground testing at Lincoln Laboratory. When illuminated, these detectors leak or induce signal onto detectors of the same band and row. By row, we mean the odd or even detector row in which the leaker is contained (odd row for band 2 and even row for band 3). Detectors of the opposing row are not affected. Additionally, when the leaky detector is not illuminated, residual cross-talk remains but is effectively removed by dark-current subtraction. Detectors that are affected by leakage will be referred hereafter as corrupted detectors. Detectors that are not affected by leakage will be referred hereafter as standard detectors.

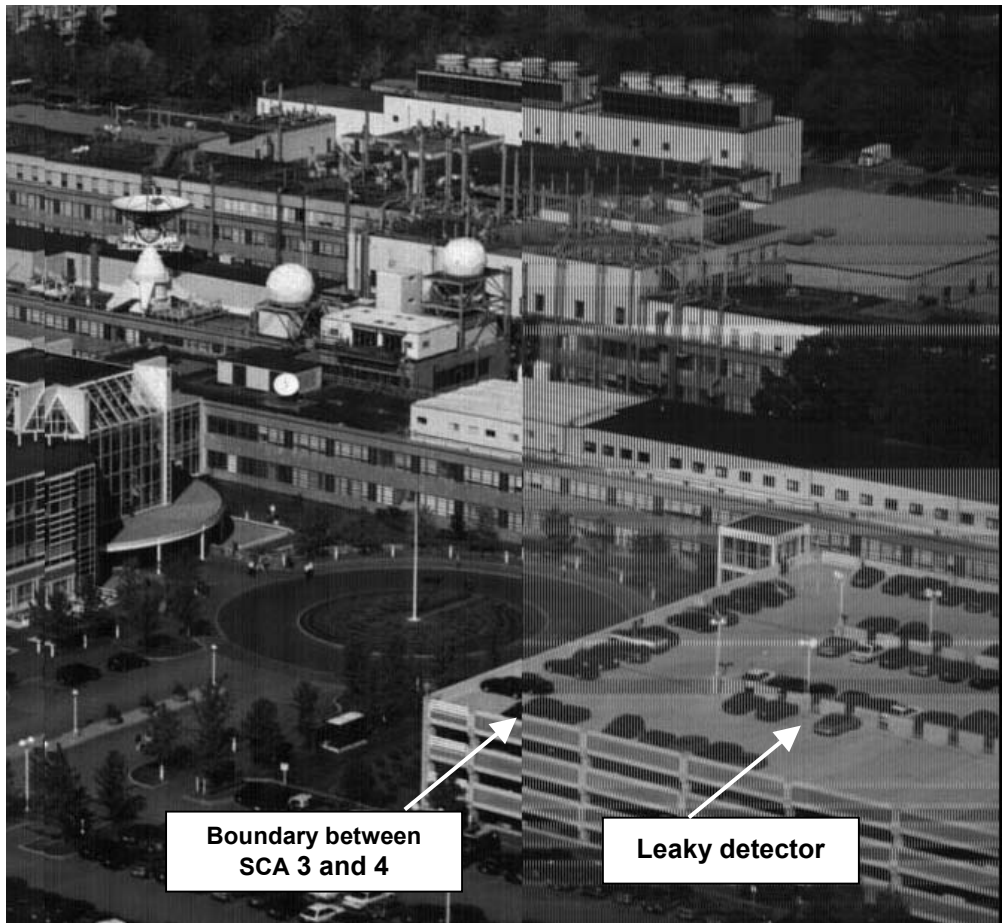


*Figure D-1: Band 2 image of Lincoln Laboratory before the effects of the leaky detector (1149) are corrected. The left portion of the image is from sensor chip assembly 3, which does not contain a leaky detector for this band.*

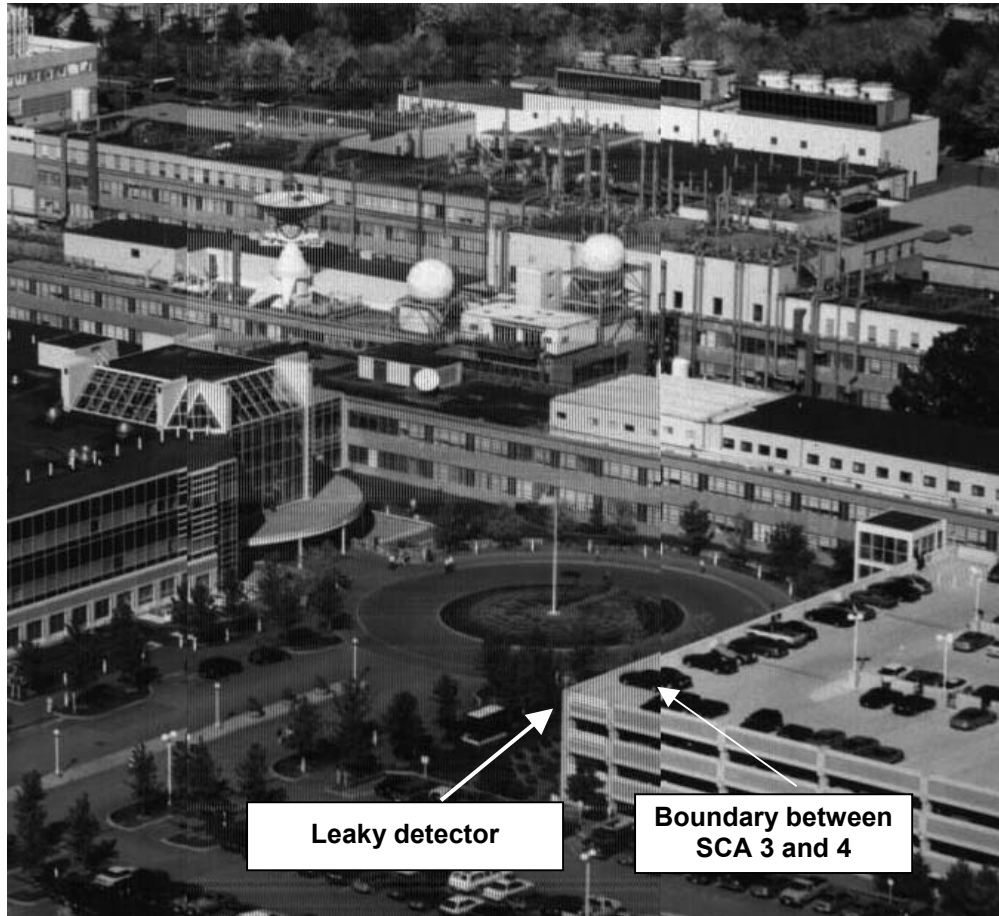


*Figure D-2: Band 3 image of Lincoln Laboratory before the effects of the leaky detector (864) are corrected. The right portion of the image is from sensor chip assembly 4, which does not contain a leaky detector for this band.*

The optical or electrical cross-talk of leaky detectors results in the corruption of portions of images when the leaky detector is illuminated. Figures D-1 and D-2 depict images of Lincoln Laboratory in bands 2 and 3 respectively, before the effects of the leaky detectors are accounted for. The approximate location of the leaky detector column is indicated by an arrow. Furthermore, abutting sensor chip assemblies are included in these images to demonstrate the quality of the data in non-leaky regions.

### *Radiometric Correction Methodology*

The radiometric response of corrupted detectors is highly dependent on leaky detector illumination. As a result, a correction procedure must be followed to radiometrically account for the effects of leakage on affected regions. Initially, an algorithm was developed to correct images for leaky detector artifacts by associating the amount of

## FINAL DRAFT

Created on 4/16/2002 9:07 PM

leakage with the dark subtracted value of the leaky detector on a frame-by-frame basis. This algorithm may be represented analytically as

$$L_N = ADN_N + BDN_L \quad (1)$$

Where  $L_N$  is the apparent radiance of corrupted detector N,  $DN_N$  is the true detector value for detector N, A is the radiometric gain coefficient for detector N,  $DN_L$  is the detector value for the leaky detector, and B is a constant which describes the fraction of the leaky detector corrupting detector N. This algorithm correctly accounted for leaky detector effects for most portions of images. However, it was quickly realized that all regions where the algorithm failed were associated with sharp edges crossing the leaky detector during the push-broom imaging of a scene. This led to the conjecture that the leak is caused by a localized defect in the detector area. For scenes with uniform illumination, the leaky detector (good and defective regions) are fully illuminated and Equation 1 is correct. For scenes with no illumination, no leakage exists and Equation 1 is again correct. However, if the leaky detector is partially illuminated, the defective region within this detector may have none, partial, or full illumination. As a result, the dependence on the leaky detector illumination is no longer valid and the original image correction process breaks down. *This leads us to the conclusion that the amount of leakage for any frame is dependent on the illumination of the leaky detector defective region and not of the entire leaky detector. Additionally, since we do not know the precise illumination of the defect a priori, we have adopted an empirical correction method to eliminate the effects of leaky detectors on ALI images (Earth Observing-1 Advanced Land Imager Flight Performance Assessment: Leaky Detector Correction).*

The empirical correction method we have adopted is implemented on a frame-by-frame basis and uses the differences between each corrupted detector and its nearest uncorrupted (standard) neighbor to derive a leakage function. The leakage function is then used to correct corrupted detectors while maintaining the unique detector-to-detector radiometric variations for that frame. This method is then repeated for all frames. The empirical correction method is implemented in the following manner:

- Correct geometrically odd and even detector offsets and SCA to SCA offsets for the entire image.
- Correct radiometrically entire image using calibration coefficients.
- Begin frame-by-frame loop
  - Generate difference array between corrupted detectors and nearest neighbors
  - Compute leakage function
  - Correct frame
- End frame-by-frame loop
- Save corrected image

### *Geometrically correct image*

The first step in correcting the effects of leaky detector corruption is to geometrically correct the entire image for odd and even detector and SCA to SCA offsets. The ALI focal plane is composed of four sensor chip assemblies, positioned in a staggered formation to provide overlap between arrays (Figure D-3). Within each array, detectors are aligned in odd and even rows for each band (Figure D-4). The SCAs are offset by 5 mm and each odd and even row is separated by 80 $\mu$ m.

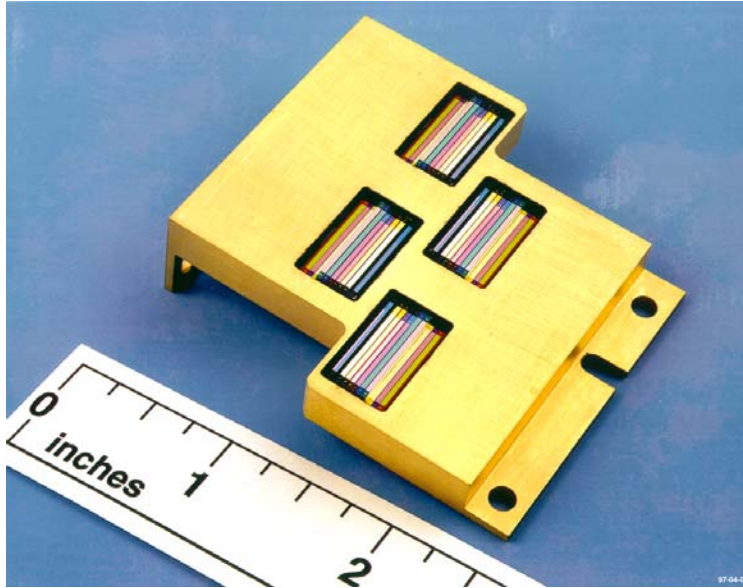


*Figure D-3: Photograph of ALI filter assembly.*

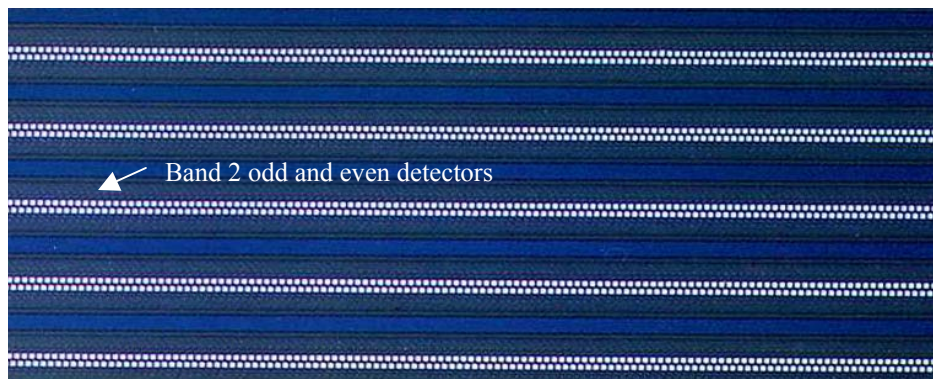


*Figure D-4: Photograph of detector rows for Bands 1-4. Odd and even rows for each band are evident. Columns in an image are formed by acquiring data from a single detector in a push-broom fashion.*

To reconstruct an ALI image, even numbered SCAs and detector columns are shifted down an integral number of frames (correction factor is different for SCAs and columns), depending on the frame rate used during the data collection. Small effects from telescope distortion must also be accounted for when properly reconstructing an

image but these effects are second order when correcting for leaky detector corruption. To illustrate the effects of detector offset shifting, subframes of the Band 2 image of Lincoln Laboratory are displayed in Figure D-5.



*Figure D-5: Example of geometric correction performed on images before the leaky detector correction is implemented. The top figure is before correction. The bottom figure is after correction.*

### *Radiometrically Correct Image*

The second step in accounting for leaky detector effects is to radiometrically calibrate the image. This involves applying radiometric calibration coefficients to transform data from digital numbers to  $W/cm^2/sr/\mu$ . For ALI data this transform is linear and may be expressed analytically as

$$L_N = A_N + B_N DN_N \quad (2)$$

Here,  $L_N$  is the radiance observed by detector N,  $A_N$  and  $B_N$  are the offset and gain calibration coefficients for detector N, and  $DN_N$  is the dark subtracted focal plane response for detector N. The calibration coefficients have been derived from laboratory measurements of the radiometric response of the focal plane to diffuse scenes of varying radiance (see *Earth Observing-1 Advanced Land Imager: Radiometric Response Calibration*). Although the response of corrupted detectors is influenced by the leaky detectors, we have found the adoption of incorrect radiometric response coefficients for these detectors are effectively accounted for during leaky detector correction. As an example of this step in the leaky detector correction process, frame 1050 of the Lincoln Laboratory image, before and after radiometric correction, are graphically displayed in Figure D-6.

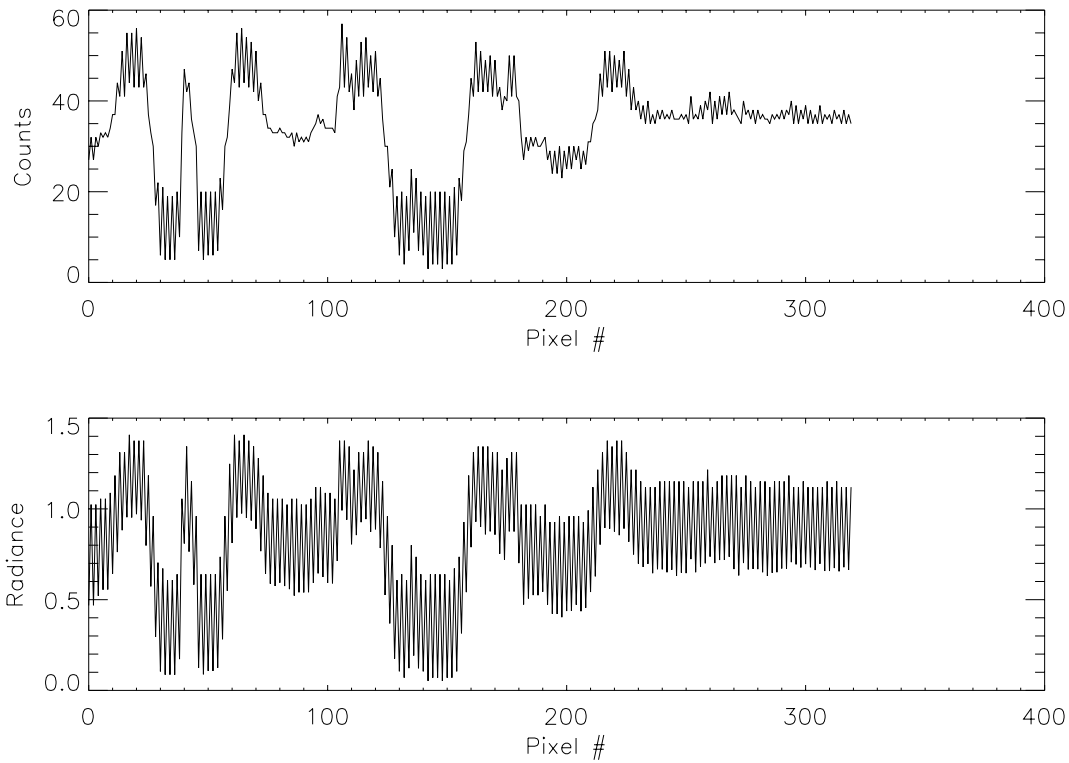


*Figure D-6: Effects of leaky detector corruption of frame 1050 of the Band 2 image of Lincoln Laboratory. The top figure is dark subtracted data. The bottom figure has been radiometrically corrected.*

### *Generate Difference Array Between Corrupted Detectors and Nearest Neighbors*

Once an image has been geometrically corrected and radiometrically calibrated, the leaky detector correction methodology focuses on a frame-by-frame correction. This correction begins with the generation of a *difference* array between corrupted detectors and nearest uncorrupted or *standard* neighbors. After an image has been geometrically corrected, each corrupted detector is abutted on either side by an uncorrupted or standard detector. A difference array between corrupted and standard detectors creates a database of leakage for a given frame. A trend of leakage versus radiance is then formed if the weighted standard detector radiance is plotted against the difference array. The difference array against radiance for frame 1050 is plotted in Figure D-7.

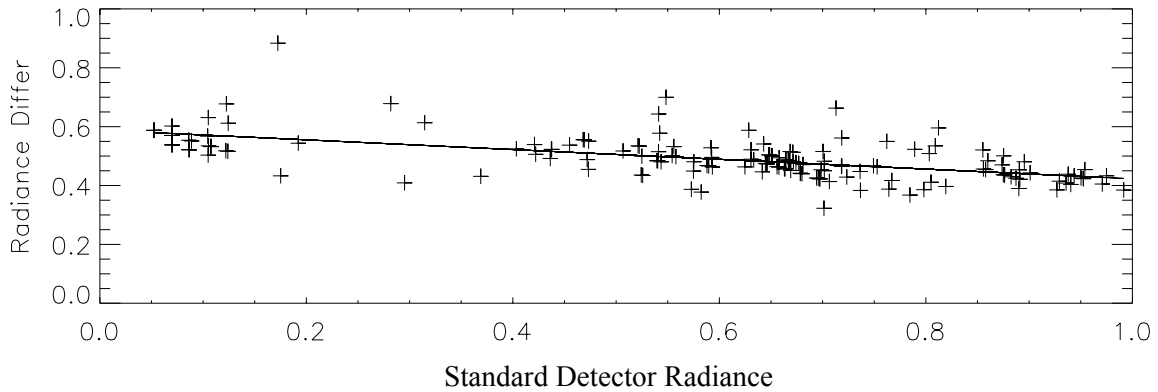


*Figure D-7: Frame 1050 difference array as a function of weighted standard detector radiance.*

### *Compute Correction Function*

The leakage correction function for each frame is calculated as a polynomial fit to the standard detector radiance and difference array data. This fit identifies the leakage observed as a function of radiance by statistically averaging the inherent standard-to-corrupted detector variations in geometrically varying scenes. The correction function for frame 1050 is shown in Figure D-8.

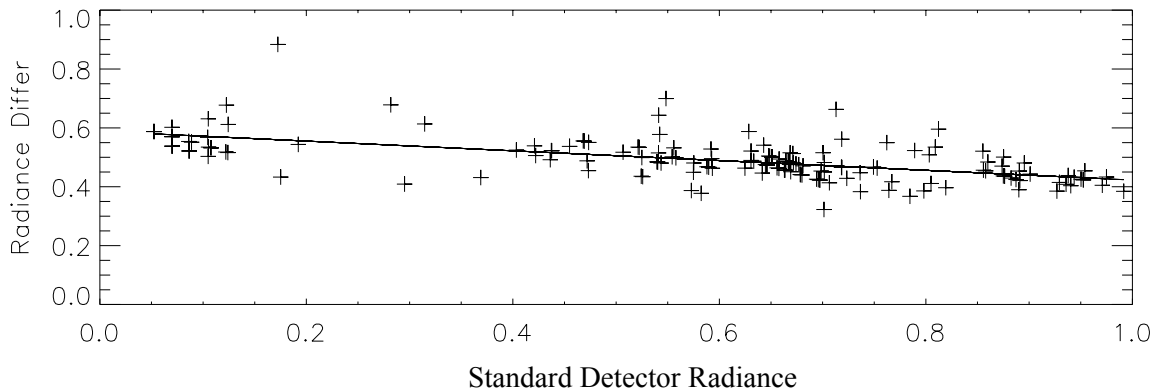


*Figure D-8: Frame 1050 difference array as a function of weighted standard detector radiance. Overlaid is the linear fit leakage function that is used to correct corrupted detectors for this frame.*

The final step in leaky detector correction is the application of the leakage correction function to individual detectors. For a given corrupted detector, a correction factor is calculated, based on the correction function and neighboring standard detector value:

$$C_N = A_{CF} + B_{CF}(R_S) + C_{CF}(R_S)^2 \quad (3)$$

# FINAL DRAFT

Created on 4/16/2002 9:07 PM

Here,  $C_N$  is the correction factor for detector N,  $A_{CF}$ ,  $B_{CF}$ ,  $C_{CF}$  are the correction factors generated from the fitting procedure described above, and  $R_S$  is the radiance of the neighboring standard detectors. Once a correction factor has been calculated, it is simply subtracted from the original radiometrically calibrated corrupted detector value. Figure D-9 depicts the effects of leaky detector correction for frame 105. As one may see, the leakage has been effectively removed, while maintaining the intrinsic detector to detector variability of the scene. This is demonstrated graphically in Figures D-10 and D-11. The images on the left are the original corrupted Band 2 and Band 3 images respectively. The images on the right are the images after leaky detector correction has been implemented.

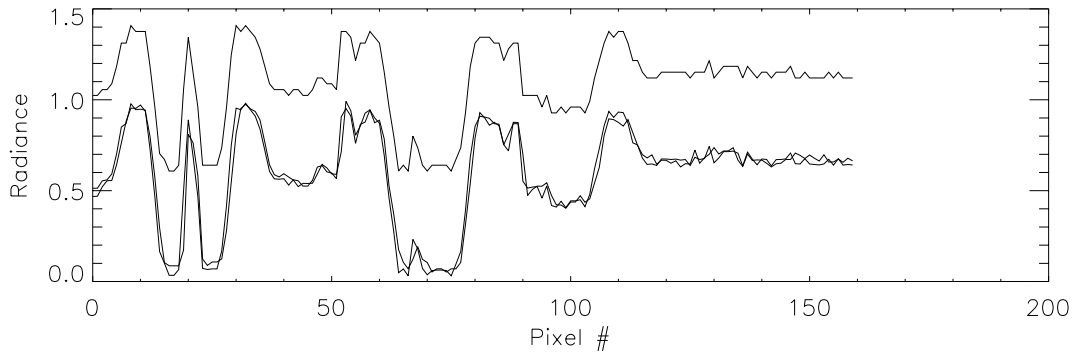


*Figure D-9: Frame 1050 with leaky detector correction applied. The data set at the top is the original radiometrically corrected corrupted detector data. The data at the bottom is an overlay of uncorrupted detector data and leaky detector corrected data.*



Figure D-10: Band 2 image of Lincoln Laboratory before (left) and after (right) leaky detector correction applied.



Figure D-11: Band 3 image of Lincoln Laboratory before (left) and after (right) leaky detector correction applied.

## FINAL DRAFT

Created on 4/16/2002 9:07 PM

### *Discussion*

The radiometric responses of corrupted detectors are highly dependent on leaky detector illumination. As a result, an empirical correction method has been developed to effectively eliminate the addition of optical or electrical cross-talk induced by leaky detectors. This method centers on the generation of a *difference* array between corrupted and neighboring *standard* detectors. This array is used to fit a correction function on a frame-by-frame basis and calculate correction factors on a detector-by-detector basis. This method has been used on various scenes collected during ground calibration at Lincoln Laboratory with excellent results.

Using the above method on a variety of scenes, one area of concern has been identified: scenes with uniform high (low) radiance levels, sparsely intermixed with a very low number of small, low (high) radiance regions. Examples of these scenes include snow covered scenes with a single road cutting across the image or ocean scenes with small, sparsely distributed clouds. The root of the problem lies in the generation of the correction function. For the above examples, an overwhelming number of detectors will have nearly the same high (low) radiances with only a handful of detectors exhibiting low (high) radiances. If the difference array for the handful of detectors cluster is not correctly calculated or has a large scatter, the resulting correction function will not be correct, resulting in poor correction for those detectors. This danger only exists for scenes where the distribution of radiance across the scene is split into large and small groups. Fortunately, by the nature of the problem, only the handful of detectors whose correction function is incorrect will be affected.

## Appendix E: Edge Response Calculation

The ALI edge responses have been derived from the spatial transfer function (MTF), which was calculated using pre-flight subsystem and system level measurements. The edge response is calculated by the following method:

- Compute modulation factor to account for motion during integration time
- Rotate two-dimensional dynamic STF (DSTF) to match angle of edge
- Multiply rotated DSTF by transform of step function
- Invert Fourier Transform to yield Edge Spread Function
- Find distance between 40% and 60% response points

All VNIR MS bands (1', 1, 2, 3, 4, and 4') satisfy this specification at the nominal integration time of 4.05 ms (duty cycle = 91.5%). SWIR bands (5', 5, and 7) meet the specification if duty cycle is reduced to 50%. The most stressing case is band 7 (2200 nm), for nominal duty cycle, and edges perpendicular to the ground track. The above statements hold true for all angles of the edge with respect to the ground track. Tables E-1 and E-2 and Figures E-1 through E-7 support these results.

Table E-1: ALI edge slopes, duty cycle = 91.53% case.

Duty cycle = 91.53%	Edge Angle from Cross -Track (deg)							Mean	Mean * GSD
	0	15	30	45	60	75	90		
ALI Band	Edge Slope (/m)								
1'	0.0269	0.0270	0.0280	0.0299	0.0313	0.0300	0.0292	0.0289	0.868
1	0.0272	0.0272	0.0283	0.0302	0.0316	0.0302	0.0293	0.0291	0.874
2	0.0274	0.0275	0.0286	0.0305	0.0319	0.0305	0.0296	0.0294	0.882
3	0.0275	0.0276	0.0287	0.0306	0.0320	0.0305	0.0296	0.0295	0.885
4	0.0275	0.0276	0.0287	0.0306	0.0320	0.0305	0.0296	0.0295	0.885
4'	0.0275	0.0276	0.0287	0.0305	0.0319	0.0305	0.0295	0.0294	0.883
5'	0.0259	0.0260	0.0270	0.0286	0.0300	0.0302	0.0302	0.0283	0.848
5	0.0253	0.0253	0.0263	0.0278	0.0291	0.0294	0.0296	0.0275	0.826
7	0.0243	0.0243	0.0252	0.0265	0.0277	0.0281	0.0285	0.0264	0.792
Pan	0.0601	0.0599	0.0610	0.0621	0.0624	0.0624	0.0641	0.0617	0.617

Table E-2: ALI edge slopes, duty cycle = 50% case.

Duty cycle = 50%	Edge Angle from Cross-Track (deg)							Mean	Mean * GSD
	0	15	30	45	60	75	90		
ALI Band	Edge Slope (/m)								
1'	0.0289	0.0293	0.0312	0.0330	0.0325	0.0301	0.0292	0.0306	0.918
1	0.0291	0.0295	0.0314	0.0333	0.0327	0.0303	0.0293	0.0308	0.924
2	0.0294	0.0298	0.0317	0.0337	0.0331	0.0305	0.0296	0.0311	0.933
3	0.0295	0.0299	0.0319	0.0338	0.0332	0.0306	0.0296	0.0312	0.936
4	0.0295	0.0299	0.0319	0.0338	0.0331	0.0305	0.0296	0.0312	0.935
4'	0.0294	0.0299	0.0318	0.0337	0.0330	0.0305	0.0295	0.0311	0.934
5'	0.0291	0.0292	0.0302	0.0312	0.0312	0.0304	0.0302	0.0302	0.907
5	0.0284	0.0285	0.0294	0.0302	0.0303	0.0296	0.0296	0.0294	0.882
7	0.0272	0.0272	0.0280	0.0287	0.0288	0.0284	0.0285	0.0281	0.844
Pan	0.0649	0.0648	0.0659	0.0656	0.0639	0.0629	0.0641	0.0646	0.646

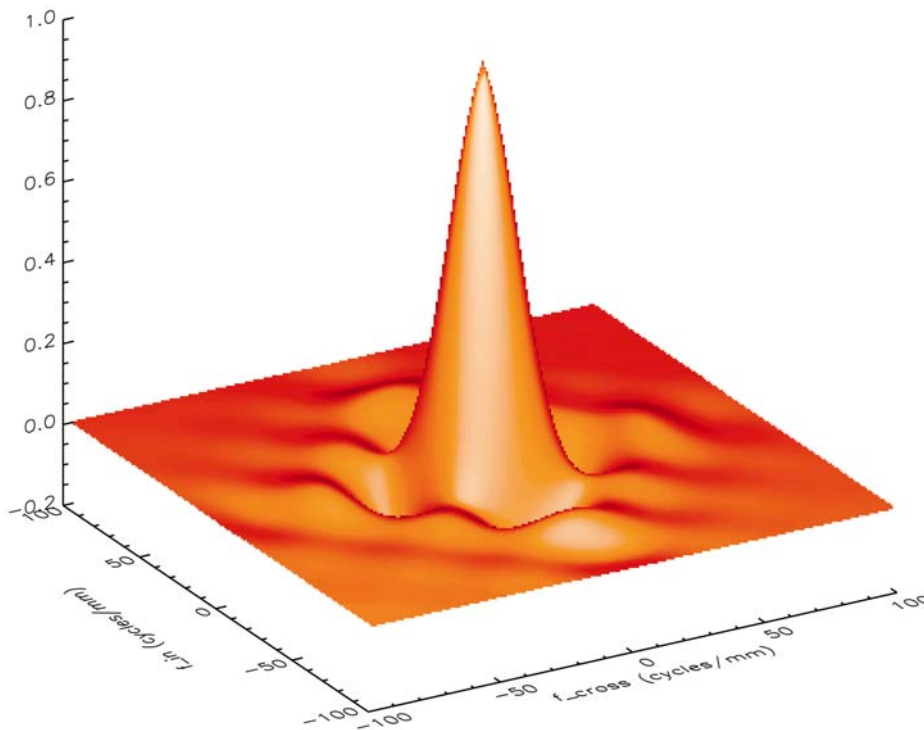


Figure E-1: ALI spatial transfer function for Band 4p (static).

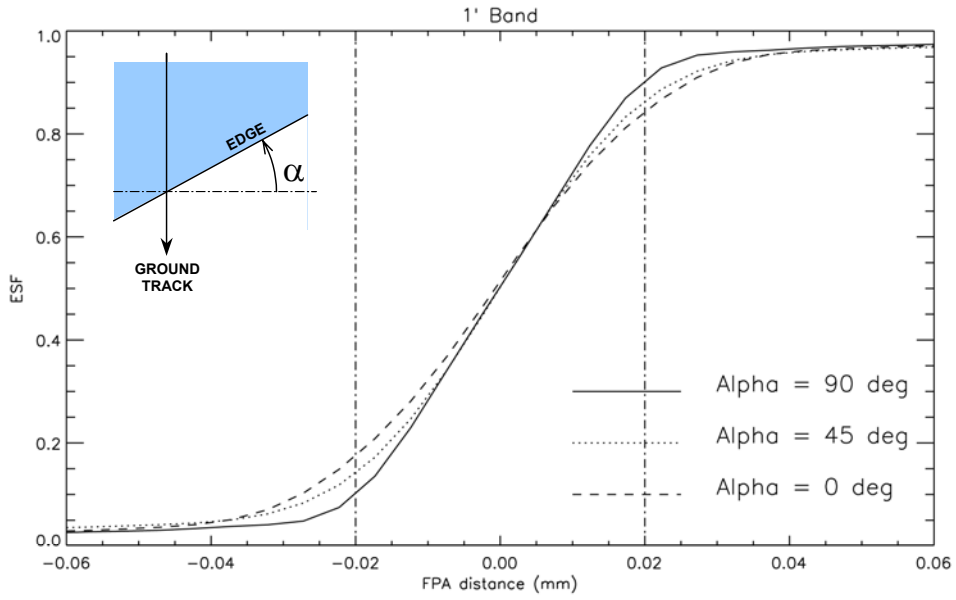


Figure E-2: ALI edge spread function, Band 1p.

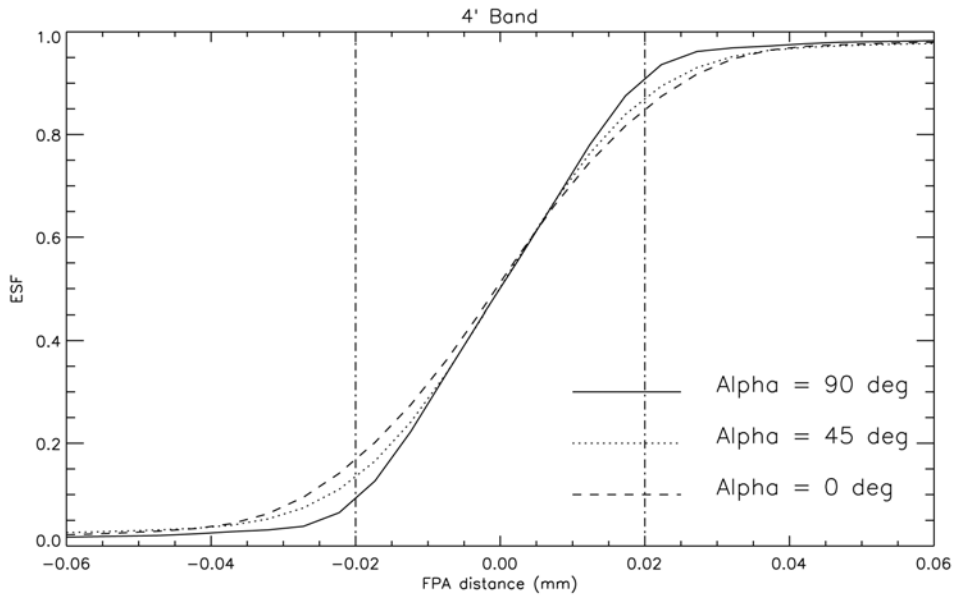


Figure E-3: ALI edge spread function, Band 4p.

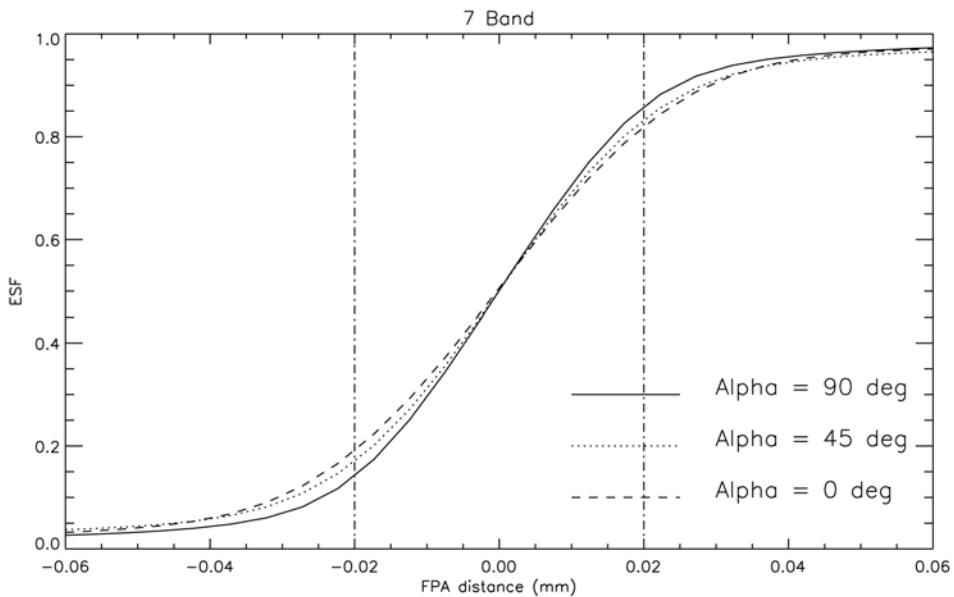


Figure E-4: ALI edge spread function, Band 7.

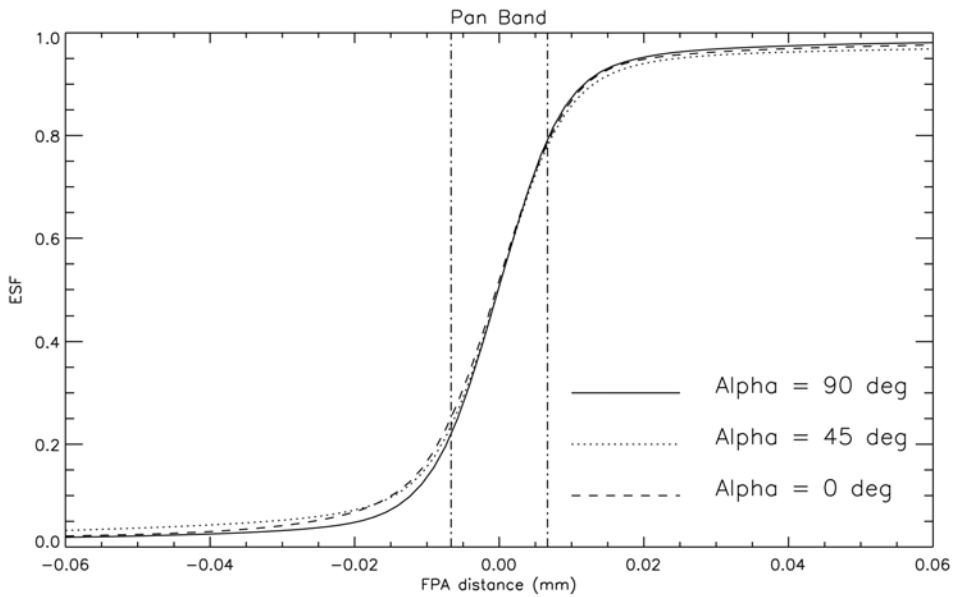


Figure E-5: ALI edge spread function, Pan band.

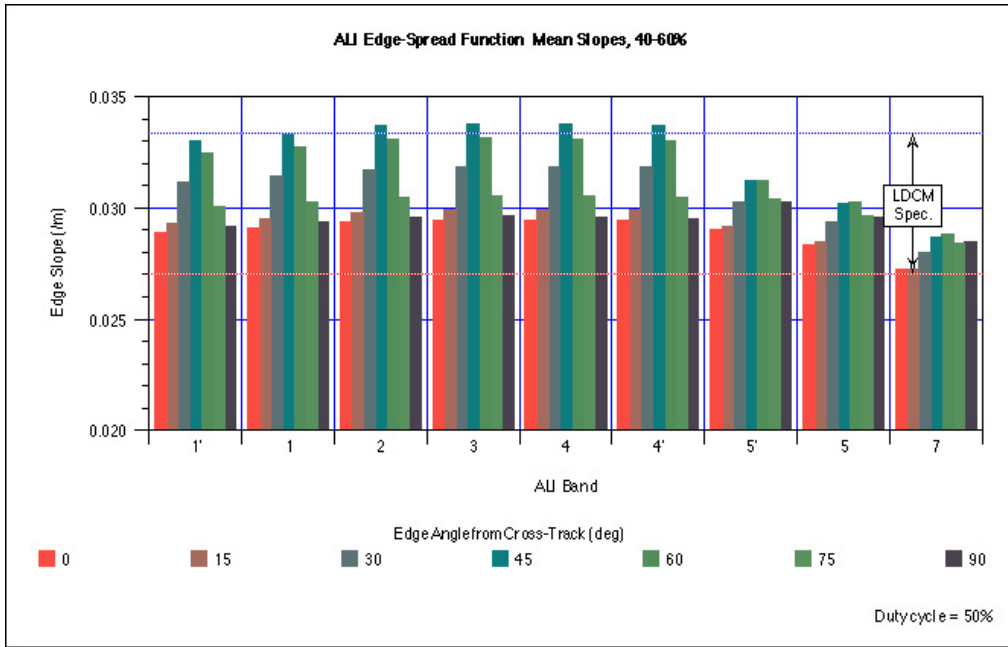


Figure E-6: Nominal ALI edge responses. Duty cycle = 50%.

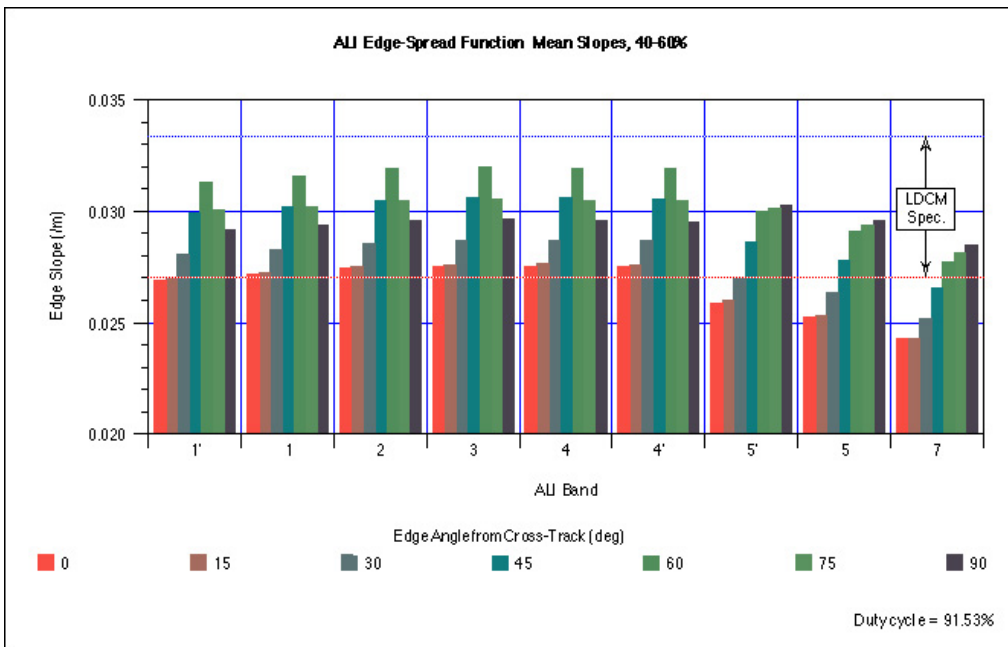


Figure E-7: Sharpened ALI edge responses. Duty cycle = 92%.

# FINAL DRAFT

Created on 4/16/2002 9:07 PM

## Appendix F: Coherent Noise

Dark data collected by the ALI during each Data Collection Event (DCE) have been extensively analyzed. In this analysis, the four SCAs were treated separately. The maximum values of the autocorrelations computed as specified are spread over a range from 0.08 to 0.60, when all bands and all SCAs are considered. There are clear differences between the SCAs, with SCA 3 having the highest autocorrelations ( $\sim 0.35$  to  $\sim 0.60$ ), and SCA 4 having the lowest range ( $\sim 0.08$  to  $\sim 0.30$ ). No secular trends are apparent in the autocorrelations, though there are considerable variations from DCE to DCE. The maximum autocorrelations for the nine DCEs analyzed so far are plotted against time in Figure F-1.

Plots of the noise autocorrelation image (or equivalently, the noise power spectral density, or PSD) provide clues to the origin of coherent noise in the instrument. The autocorrelation shows sinusoidal ripples at various angles, corresponding to localized peaks in the PSD. These are apparently caused by *pickup of periodic signals* from other circuits. A prominent feature of the autocorrelation is a ridge of high values in the row with zero frame (temporal) lag. This corresponds to a column of high PSD values at zero spatial frequency. Any source of *common-mode noise*, affecting all detectors, can cause this. The zero-frame lag row also shows that the even spatial lags (0, 2, 4, ...) are much higher than the odd lags. The maximum autocorrelation almost always occurs in these lag elements. This feature corresponds to a column of high PSD values at the Nyquist spatial frequency. Since all of the even-numbered detectors in each row of the SCA have a separate signal path from the odd-numbered detectors, random noise components in the separate paths will give rise to this *odd-even noise* effect. Finally, we point out that any residual error in subtracting the DC offsets of the detectors before noise processing will give rise to a row of high PSD values at zero temporal frequency, and a column of high autocorrelations at zero spatial lag. This component was absent in our analysis of the dark data alone, since the DC values were forced to be zero. In an earth scene however, the dark DC values are subtracted from the scene values, and some statistical error in the *estimates of the dark values* is inevitable.

It was instructive to simulate all of the effects just described. The magnitude of each noise component in relation to the white noise could be adjusted arbitrarily. We discovered a simple relationship between the maximum value of the autocorrelation,  $A_{max}$ , and the variances of the several noise contributors:

$$A_{max} = \frac{P_{coh}}{P_{total}} ,$$

where

$$P_{coh} = \sum_{\{coherent\}} \sigma_i^2 , \text{ for all } coherent \text{ noise sources,}$$

$$P_{total} = \sum_{\{all\}} \sigma_i^2 , \text{ for all noise sources, and}$$

$\sigma_i^2$  is the variance of noise source  $i$ .

**FINAL DRAFT**  
Created on 4/16/2002 9:07 PM

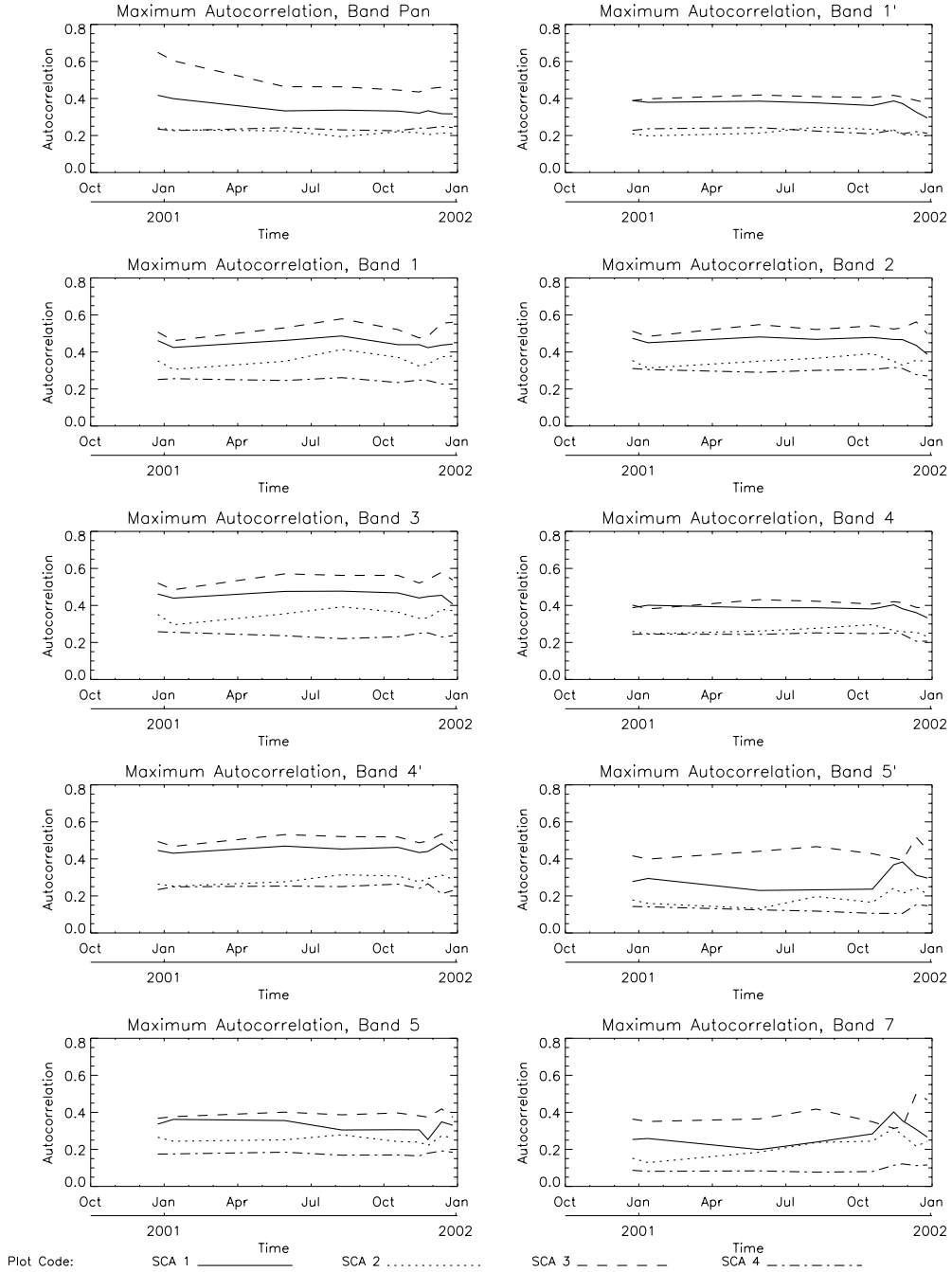


Figure F-1: Maximum autocorrelations in ALI dark data, plotted by band and Sensor Chip Assembly.

# FINAL DRAFT

Created on 4/16/2002 9:07 PM

A simulation with the following noise component variances produced an autocorrelation image, which qualitatively mimicked the observed ALI autocorrelations well:

white noise = 1.0 (by definition),

common-mode noise = 0.25,

odd-even noise = 0.25,

sinusoidal pickup = 0.125 (peak amplitude = 0.5).

For this example,  $\langle A_{max} \rangle = 0.385$ , and the coherent noise RMS amplitude is then 62% of the white noise. A plot of the simulated noise and autocorrelation (for 160 detectors) is shown in Figure F-2.

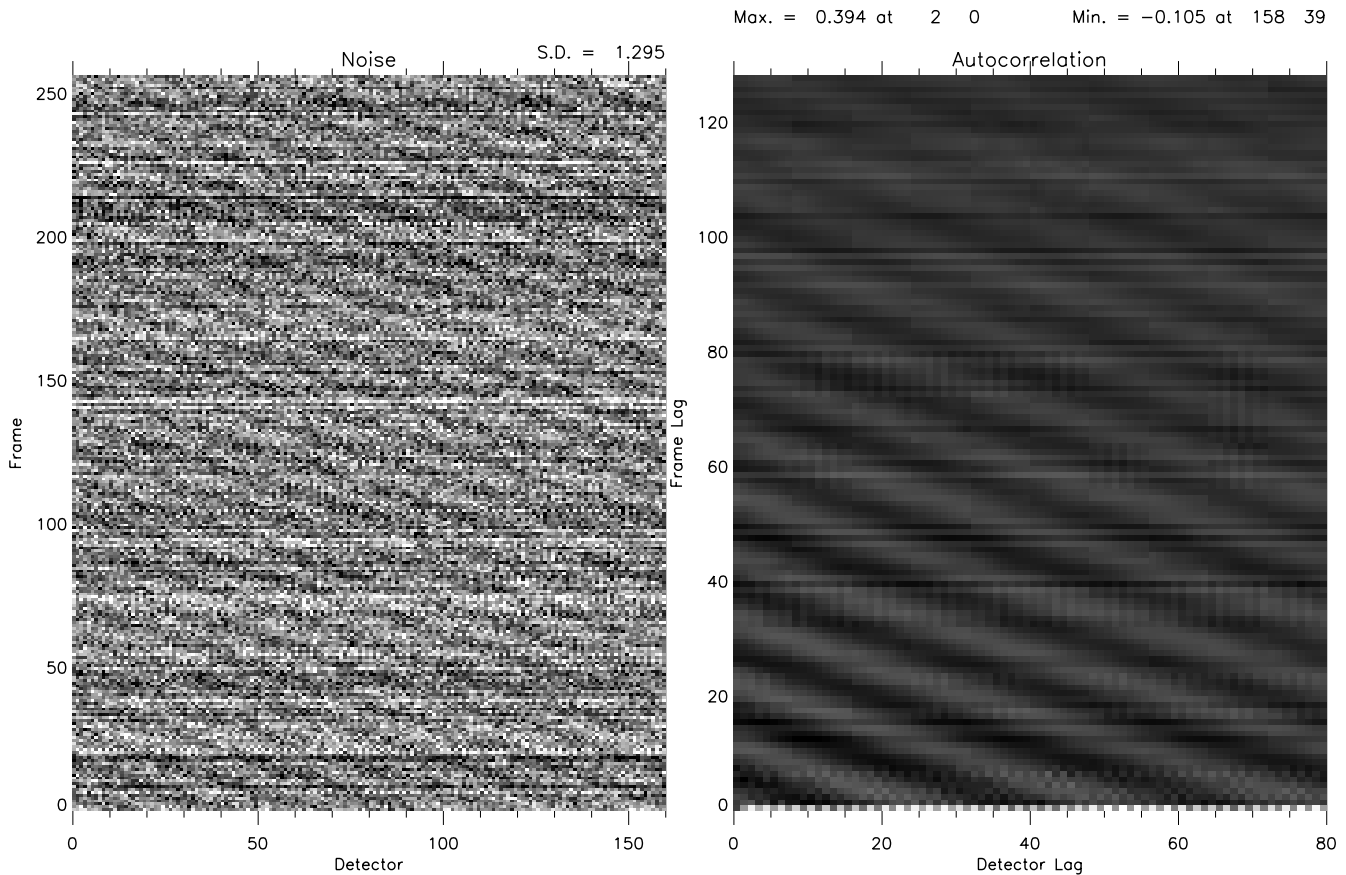


Figure F-2: Simulated noise and autocorrelation, with common-mode variance = 0.25, odd-even variance = 0.25, peak sine amplitude = 0.5 (all relative to white noise variance = 1.0).

The present results are consistent with the coherent noise analysis given earlier (Report EO-1-5), except that common-mode noise and odd-even noise were not included in the coherent noise total for that report.

Notwithstanding the identification of coherent noise components in the ALI dark data, coherent noise artifacts are difficult to find in ALI images of earth scenes. To do so requires the study of very uniform areas, with highly stretched contrast.

## FINAL DRAFT

Created on 4/16/2002 9:07 PM

### Appendix G: Publications

1. D. E. Lencioni and D. R. Hearn, "New Millennium EO-1 Advanced Land Imager," *International Symposium on Spectral Sensing Research*, San Diego, Dec. 13-19, 1997.
2. "Report and Recommendations from EO-1 ALI SiC Optics Performance Workshop", May 29, 1998, found at <http://eo1.gsfc.nasa.gov/Technology/StrayLightIssues.html>
3. "Stray Light Analysis Report No. 3" - prepared by Lambda Research Corporation, Littleton, MA 01460-4400, May 4, 1998.
4. C. J. Digenis, D. E. Lencioni 4/17/024/17/02 and W. E. Bicknell, "New Millennium EO-1 Advanced Land Imager," *SPIE Conference on Earth Observing Systems III*, San Diego, California, Proc. SPIE, Vol. 3439, pp. 49-55, July 1998.
5. J. A. Mendenhall, D. E. Lencioni, D. R. Hearn and A. C. Parker, "EO-1 Advanced Land Imager preflight calibration," Proc. SPIE, Vol. 3439, pp. 390-399, July 1998.
6. D. R. Hearn, "Characterization of instrument spectral resolution by the spectral modulation transfer function," Proc. SPIE, Vol. 3439, pp. 400-407, July 1998.
7. J. A. Mendenhall, D. E. Lencioni, D. R. Hearn and A. C. Parker, "EO-1 Advanced Land Imager in-flight calibration," Proc. SPIE, Vol. 3439, pp. 416-422, July 1998.
8. W. E. Bicknell, C. J. Digenis, S. E. Forman and D. E. Lencioni, "EO-1 Advanced Land Imager," *SPIE Conference on Earth Observing Systems IV*, Denver, Colorado, Proc. SPIE, Vol. 3750, pp. 80-88, July 1999.
9. D. E. Lencioni, D. R. Hearn, J. A. Mendenhall and W. E. Bicknell, "EO-1 Advanced Land Imager calibration and performance," *SPIE Conference on Earth Observing Systems IV*, Denver, Colorado, Proc. SPIE, Vol. 3750, pp. 89-96, July 1999.
10. D. R. Hearn, J. A. Mendenhall and B. C. Willard, "Spatial calibration of the EO-1 Advanced Land Imager," *SPIE Conference on Earth Observing Systems IV*, Denver, Colorado, Proc. SPIE, Vol. 3750, pp. 97-108, July 1999.
11. J. A. Mendenhall and A. C. Parker, "Spectral calibration of the EO-1 Advanced Land Imager," *SPIE Conference on Earth Observing Systems IV*, Denver, Colorado, Proc. SPIE, Vol. 3750, pp. 109-116, July 1999.
12. J. A. Mendenhall, D. E. Lencioni and A. C. Parker, "Radiometric calibration of the EO-1 Advanced Land Imager," *SPIE Conference on Earth Observing Systems IV*, Denver, Colorado, Proc. SPIE, Vol. 3750, pp. 117-131, July 1999.
13. H. Viggh, J. Mendenhall, R. Sayer, J. S. Stuart and M. Gibbs, "An Automated Ground Data Acquisition and Processing System for Calibration and Performance Assessment of the EO-1 Advanced Land Imager," *SPIE Conference on Earth Observing Systems IV*, Denver, Colorado, Proc. SPIE, Vol. 3750, pp. 132-140, July 1999.
14. H. Viggh, J. S. Stuart, R. Sayer, J. Evans, J. A. Mendenhall and M. Gibbs, "Performance Assessment Software for the EO-1 Advanced Land Imager," *SPIE Conference on Earth Observing Systems IV*, Denver, Colorado, Proc. SPIE, Vol. 3750, pp. 141-152, July 1999.
15. J. Evans and H. Viggh, "Radiometric Calibration Pipeline for the EO-1 Advanced Land Imager," *SPIE Conference on Earth Observing Systems IV*, Denver, Colorado, Proc. SPIE, Vol. 3750, pp. 153-161, July 1999.
16. B. C. Willard, "Wide field-of-view Schmidt-sphere imaging collimator," *SPIE Conference on Earth Observing Systems IV*, Denver, Colorado, Proc. SPIE, Vol. 3750, pp. 286-296, July 1999.
17. D. R. Hearn, "Vacuum Window Optical Power Induced by Temperature Gradients," *SPIE Conference on Earth Observing Systems IV*, Denver, Colorado, Proc. SPIE, Vol. 3750, pp. 297-308, July 1999.

## FINAL DRAFT

Created on 4/16/2002 9:07 PM

18. D. E. Lencioni, C. J. Digenis, W. E. Bicknell, D. R. Hearn and J. A. Mendenhall, "Design and Performance of the EO-1 Advanced Land Imager," *SPIE Conference on Sensors, Systems, and Next Generation Satellites III*, Florence, Italy, 20 September 1999.
19. D. R. Hearn, "EO-1 Advanced Land Imager Modulation Transfer Functions," *MIT Lincoln Laboratory Technical Report 1061*, 22 March 2000.
20. J. A. Mendenhall (Editor), "Earth Observing-1 Advanced Land Imager: Instrument and Flight Operations Overview," MIT/LL Project Report EO-1-1, 23 June 2000.
21. J. A. Mendenhall and D. P. Ryan-Howard, "Earth Observing-1 Advanced Land Imager: Spectral Response Calibration," MIT/LL Project Report EO-1-2, 20 September 2000.
22. J. A. Mendenhall, D. E. Lencioni and J. B. Evans, "Earth Observing-1 Advanced Land Imager: Radiometric Response Calibration," MIT/LL Project Report EO-1-3, 29 November 2000.
23. D. R. Hearn, "Earth Observing-1 Advanced Land Imager: Detector Line-of-Sight Calibration," MIT/LL Project Report EO-1-4, 29 December 2000.
24. J. A. Mendenhall, "Earth Observing-1 Advanced Land Imager: Dark Current and Noise Characterization and Anomalous Detectors," MIT/LL Project Report EO-1-5, 7 May 2001.
25. J. A. Mendenhall and M. D. Gibbs, "Earth Observing-1 Advanced Land Imager Flight Performance Assessment: Noise and Dark Current Trending for the First 60 Days," MIT/LL Project Report EO-1-7, 1 June 2001.
26. J. A. Mendenhall, "Earth Observing-1 Advanced Land Imager Flight Performance Assessment: Investigating Dark Current Stability Over One-half Orbit Period During the First 60 Days," MIT/LL Project Report EO-1-6, 1 July 2001.
27. D. R. Hearn, C. J. Digenis, D. E. Lencioni, J. A. Mendenhall, J. B. Evans and R. D. Welsh, "EO-1 Advanced Land Imager Overview and Spatial Performance ", IGARSS 2001, Sydney, 9 July 2001.
28. J. A. Mendenhall, D. R. Hearn, J. B. Evans, D. E. Lencioni, C. J. Digenis and R. D. Welsh, "Initial Flight Test Results from the EO-1 Advanced Land Imager: Radiometric Performance", IGARSS 2001, Sydney, 9 July 2001.
29. D. E. Lencioni, J. A. Mendenhall and D. P. Ryan-Howard, "Solar Calibration of the EO-1 Advanced Land Imager", IGARSS 2001, Sydney, 9 July 2001. (Poster Session).
30. J. B. Evans, C. J. Digenis, M. D. Gibbs, D.R. Hearn, D.E. Lencioni, J.A. Mendenhall and R.D. Welsh, "On-Orbit Test Results from the EO-1 Advanced Land Imager", SPIE Conference, San Diego, July 2001.
31. J. A. Mendenhall and D. E. Lencioni, "EO-1 Advanced Land Imager On-Orbit Radiometric Calibration", IGARSS 2002, Toronto, 24-28 June 2002 (in USAF release review).
32. J. A. Mendenhall and D. E. Lencioni, "EO-1 Advanced Land Imager Stray Light Analysis and Impact on Flight Data", IGARSS 2002, Toronto, 24-28 June 2002 (in USAF release review).
33. J. A. Mendenhall, D. R. Hearn and D. E. Lencioni, "Comparison of Earth Observing-1 Advanced Land Imager Performance with the Landsat Data Continuity Mission Specification", MIT/LL Project Report in preparation – Review copy target: March 18, 2002.
34. J. A. Mendenhall and D. E. Lencioni, "Earth Observing-1 Advanced Land Imager Flight Performance Assessment: Absolute Radiometry and Stability During the First Year," MIT/LL Project Report in preparation – Review copy target: March 22, 2002.
35. J. A. Mendenhall et al., "EO-1 Advanced Land Imager Technology Validation Report", MIT/LL Project Report in preparation – Review copy target: March 22, 2002.
36. J. A. Mendenhall and D. E. Lencioni, "Earth Observing-1 Advanced Land Imager Flight Performance Assessment: Leaky Detector Correction," MIT/LL Project Report in preparation – Review copy target: April 5, 2002.

## **FINAL DRAFT**

Created on 4/16/2002 9:07 PM

37. D. R. Hearn, " Earth Observing-1 Advanced Land Imager: Spatial Imaging Performance On-Orbit," MIT/LL Project Report in preparation, – Review copy target: April 15, 2002.
38. J. A. Mendenhall and M. D. Gibbs, "Earth Observing-1 Advanced Land Imager Flight Performance Assessment: Dark Current and Noise Stability during the first Year," MIT/LL Project Report in preparation – Review copy target: April 19, 2002.
39. D. E. Lencioni, J. A. Mendenhall , D. R. Hearn and C. J. Digenis, "On-Orbit Calibration, Performance, and Characterization Results from the EO-1 Advanced Land Imager", SPIE 2002, 7-11 July, 2002 ( in preparation).